Mass Spectrometry-Based Quantitative Proteomics for Drug-Metabolizing Enzymes

By

Yao Chen

Submitted to the graduate degree program in Pharmaceutical Chemistry and the Graduate Faculty of the University of Kansas in partial fulfillment of the requirements for the degree of Doctor of Philosophy.

_____

Chairperson: M. Z. Wang, Ph.D.

_____

V. J. Stella, Ph.D.

_____

J.F.Stobaugh, Ph.D.

_____

C.J. Berkland, Ph.D.

_____

J.L. Staudinger, Ph.D.

Date Defended: 22Aug16

The Dissertation Committee for Yao Chen

Certifies that this is the approved version of the following dissertation:

Mass Spectrometry-Based Quantitative Proteomics for Drug-Metabolizing Enzymes

_____

Chairperson: M. Z. Wang, Ph.D.

Date approved: 22Aug16

ABSTRACT

Quantification of highly homologous human liver drug-metabolizing enzymes (DMEs) has been a challenging task in drug metabolism and disposition research, due to a lack of specific antibodies and marker substrates. Mass spectrometry (MS) techniques and applications have evolved significantly, striving to achieve absolute and specific quantification of these enzymes. Since the first absolute quantification of cytochrome P450s (CYPs) using the attachment of isotope tags to free thiols (iCAT), MS-based quantification has become much more versatile, cheaper, and easier to use. Today, variations of liquid chromatography-multiple reaction monitoring (LC-MRM)-based targeted proteomics, such as AQUA (absolute quantification) and QconCAT (concatenated signature peptides), have become the gold standards for quantification. These new methods have driven the absolute quantification of DMEs to become a routine laboratory task.

Many drug metabolism-related projects require absolute enzyme quantification. For example, precise knowledge of enzyme expression during ontogeny is a necessity to aid pharmacists in planning drug-dosing regimens for patients of different age groups. Additional examples include the need for accurate cellular enzyme expression profiles when establishing new drug-screening cell models and when elucidating molecular mechanisms underlying hypothesized drug-drug interactions. This dissertation demonstrates how an LC-MRM targeted approach contributes to these three areas. First, an ultra-performance liquid chromatography (UPLC)-MRM targeted quantification method was developed and validated, focusing specifically on the quantification of CYP2C and flavin-containing monoxoygenase (FMO) isoforms. Second, the newly developed, as well as existing, UPLC-MRM quantification methods were used to confirm previously reported DME ontogeny patterns and establish patterns for CYP4F and FMO5. Third, targeted

proteomic quantification was employed for the absolute quantification of CYPs 1A1, 1A2 and 1B1 in KLE cells and different human tissue microsomes to aid the establishment of CYP1B1-dependent cell models for the screening of anticancer prodrugs. Lastly, CYP4F2-specific targeted quantification was used to confirm the mechanism underlying a potential drug-drug interaction between warfarin and lovastatin.

UPLC-MRM-based targeted proteomic techniques have many advantages, but the cost and time required for method development rises linearly with an increase in the number of targeted proteins. An emerging technique utilizing label-free data independent analysis (DIA) with high-resolution mass spectrometry (HDMS) offers the global quantification of hundreds of proteins at a negligible cost; however, there are numerous hurdles when using this technique. We introduced a new sample processing method, quantitative filter-assisted sample preparation (qFASP), which allows full recovery and analysis of clean, digested proteomic peptides. With qFASP and additional optimized procedures, many of the hurdles encountered with DIA quantification were mitigated. Very strong quantitative correlations were observed between the new DIA/ HDMS technique and the well-established targeted proteomics for DME quantification.

In summary, this dissertation describes a targeted and an untargeted (DIA) quantitative proteomic method for the multiplexed absolute quantification of human hepatic DMEs and their applications to developmental pharmacology. Quantification coherence achieved between the targeted and the untargeted proteomic methods was made possible by a newly developed qFASP sample preparation protocol, which allowed quantitative and reproducible recovery of peptides after filter-assisted sample cleanup and protein digestion. These methods are expected to enrich our knowledge regarding ontogenetic changes of human DMEs and establish necessary quantitative information to construct predictive physiologically-based pharmacokinetic models.

ACKNOWLEDGEMENTS

I sincerely appreciate my mentor and advisor, dear friend and strong leader, Professor Michael Wang, for countless times of his patiently mentoring, teaching, advising, especially his enormous support at my most difficult times of graduate studies. Thank you so much for the support you gave when I was/am not skillful, not wise, so confused and did not know what to do. Thank you for giving me so much spaces and opportunities to find out my passion in analytics and instrumentations. I cannot count how much I learnt through our discussions in individual or lab meetings; how much I benefited from your corrections in my presentations, posters, and publication drafts; how much life mistakes I could have been made without your advises. Your countless efforts have elevated me.

I am very grateful to Dr. Judy Wu. The stories you told, the conversations we had, the lab technique demonstrations you showed all enlightened me. You could arouse hope from hopeless, awaken passion from desperate, and spark innovation from dead-end. I'll bear in mind your optimism and spirit to innovate.

I would like to give special thanks to our dear partner and collaborator Dr. Nicole R. Zane. You opened up a new window for me to do science; reminded me how much I could do with the analytical skills; offered me opportunities to collaborate, communicate, and publish. You taught me important lessons of trying hard, not giving up, not compromise. You made my graduate studies completely different.

I would like to thank Dr. Oliver Mozziconacci for your patience in our discussions on instrumentations, projects, and analytics. I admire your passion for science and spirit to perfection. It's a great pleasure to know you during my last a year and half of graduate studies.

You are an influencer capable of impacting other people's paths. You have definitely impacted mine.

I would like to thank previous and current lab member, Dr. Kuan-Wei Peng, Dr. Zhiying Wang, Dr. Ju Wujian, Dr. Sihyung Yang, Diana Scherier, Laura Drbohlav, and Mei Feng. I had great time and nice collaborations with you. It was great please to learn, hear, and work with you. You made by graduate study different.

I want to thank my committee professors for your time and advise on my path of search, for your professional opinions and new ideas when my project was not flowing smoothly.

Great thanks for my parents, families, and friends, without your support I would not be able to finish my graduate studies.

Lastly and very importantly, I am so grateful for my American mom, Pilduck Lee for your selflessly and passionate care and support in every possible way of my life. It's a great luck and fortune of my life to have you.

Thank you all so very much, sincerely.

Mass Spectrometry-Based Quantitative Proteomics for Drug-Metabolizing Enzymes

TABLE OF CONTENTS

APPENDICES

Chapter I: Brief History of Mass Spectrometry-Based Absolute Quantification of Drug-Metabolizing Enzymes

TABLE OF CONTENTS

1.1 Overall Goal of Dissertation

Human hepatic DMEs play a critically important role in drug metabolism. Advances in the pharmaceutical industry combined with new drug discovery require more effort in the discovery and research of DMEs and their impact in the field. Mass spectrometry-based DME measurements bring unprecedented accuracy, simplicity, and multiplexing to drug metabolism and disposition research. This dissertation details the development of methods to quantify DMEs using MS-based targeted proteomics and how targeted proteomics can be applied to research focused on age-dependent DME expression, the establishment of cell models for CYP dependent anticancer prodrug screening, and investigation of potential drug-drug interactions. Finally, attempts are made to solve the problems of label-free DIA quantification and apply the use of this technique to quantitative DME analysis.

1.2 Significance and Nomenclature of Human Liver CYPs and FMOs

Cytochrome P450s (CYPs) are a superfamily of oxidoreductases that catalyze the oxidation of food, pharmaceuticals, environmental chemicals, and endogenous substances. CYPs exist in almost all living organisms, including animals, plants, bacteria, fungi, archaea and viruses (1). Over 350 families and 3000 unique sequences encoding this class of enzymes have been discovered, and these numbers continue to grow (2). CYPs are of critical importance to the pharmaceutical industry as they are responsible for the phase I metabolism of a majority of clinically used small molecule pharmaceuticals (3). CYPs not only metabolize and detoxify drugs, they also catalytically activate pro-toxins and pro-carcinogens. The capability of CYPs to activate toxins has been used against cancers; some chemotherapy drugs, such as ifosfamide,

cyclophosphamide and dacarbazine, are specifically activated in tumor tissues (4). CYPs are known to mediate drug-drug interactions. Patients taking amiodarone or metronidazole have an increased risk of bleeding if they also are on warfarin, as amiodarone and metronidazole are inhibitors of the warfarin-metabolizing enzymes CYP3A4 and/or CYP2C9 (5). CYP expression levels change drastically at different human developmental stages, which can affect drug clearance. For example, both diazepam and theophyline have low clearance rates in neonates, newborns and seniors, while adults have higher clearance rates. These differences can impact greatly the design of new drug dosing regimens for people of different age groups (6).

Fifty-seven CYP genes have been identified in humans. A nomenclature system helps to identify each individual isoform. All enzymes share the superfamily root symbol "CYP". The first number that follows CYP (*e.g.*, CYP1, CYP2 and CYP3) codes for the family. Enzymes falling into the same family share over 40% amino acid sequence identity. The letter that follows (*e.g.*, CYP1A and CYP1B) identifies the subfamily, in which enzymes share greater than 55% amino acid identity. The final number (*e.g.*, CYP3A4, CYP3A5 and CYP3A7) indicates the individual isoform (7). Many CYP enzymes are highly homologous; for example, CYP3A4 and CYP3A5 share 87% sequence identity and CYP4F2 and CYP4F3B share 93% sequence identity (8).

Flavin-containing monooxygenases (FMOs; EC 1.14.13.8) are flavin adenine dinucleotide (FAD)- and Nicotinamide adenine dinucleotide phosphate (NADPH)-dependent microsomal enzymes that have a significant role in the metabolism and detoxification of pharmaceuticals, endogenous substances and environmental compounds. FMOs catalyze the oxygenation of soft nucleophilic heteroatom-containing (*e.g.*, N, S and P) organic substances, converting them to more readily excreted polar metabolites. Five functional human FMO isozymes (FMO1- FMO5)

have been discovered; among these, FMOs 1, 3 and 5 are relevant to hepatic drug metabolism (9-11).

Human liver has the most CYPs and FMOs expressed; expression of these enzymes dictates drug pharmacokinetics, toxicity, and efficacy (12). Thus, quantification of these hepatic enzymes is practiced regularly in pharmaceutical research and development.

1.3 Basic Principles and Advantages of Mass Spectrometry-Based Quantification of Drug-Metabolizing Enzymes

Drug-metabolizing enzyme (DME) expression has been quantified traditionally using immuno-blotting based techniques such as an ELISA (enzyme-linked immunosorbent assay) or Western blot. These techniques are sensitive, versatile, and easy to use; however, they suffer from limited dynamic range, limited multiplexing, or lack specificity to differentiate highly homologous DME isozymes (8). Mass spectrometry (MS)-based proteomic quantification was developed to answer these challenges. Fundamentally, protein mixtures are digested by endo-proteases, yielding predictable sequences of peptides. All peptides are subjected to liquid chromatography (LC) separation and MS analysis. The peptides with sequences that are unique to the protein of interest are called signature peptides. Each signature peptide has a specific chromatographic retention time (RT) and mass-to-charge ratio (m/z) which are measured by (U)HPLC and MS, respectively. By measuring how much signature peptides are present, the concentrations of the corresponding protein can be extrapolated using known concentrations of (calibration) standards (Figure 1). This signature peptide-based protein quantification has been proven to provide a large linear quantification range, great level of multiplexing, and excellent selectivity. In addition, synthesizing signature peptides is far easier and cheaper than the production of new specific antibodies. Thus, the development of MS-based assays for protein quantification is cheaper and

faster than that of immuno-blotting-based techniques.

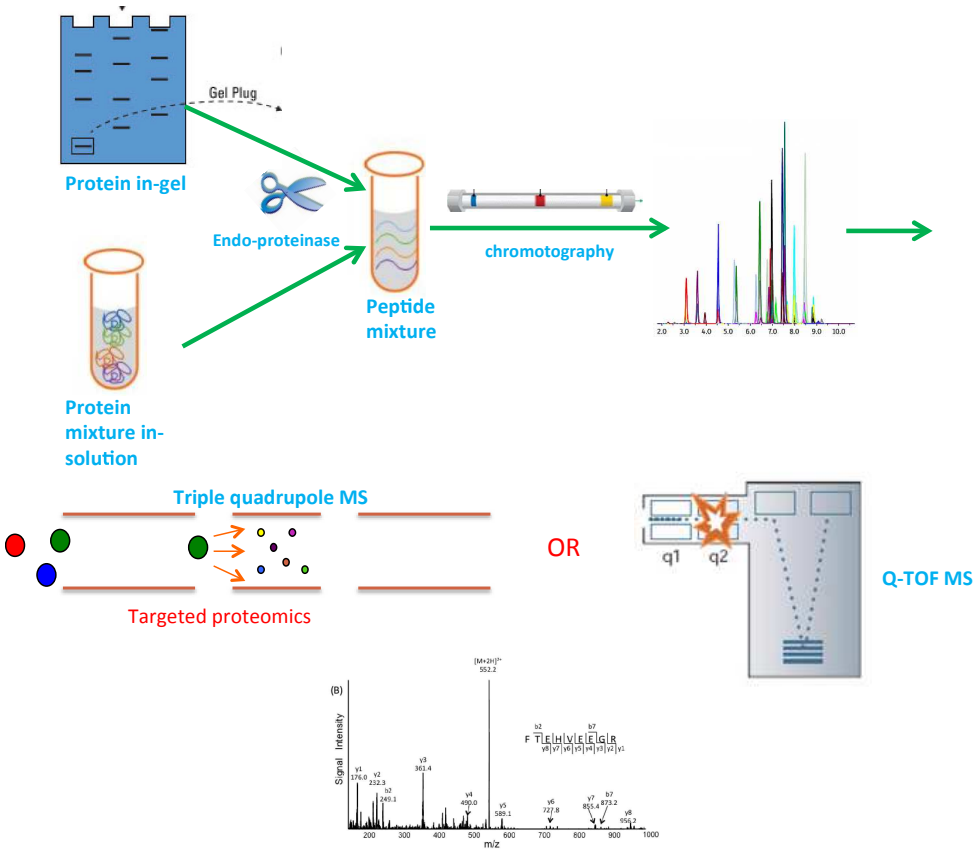

Figure 1. Illustration of basic principle of signature peptide-based MS protein quantification.

Presently, the quantification of DMEs is much more simplified and well developed than in the past. However, the simplicity and sophistication of such techniques was not achieved in a day. The sections following discuss very brief histories of the evolution of MS-based absolute quantification of DMEs.

1.4 The First Mass Spectrometry-Based Absolute Quantification of CYPs in Mice Through ICAT® Labeling

The first absolute quantification of CYP enzymes by MS was published in 2006 by Jenkins *et. al.* (13). At that time, quantification of relative protein expression via MS was enabled by isotope tagging. Control and experimental samples were labeled with light (^{12}C, ^{14}N or ^{1}H) and heavy

(^{13}C, ^{15}N or ^{2}H) isotope tags, respectively. The light and heavy tagged proteins then were mixed together, digested, and analyzed by LC-MS/MS. Signature peptides from control and experimental samples were differentiated by mass; they have similar chemical properties that result in the same retention time on LC columns and signal response in mass spectrometer. Comparison of the labeled peptides revealed relative protein abundance (14). Jenkins *et. al.* used the isotope coded affinity tag (iCAT) technique, in which the tag was incorporated with heavy ^{2}H or light ^{1}H and was conjugated to free cysteines in peptides. The tag also was linked to biotin, which has a high affinity for avidin, so that avidin affinity chromatography selectively pulled out tagged peptides. The biotin linker then was cleaved, freeing captured signature peptides for MS analysis. iCAT allowed Jenkins *et. al.* to do proteomic profiling of DMEs in mouse liver microsomes. The control and experimental samples and synthetic signature peptides were all labeled with heavy iCAT tags. The MS response of the signature peptides in the control and experimental samples were calibrated using known concentrations of synthetic peptides. The absolute quantities of eight mouse CYP proteins were measured for the first time by MS.

Despite the successful first leap in MS-based absolute CYP quantification, the limitation of the method was quite obvious. The iCAT technique only labels free thiol groups. If CYP isozymes can be differentiated only by cysteine-lacking signature peptides, they will not be able to be quantified specifically by such a technique.

1.5 Other Peptide Labeling Techniques That Attempted to Overcome iCAT Limitations

To overcome the limitation of iCAT to solely label free thiol-containing peptides, C.S. Lane *et. al.*, in 2007, attempted to label CYP peptides with ^{18}O (2). Equal amounts of microsomes from normal and chemical-treated mice were separated on a PAGE gel. Protein bands were excised and subjected to in-gel tryptic digestion. Tryptic peptides from treated animals were incubated

with $H_2{}^{18}O$-containing trypsin, while those from control animals were dissolved in $H_2{}^{16}O$-containing trypsin. Trypsin is able to incorporate ^{18}O or ^{16}O into peptides. The resulting peptides were combined and analyzed by LC-MS/MS. Peptides incorporating ^{18}O or ^{16}O were co-eluted during LC and could be differentiated only by their mass. Relative CYP expressions were measured by comparing peak areas of signature peptides that had been labeled with ^{18}O or ^{16}O. Using the $^{18}O/^{16}O$ labeling technique, C.S. Lane *et. al.* were able to identify 9 CYPs that were up-regulated and 4 CYPs that were down regulated as a result of chemical treatment. The authors did admit they were unable to differentiate some of the highly homologous mouse hepatic CYP enzymes, such as CYP2A4/5.

Another chemical labeling technique is iTRAQ (isotope tags for relative or absolute quantification). Briefly, proteins isolated from normal and treated subjects were separated on a gel; equivalent bands were excised. Following in-gel tryptic digestion, the iTRAQ reagent containing reactive groups conjugate with primary amines was added to the digests, labeling peptides on the N-terminal amines. The iTRAQ reagent also contains isotopes of different weights, allowing mixed peptides to be differentiated by MS/MS. Relative CYP expressions were measured in the same manner as by $^{16/18}O$ labeling (14).

Isotope chemical labeling MS quantifications are usually incredibly expensive, laborious, and low throughput. Simplification of these processes calls for new experimental design.

1.6 Gel-Free Absolute Quantification of Human Liver Microsomal CYP Proteins - The First MS-Based Absolute Quantification of Human Liver CYPs

A simpler solution for MS-based absolute protein quantification was published in 2003. S. A. Gerber et. al. quantified proteins and phospho-proteins in yeast using the AQUA (absolute

quantification) technique (15). Basically, stable isotope-labeled (2H, 13C or 15N) peptides that have the same sequences as targeted signature peptides of the proteins of interest were synthesized and/or chemically modified by phosphorylation, methylation, or acetylation to mimic the natural peptide. Proteins extracted from yeast were subjected to gel electrophoresis and tryptic digestion. Known concentrations of recombinant proteins were treated in the same manner and served as calibration standards. Resulting peptides were extracted from gel, spiked with stable isotope-labeled synthetic peptide counterparts and injected for LC-SRM (single reaction monitoring) using a tendon MS. SRM precursor and product ion transitions unique to the natural and synthestic peptides were selected.

The peak ratios between natural and stable isotope-labeled peptides from the yeast were compared to the ratio of recombinant calibration standards to extrapolate targeted protein concentrations.

By adopting the AQUA technique, M. Z. Wang *et. al.* first quantified human liver microsomal CYP3A4, CYP3A5, and combined CYP3A (CYP3A4, CYP3A5 and CYP3A7) by LC-MRM (multiple reaction monitoring) with absolute quantity in 2008 (8). He further simplified the technique by removing in-gel digestion and replacing it with a much simpler and faster process involving protein reduction, denaturation, alkylation and digestion that takes place in solution. By avoiding in-gel digestion, Wang *et. al.* also were able to eliminate peptide loss during gel extraction, resulting in a more accurate quantification. Good assay robustness and quantification accuracy were demonstrated by 1) consistent quantification of two signature peptides digested from the same protein and 2) a strong correlation between LC-MRM measured CYP3A quantity and Western blot densitometry measured CYP3A quantity or specific CYP3A marker substrate activities. Nowadays, gel-free LC-MRM-based targeted protein quantification has been adopted

for the measurement of UGTs, drug transporters, and many other proteins of interest. It also is considered the gold standard for protein quantification (8, 12, 16-19). Quantification method development is far cheaper and more convenient at this stage. Another variation of AQUA further reduces the cost for large numbers of targeted protein quantifications.

1.7 QconCAT, an AQUA Variant, Decreases the Cost of Large Scale Targeted Proteomic Quantification

In 2005, R. J. Beynon *et. al.* described a method by which proteins made of concatenated signature peptides (QconCAT) could be constructed in *E. coli* that grow in isotope enriched cell medium after being transformed with an artificial gene in a high expression vector (20). The constructed protein contained at least 50 stable isotope-labeled signature peptides (50-100 kDa) and served as an internal standard or calibration standards for the absolute quantification of different targeted proteins. Compared to synthesizing the same number of stable isotope-labeled peptides, QconCAT is more cost-effective. Since then, QconCAT has been used for many applications, including the proteomic quantification of *E. coli*, animals, yeast and humans, and as a universal construct protein standard (QCAL) for the calibration of different MS platforms (21-25).

In 2013, M. R. Russell *et. al.* first applied the QconCAT approach for the quantification of 15 CYPs and 10 5′-diphospho-glucuronosyltransferase (UGT) enzymes, with 2 signature peptides per targeted enzyme in the artificial protein. The initial expression of the artificial protein by the authors was unsuccessful until the peptide concatenation sequence was re-shuffled and the expression strategy changed (26).

AQUA and QconCAT gave unprecedented versatility, ease of use, and accuracy in method development for LC-MRM-based protein quantification. However, cost will remain relatively

high as long as isotope labeling is utilized. In addition, QconCAT method development is riskier due to possible expression failure.

1.8 Label-Free Data Independent Global Scale Absolute Protein Quantification with NanoUPLC-Q-TOF

In 2006, Jeffrey C. Silva *et. al*. discovered that the intensity of the top three ionizing peptides of a protein is directly correlated to the protein concentration within complex biological matrices when the label-free data independent acquisition (DIA; MS^E technique is the Waters version of DIA) strategy is applied to quadrupole-time of flight (Q-TOF) MS (27). The authors spiked six non-host recombinant proteins of known concentrations into an *E. coli* proteome digest and analyzed the results using the label-free DIA approach. The measured concentrations of the six spiked proteins differed from the theoretical concentrations by less than 15%. They also quantified well-characterized proteins in human serum and in *E. coli* digest; the label-free DIA measured values showed good correlation with historical reports.

Label-free Q-TOF MS^E-based protein quantification removes the need of isotope labeling and calibration standards, resulting in highly simplified method development and reduced experiment workload while quantifying hundreds of proteins simultaneously. Because of lower cost, greater multiplexing and simplicity, this technique has been adopted widely in the proteomic analysis of *E. coli*, plants, and human tissues and bodily fluids (28-32). However, due to several problematic factors, it has not been reported for the quantification of human liver DMEs. These factors include large variability in digestion and peptide loss with various protein cleanup methods (33-35) and sample storage (36, 37), poor peptide recovery following solid phase extraction during sample preparation or online trap LC columns, and ill-investigated quantification inconsistency between label-free MSE and labeled targeted proteomics (38-40). Identifying and solving these

problems requires a new approach for sample preparation, which will be discussed further in Chapter 6.

1.9 References

1. Lamb DC, Lei L, Warrilow AG, Lepesheva GI, Mullins JG, Waterman MR, et al. The first virally encoded cytochrome p450. J Virol. 2009;83(16):8266-9.

2. Lane CS, Wang Y, Betts R, Griffiths WJ, Patterson LH. Comparative cytochrome P450 proteomics in the livers of immunodeficient mice using 18O stable isotope labeling. Mol Cell Proteomics. 2007;6(6):953-62.

3. Evans WE, Relling MV. Pharmacogenomics: translating functional genomics into rational therapeutics. Science. 1999;286(5439):487-91.

4. Patterson LH, Murray GI. Tumour cytochrome P450 and drug activation. Curr Pharm Des. 2002;8(15):1335-47.

5. Lynch T, Price A. The effect of cytochrome P450 metabolism on drug response, interactions, and adverse effects. Am Fam Physician. 2007;76(3):391-6.

6. Yokoi T. Essentials for starting a pediatric clinical study (1): Pharmacokinetics in children. J Toxicol Sci. 2009;34 Suppl 2:SP307-12.

7. Nelson DR. The cytochrome p450 homepage. Hum Genomics. 2009;4(1):59-65.

8. Wang MZ, Wu JQ, Dennison JB, Bridges AS, Hall SD, Kornbluth S, et al. A gel-free MS-based quantitative proteomic approach accurately measures cytochrome P450 protein concentrations in human liver microsomes. Proteomics. 2008;8(20):4186-96.

9. Krueger SK, Williams DE. Mammalian flavin-containing monooxygenases: structure/function, genetic polymorphisms and role in drug metabolism. Pharmacology & therapeutics. 2005;106(3):357-87.

10. Cashman JR, Zhang J. Human flavin-containing monooxygenases. Annual review of pharmacology and toxicology. 2006;46:65-100.

11. Mitchell SC. Flavin mono-oxygenase (FMO)--the 'other' oxidase. Curr Drug Metab. 2008;9(4):280-4.

12. Chen Y, Zane NR, Thakker DR, Wang MZ. Quantification of Flavin-containing Monooxygenases 1, 3 and 5 in Human Liver Microsomes by UPLC-MRM-based Targeted Quantitative Proteomics and Its Application to the Study of Ontogeny. Drug Metab Dispos. 2016;44(7):975-83.

13. Jenkins RE, Kitteringham NR, Hunter CL, Webb S, Hunt TJ, Elsby R, et al. Relative and absolute quantitative expression profiling of cytochromes P450 using isotope-coded affinity tags. Proteomics. 2006;6(6):1934-47.

14. Wang Y, Al-Gazzar A, Seibert C, Sharif A, Lane C, Griffiths WJ. Proteomic analysis of cytochromes P450: a mass spectrometry approach. Biochem Soc Trans. 2006;34(Pt 6):1246-51.

15. Gerber SA, Rush J, Stemman O, Kirschner MW, Gygi SP. Absolute quantification of proteins and phosphoproteins from cell lysates by tandem MS. Proc Natl Acad Sci U S A. 2003;100(12):6940-5.

16. Kawakami H, Ohtsuki S, Kamiie J, Suzuki T, Abe T, Terasaki T. Simultaneous absolute quantification of 11 cytochrome P450 isoforms in human liver microsomes by liquid chromatography tandem mass spectrometry with in silico target peptide selection. J Pharm Sci. 2011;100(1):341-52.

17. Sakamoto A, Matsumaru T, Ishiguro N, Schaefer O, Ohtsuki S, Inoue T, et al. Reliability and robustness of simultaneous absolute quantification of drug transporters, cytochrome P450 enzymes, and Udp-glucuronosyltransferases in human liver tissue by multiplexed MRM/selected reaction monitoring mode tandem mass spectrometry with nano-liquid chromatography. J Pharm Sci. 2011;100(9):4037-43.

18. Michaels S, Wang MZ. The revised human liver cytochrome P450 "Pie": absolute protein quantification of CYP4F and CYP3A enzymes using targeted quantitative proteomics. Drug Metab Dispos. 2014;42(8):1241-51.

19. Peng KW, Bacon J, Zheng M, Guo Y, Wang MZ. Ethnic variability in the expression of hepatic drug transporters: absolute quantification by an optimized targeted quantitative proteomic approach. Drug Metab Dispos. 2015;43(7):1045-55.

20. Beynon RJ, Doherty MK, Pratt JM, Gaskell SJ. Multiplexed absolute quantification in proteomics using artificial QCAT proteins of concatenated signature peptides. Nat Methods. 2005;2(8):587-9.

21. Mirzaei H, McBee JK, Watts J, Aebersold R. Comparative evaluation of current peptide production platforms used in absolute quantification in proteomics. Mol Cell Proteomics. 2008;7(4):813-23.

22. Rivers J, Simpson DM, Robertson DH, Gaskell SJ, Beynon RJ. Absolute multiplexed quantitative analysis of protein expression during muscle development using QconCAT. Mol Cell Proteomics. 2007;6(8):1416-27.

23. Eyers CE, Simpson DM, Wong SC, Beynon RJ, Gaskell SJ. QCAL--a novel standard for assessing instrument conditions for proteome analysis. J Am Soc Mass Spectrom. 2008;19(9):1275-80.

24. Carroll KM, Simpson DM, Eyers CE, Knight CG, Brownridge P, Dunn WB, et al. Absolute quantification of the glycolytic pathway in yeast: deployment of a complete QconCAT approach. Mol Cell Proteomics. 2011;10(12):M111 007633.

25. Ding C, Li Y, Kim BJ, Malovannaya A, Jung SY, Wang Y, et al. Quantitative analysis of cohesin complex stoichiometry and SMC3 modification-dependent protein interactions. J Proteome Res. 2011;10(8):3652-9.

26. Russell MR, Achour B, McKenzie EA, Lopez R, Harwood MD, Rostami-Hodjegan A, et al. Alternative fusion protein strategies to express recalcitrant QconCAT proteins for quantitative proteomics of human drug metabolizing enzymes and transporters. J Proteome Res. 2013;12(12):5934-42.

27. Silva JC, Gorenstein MV, Li GZ, Vissers JP, Geromanos SJ. Absolute quantification of proteins by LCMSE: a virtue of parallel MS acquisition. Mol Cell Proteomics. 2006;5(1):144-56.

28. Cheng FY, Blackburn K, Lin YM, Goshe MB, Williamson JD. Absolute protein quantification by LC/MS(E) for global analysis of salicylic acid-induced plant protein secretion responses. J Proteome Res. 2009;8(1):82-93.

29. Bostanci N, Heywood W, Mills K, Parkar M, Nibali L, Donos N. Application of label-free absolute quantitative proteomics in human gingival crevicular fluid by LC/MS E (gingival exudatome). J Proteome Res. 2010;9(5):2191-9.

30. Farrell A, Mittermayr S, Morrissey B, Mc Loughlin N, Navas Iglesias N, Marison IW, et al. Quantitative host cell protein analysis using two dimensional data independent LC-MS(E). Anal Chem. 2015;87(18):9186-93.

31. Finamore F, Pieroni L, Ronci M, Marzano V, Mortera SL, Romano M, et al. Proteomics investigation of human platelets by shotgun nUPLC-MSE and 2DE experimental strategies: a comparative study. Blood Transfus. 2010;8 Suppl 3:s140-8.

32. Mbeunkui F, Goshe MB. Investigation of solubilization and digestion methods for microsomal membrane proteome analysis using data-independent LC-MSE. Proteomics. 2011;11(5):898-911.

33. Cunningham R, Wang J, Wellner D, Li L. Investigation and reduction of sub-microgram peptide loss using molecular weight cut-off fractionation prior to mass spectrometric analysis. J Mass Spectrom. 2012;47(10):1327-32.

34. Lin Y, Liu Y, Li J, Zhao Y, He Q, Han W, et al. Evaluation and optimization of removal of an acid-insoluble surfactant for shotgun analysis of membrane proteome. Electrophoresis. 2010;31(16):2705-13.

35. Speicher KD, Kolbas O, Harper S, Speicher DW. Systematic analysis of peptide recoveries from in-gel digestions for protein identifications in proteome studies. J Biomol Tech. 2000;11(2):74-86.

36. Kristensen K, Henriksen JR, Andresen TL. Adsorption of cationic peptides to solid surfaces of glass and plastic. PLoS One. 2015;10(5):e0122419.

37. Horinek D, Serr A, Geisler M, Pirzer T, Slotta U, Lud SQ, et al. Peptide adsorption on a hydrophobic surface results from an interplay of solvation, surface, and intrapeptide forces. Proc Natl Acad Sci U S A. 2008;105(8):2842-7.

38. Al Feteisi H, Achour B, Rostami-Hodjegan A, Barber J. Translational value of liquid chromatography coupled with tandem mass spectrometry-based quantitative proteomics for in vitro-in vivo extrapolation of drug metabolism and transport and considerations in selecting appropriate techniques. Expert Opin Drug Metab Toxicol. 2015;11(9):1357-69.

39. Achour B, editor A Cross-Laboratory Comparison of Enzyme and Transporter Abundance Quantification. 2015 AAPS Annual Meeting and Exposition; 2015 October 29; Orlando, FL, USA.

40. Wegler C, editor Quantification of ADME Proteins: An Inter-laboratory Comparison. AAPS Annual Meeting and Exposition; 2015 October 29th; Orlando, FL, USA.

Chapter II: Development of Quantification Method for FMOs and CYP2Cs in Human Liver Microsomes Using UPLC-MRM-Based Targeted Proteomics

TABLE OF CONTENTS

LIST OF TABLES

LIST OF FIGURES

2.1 Introduction

Flavin-containing monooxygenases (FMOs; EC 1.14.13.8) are FAD- and NADPH-dependent microsomal enzymes that have a significant role in the metabolism and detoxification of pharmaceutical, endogenous substances and environmental compounds. FMOs catalyze the oxygenation of soft nucleophilic heteroatom-containing (*e.g.*, N, S and P) organic substances, converting them to more readily excreted polar metabolites. Five functional human FMO isozymes have been discovered; among these, FMOs 1, 3 and 5 are relevant to hepatic drug metabolism (1-3).

CYP2Cs are another important subfamily among human hepatic DMEs. It occupies close to one fifth of total human hepatic CYP expression and involved in the metabolism of 20% of small molecule pharmaceuticals (4, 5). There are four members in the CYP2C subfamily—CYP2C8, CYP2C9, CYP2C18, and CYP2C19. Among them, CYP2C9 and CYP2C19 are relatively more important as they are responsible for the clearance of many frequently used drugs. For example, CYP2C9 oxidizes tolbutamide, phenytoin, warfarin, ibuprofen, and diclofenac (6). CYP2C19 metabolizes omeprazole, diazepam, and some barbiturates (5).

Traditionally, FMO enzyme quantification has relied on isozyme-specific antibody-based immunoquantification via Western blots. For absolute quantification, FMO content has been determined based on FAD content, the tightly-bound prosthetic group required for the catalytic activity of FMO holoproteins (7). Recombinant FMOs (*e.g.*, heterologously expressed in baculovirus-infected insect cells or Supersomes) have served as calibration standards (8, 9). Thus, previous studies have reported the quantification of FMO holoproteins, rather than total FMO proteins (*i.e.*, holoprotein + apoprotein). CYP2C9 and CYP2C19 have been quantified by

both Western blot and MS-based targeted proteomic approaches, but the quantification was not thoroughly verified by the correlation between the quantified amount and enzyme specific marker substrate activities (10).

To overcome the common limitations of immunoquantification (*i.e.*, cross-reactivity, dynamic range, reproducibility and multiplexity), liquid chromatography-tandem mass spectrometry (LC-MS/MS)- and multiple reaction monitoring (MRM)-based targeted quantitative proteomic methods have been developed for the absolute quantification of cytochrome P450s (CYPs), UDP-glucuronosyltransferases (UGTs) and membrane drug transporters (4, 11-13). However, targeted quantitative proteomic methods for FMOs have yet to be reported. The term "absolute" quantification in these publications and the report herein refers to a type of proteomic quantification that produces protein concentration or amount, rather than "relative" protein expression profiles. A targeted quantitative proteomic method for absolute protein quantification relies on the use of either synthetic signature peptides of known concentration or signature peptides derived from the tryptic digest of target proteins of known concentration as calibration standards. The selection of appropriate signature peptides involves the *in silico* tryptic digestion of target proteins, followed by evaluation of the resulting candidate peptides based on several selection criteria to ensure specificity, stability and digestion efficiency (4, 14, 15). Candidate signature peptides (usually at least two for each protein) then can be synthesized and used to tune the MS (typically, a triple-quadrupole MS) for optimal MRM detection. However, some candidate signature peptides may not perform optimally due to poor digestion efficiency, chromatography or ionization during MS analysis, therefore rendering expensive signature peptides useless. Hence, it is desirable to incorporate an additional process(es) to verify candidate signature peptides following *in silico* prediction but prior to their synthesis.

The objective of the current chapter was to develop an UPLC-MRM-based targeted quantitative proteomic method for the absolute quantification of FMO1, FMO3 and FMO5 in human liver microsomes (HLM) and evaluate the quantification method by correlating quantified FMOs and CYP2Cs amounts to their specific substrate activities.

2.2 Materials and Methods

2.2.1 Chemicals, Enzymes, and Liver Tissues. Optima-grade acetonitrile, water, formic acid, and acetic acid were obtained from Fisher Scientific (Pittsburgh, PA). Ammonium bicarbonate, dimethylsulfoxide, dithiothreitol, iodoacetamide, and cimetidine were purchased from Sigma-Aldrich (Saint Louis, MO). Cimetidine sulfoxide was acquired from Abcam Biochemicals (Cambridge, UK). Famotidine sulfoxide was acquired from Toronto Research Chemicals (Toronto, Canada). Recombinant human FMO1, FMO3, FMO5, CYP2C9, and CYP2C19 Supersomes, prepared from baculovirus-infected insect cells expressing human FMO enzymes, were purchased from Corning Gentest (Woburn, MA). The FMO concentration (pmol/mL and pmol/mg protein) of each Supersomes, based on the FAD content determined by an HPLC-fluorescence method or by CO difference spectrum assay (7, 16), was provided by the supplier. Control Supersomes (Corning Gentest) contained microsomes from insect cells infected with wild-type baculovirus. Synthetic unlabeled AQUA Ultimate-grade signature peptides (5 pmol/μL ± 5% by amino acid analysis) were ordered from Thermo Scientific (Ulm, Germany). Peptide purity (>97%), determined by RP-HPLC UV (detection wavelength of 215 nm) and MALDI-TOF MS, was provided by the manufacturer. Synthetic ^{13}C and ^{15}N stable isotope-labeled crude signature peptides also were acquired from Thermo Scientific. All synthetic peptide sequences

were confirmed by MS/MS fragmentation analysis using a Waters Xevo TQ-S triple-quadrupole MS (Milford, MA). Sequencing-grade modified trypsin (cat. # V5113, lot 104493) was purchased from Promega (Madison, WI). Pooled HLM (XTreme 200) and nine individual adult donor HLM (Table 1) were purchased from XenoTech, LLC (Lenexa, KS). Liver tissues from seven fetal (14-20 weeks gestation) donors and sixteen pediatric (aged 5 months-10 years) donors were obtained from the NICHD Brain and Tissue Bank for Developmental Disorders (Contract #HHSN275200900011C, Ref. No. NO1-HD-9-0011; Baltimore, MD) under an approved UNC-Chapel Hill IRB and were used to prepare fetal and pediatric HLM (Table 1).

Table 1. Donor information for individual donor human liver microsomes.

Group	Sample	Gender	Age	Race
Adult	H0024	Male	47 years	Caucasian
	H0079[a]	Female	56 years	Caucasian
	H0081[b]	Female	67 years	Caucasian
	H0134	Female	61 years	Caucasian
	H0199	Female	48 years	African American
	H0232	Male	43 years	Caucasian
	H0246	Female	40 years	Caucasian
	H0292	Male	65 years	African American
	H0307	Male	39 years	Caucasian
Fetal[c]	F1	Female	18 weeks	African American
	F5	Male	15 weeks	African American
	F6	Female	20 weeks	African American
	F7	Male	16 weeks	African American
	F8	Male	15 weeks	African American
	F9	Male	19 weeks	Caucasian
	F10	Male	16 weeks	African American
Pediatric	P1	Male	6 years	Caucasian
	P2	Male	4 years	Caucasian
	P3	Male	2 years	African American
	P4	unknown	2 years	unknown
	P5	unknown	1 years	unknown
	P6	unknown	4 months	unknown
	P7	Male	4 years	Caucasian
	P8	Male	8 years	Caucasian
	P9	Male	2 years	African American
	P10	Female	9 years	Hispanic
	P11	Female	111 days	Caucasian
	P12	Female	92 days	Caucasian
	P13	Male	63 days	African American
	P14	Female	57 days	African American
	P15	Female	97 days	African American
	P16	Male	71 days	African American

a 5-6 cigarettes/day for 40 years
b 1 pack/day for 40 years and 1 beer/month
c age for fetal donors is gestational age

2.2.2 *In Silico* Selection of FMO, CYP2C Signature Peptides. Candidate tryptic signature peptides for FMO quantification were selected *in silico* using criteria described previously (4, 14, 15). The selected candidate peptides for each FMO protein are listed in Table 2.

Table 2. Candidate signature peptides identified for human FMO1, FMO3, FMO5, CYP2C9 and CYP2C19 based on in silico selection criteria.

Protein	Candidate Signature Peptide	Peptide Sequence	Start-End[a]	Average Mass MH+ (Da)[b]
FMO1	**FMO1_pep1_L**	**FTEHVEEGR**	**43-51**	**1104.2**
	FMO1_pep2_L	**VEDGQASLYK**	**345-354**	**1110.2**
	FMO1_pep3_L	HIQFK	103-107	672.8
	FMO1_pep4_L	HPDIFK	178-183	756.9
	FMO1_pep5_L	EFVLNDELPGR	281-291	1289.4
	FMO1_pep6_L	VAIVGAGVSGLASIK	42509	1342.6
	FMO1_pep7_L	VVQESPSPFESFLK	503-516	1594.8
FMO3	**FMO3_pep1_L**	**FSDHAEEGR**	**43-51**	**1048.1**
	FMO3_pep2_L	NNEIILFK	347-354	991.2
	FMO3_pep3_L	VAIIGAGVSGLASIR	42509	1384.7
	FMO3_pep4_L	**SNDIGGLWK**	**34-42**	**990.1**
	FMO3_pep5_L	TFVSSVNK	108-115	882
	FMO3_pep6_L	WAAQVIK	388-394	816
	FMO3_pep7_L	LVGPGQWPGAR	473-483	1138.3
	FMO3_pep8_L	NAILTQWDR	484-492	1117.3
FMO5	**FMO5_pep1_L**	**FQENPEEGR**	**44-52**	**1106.1**
	FMO5_pep3_L	IAVIGGGVSGLSSIK	42541	1358.6
	FMO5_pep4_L	TDDIGGLWR	35-43	1033.1
	FMO5_pep6_L	**WATQVFK**	**388-394**	**880**
	FMO5_pep7_L	VQGPGK	475-480	585.7
	FMO5_pep8_L	IISGLVK	293-299	729.9
	FMO5_pep9_L	GAWILNR	218-224	823
	FMO5_pep10_L	AILTTDDR	487-494	905
	FMO5_pep11_L	LTHFIWK	240-246	945.2
	FMO5_pep12_L	VGDYGYPADVLFSSR	225-239	1646.8
CYP2C9	**CYP2C9_PEP1_L**	**GIFPLAER**	**98-105**	**903.2**
	CYP2C9_PEP2_L	**SLVDPK**	**460-465**	**656.8**
	CYP2C9_PEP3_L	GTTILISLTSVLHDNK	384-399	1712.6
CYP2C19	**CYP2C19_PEP1_L**	**GHFPLAER**	**98-105**	**917.2**
	CYP2C19_PEP3_L	GTTILTSLTSVLHDNK	384-399	1692.4

[a] Start and end residue positions of peptides in the corresponding full-length protein.
[b] Theoretical average mass of mono-protonated molecular ion.
[c] Signature peptides used in this study are highlighted in bold font.

2.2.3 Trypsin Digestion. The tryptic digestion of FMO Supersomes and HLM was performed as described previously with minor modifications (4, 15). Briefly, protein samples (30 μg) were reduced in ammonium bicarbonate buffer (pH 8.0, 50 mM final concentration) containing dithiothreitol (4 mM final concentration) and heated at 60°C for 60 min to denature the proteins. After cooling to room temperature, the samples (90 μL total volume) were alkylated with iodoacetamide (10 mM final concentration) for 20 min in the dark prior to digestion with 1 μg trypsin at 37°C for 4 h unless stated otherwise. All reactions were carried out in Eppendorf Protein LoBind microcentrifuge tubes (Hamburg, Germany) to minimize protein and peptide loss due to binding. Solvent evaporation during the incubations was minimized by sealing the capped tubes with parafilm and applying pressure with an aluminum block. To optimize the trypsin digestion protocol, different digestion times (0.5, 1, 2, 4, 6, 8, 12 and 24 h) and protein-to-trypsin ratios (10, 20, 30, 40, 50, 60, 80 and 100:1) were examined. Reactions were cold-quenched with storage at -80°C. A mixture of stable isotope-labeled signature peptides (1 μL; internal standards) was spiked into the thawed samples prior to loading into a 6°C autosampler.

2.2.4 Signature Peptide Verification by Post-*In Silico* Product Ion Screening. After vortexing and centrifugation (16,000 *g* for 10 min at 4°C), the supernatants (10 μL) of the quenched digestion mixtures underwent UPLC-MS/MS analysis. The UPLC-MS/MS instrument, consisting of a Waters Acquity UPLC I-class binary solvent manager coupled with a Waters Xevo TQ-S triple-quadrupole MS, was operated under positive electrospray ion mode. Chromatographic separation of the peptides was carried out on a reversed-phase column (Waters UPLC BEH-C18, 1.7 μm, 2.1 x 100 mm), fitted with an in-line column filter and a VanGuard™ guard-column (Waters). The mobile phases consisted of (A) water containing 0.1% (v/v) formic acid and (B) acetonitrile containing 0.1% (v/v) formic acid. A 13.5 min gradient (0.4 mL/min)

began with 2% B held for 1 min, followed by an increase to 15% B over 2 min, and to 30% B over the next 7 min. The column was washed with 95% B for 1.5 min and then re-equilibrated with 2% B for 2 min prior to the next injection.

To detect the *in silico*-selected candidate signature peptides, product ion scans were set up using selected precursor ions corresponding to the doubly protonated ions of the candidate peptides in the Q1 quadrupole, fragmenting these precursor ions with a collision energy ramp (15-40 V) in the Q2 quadrupole, and mass analysis of the product ions in the Q3 quadrupole mass analyzer under a scan rate of 5000 amu/s. Extracted product ion (EPI) chromatograms of all the possible *y* ions of each candidate peptide were generated using Masslynx (Version 4.1; Waters) to allow visual inspection for product ion screening. A salient peak shared by most or all *y* ion EPI chromatograms verified the detection of the corresponding signature peptide. Upon detection verification, the signature peptide sequences were sent for synthesis (Thermo Scientific).

2.2.5 UPLC-MRM Analysis. Lyophilized stable isotope-labeled signature peptides were dissolved in 1 mL of 1:1 (v/v) acetonitrile:water solution. The solution was diluted further to approximately 2-4 μg/mL and then infused into the Xevo TQ-S MS at 5 μL/min with an LC flow of 50% B at 0.4 mL/min. MRM parameters were optimized using IntelliStart (Waters) under positive electrospray ion mode: capillary voltage, 1.5 kV; cone voltage, 40 V; source offset, 40 V; dissolvation temperature, 500°C; dissolvation gas, 1000 L/h; nebulizer gas, 7 bar. The optimum collision energy and precursor/production masses for the signature peptides are summarized in Table 3. UPLC-MRM quantification was performed using the peak area ratios of signature peptides to corresponding stable isotope-labeled signature peptides (internal standards).

2.2.6 Preparation of Calibration Standards. Two types of calibration standards were prepared for the absolute quantification of FMOs in HLM. First, recombinant FMO1, FMO3, FMO5, CYP2C9, and CYP2C19 Supersomes of known concentrations (based on FAD and heme content) were used to build calibration standards. Quality controls (QCs), consisting of FMO Supersomes at 0.2, 1 and 10 pmol/digestion, were prepared in triplicate. All recombinant protein standards and QCs were denatured, alkylated and trypsin-digested as described above, prior to UPLC-MRM analysis. Due to the varying amount of total proteins in the standards, additional trypsin (2 μg total) was used to keep the protein:trypsin ratio ≤ 30:1 in the high concentration standards. Second, synthetic signature peptides of known concentrations (based on amino acid analysis) were used to build calibration standards (0.02 to 20 pmol/digestion). To normalize total protein loading, control Supersomes (30 μg) were spiked into the peptide standards. The spiked peptide standards also were denatured, alkylated and trypsin-digested prior to UPLC-MRM analysis. The lower limit of quantification was defined as the lowest standard concentration with signal-to-noise ratio > 5 and acceptable precision and accuracy (within 20%).

2.2.7 FMO and CYP2C Marker Substrate Activities. Cimetidine sulfoxidation is considered specific to the activities of FMO enzymes. The cimetidine-FMO functional activity was measured as described previously (17, 18). Cimetidine (1 mM; reported K_m values are 4 mM for FMO3 and >10 mM for FMO5) was pre-incubated with HLM (0.1 mg/mL) in a phosphate buffer (pH 7.4, 100 mM) containing 3.3 mM $MgCl_2$ for 5 min at 33°C. No FMO activity lost was detected during the 5 min of FMO cimetidine pre-incubation (data not shown). Reactions (200 μL final volume) were initiated by the addition of 1/10 the reaction volume of NADPH solution (1 mM final concentration). Aliquots (10 μL each) were removed from each reaction at 1 and 5 min and transferred to tubes containing ice-cold acetonitrile (300 μL) and famotidine sulfoxide

(10 nM; internal standard). Quenched reaction mixtures were centrifuged (2250 *g* for 20 min at 4°C) and the resulting supernatants (100 μL) evaporated under nitrogen at 50°C. The evaporation was very brief to reduce the organic content. Complete dryness resulted in poor reconstitution and bad measurement reproducibility. The evaporated samples were reconstituted in water (150 μL) prior to UPLC-MS/MS quantification of cimetidine sulfoxide using the Xevo TQ-S triple-quadrupole MS operated under positive electrospray ion mode. Analytes were separated on a reversed-phase analytical column (Thermo Scientific Aquasil C18, 2.1 × 50 mm, 3 μm; Bellefonte, PA). The gradient (0.4 mL/min) began at 0% B for 0.5 min, then quickly increased to 5% B and was held there for 3 min. The column was washed with 100% B for 1 min and re-equilibrated at 0% B for 0.5 min prior to the next injection. UPLC-MRM quantification was performed using the peak area ratios of cimetidine sulfoxide to famotidine sulfoxide. Cimetidine sulfoxide calibration standards ranged from 0.1 to 100 μM. Cimetidine sulfoxidation rates were determined from the amount of metabolite generated between the 1 and 5 min reaction times. Cimetidine sulfoxide formation was linear for a minimum of 30 min under the described conditions (data not shown). Since FMO enzymes are heat labile in the absence of NADPH, their stability was examined during the pre-incubation (5 min at 33°C) with substrate only. Results showed no significant difference in cimetidine sulfoxidation activities of recombinant FMO1, FMO3, and the pooled HLM between pre-incubation with substrate cimetidine only and pre-incubation with NADPH (data not shown), indicating stability of FMO enzymes during the pre-incubation with substrate only. The CYP2C9 and CYP2C19 specific activities were provided from vendor.

2.2.8 Data Analysis. The final FMO and CYP2C protein concentrations were the average value determined using two signature peptides for each protein. All average values were calculated as

the mean. The slope and Y-intercept values were determined by least-square linear regression analysis. Student's *t* tests (two-tailed, unpaired) were used to compare the pairs of signature peptides. All data analyses were performed using GraphPad Prism (v. 5.0; San Diego, CA).

2.3 Results

2.3.1 Verification of FMO Signature Peptides by Post-*In Silico* Product Ion Screening. After the initial *in silico* selection of human FMO3 signature peptides, eight candidate peptides (Table 2) satisfied every selection criteria described previously (4, 14). To select the final signature peptides (two for each protein) from the candidate peptides, recombinant FMO3 was reduced, alkylated and trypsinized, and the resulting digest separated on a UPLC analytical column. Analysis was completed through product ion screening of the doubly charged ions of the candidate peptides. Representative EPI chromatograms of predicted *y* ions for the two final FMO3 signature peptides selected for use in this study (FMO3_pep1_L and FMO3_pep4_L; Table 1) are shown in Figures 1A and 1B, respectively. The signature peptides produced salient peaks in each EPI chromatogram (2.5 min peak for FMO3_pep1_L and 5.5 min peak for FMO3_pep4_L) and the product ion mass spectra integrated across the peaks matched each peptide sequence (Figures 1C and 1D). In addition, EPI chromatograms of predicted *y* ions for the remaining six FMO3 candidate signature peptides are shown in Figure 1. Likewise, EPI chromatograms of predicted *y* ions for the final FMO1, FMO5, CYP2C9, and CYP2C19 signature peptides (Table 3) also were examined and verified for optimal UPLC-MRM detection (data not shown).

Figure 1.

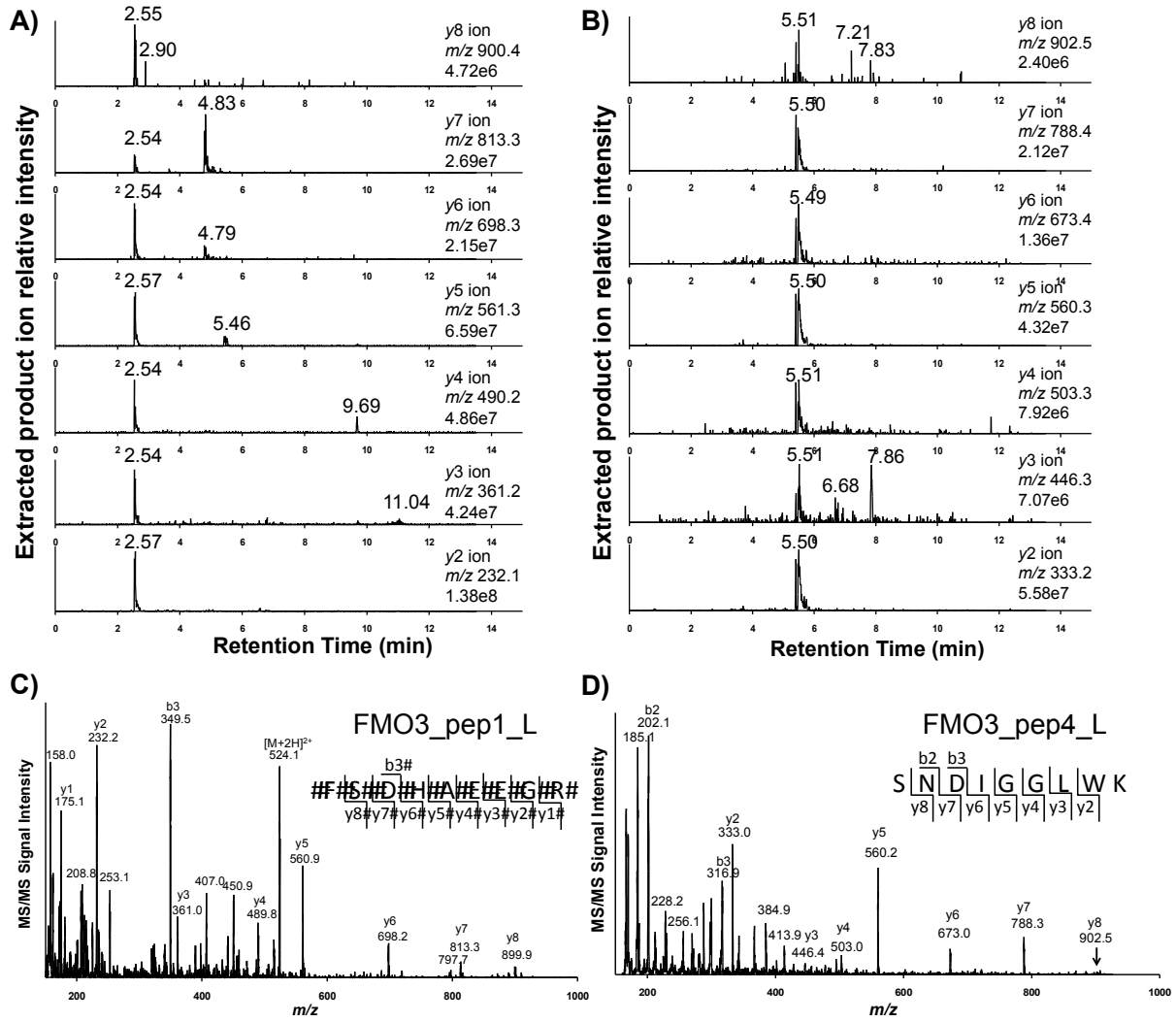

Figure 1. Post-*in silico* product ion screening of FMO3 signature peptides (FMO3_pep1_L and FMO3_pep4_L). Extracted product ion chromatograms of predicted *y* ions (**A** and **B**) and MS/MS spectra (**C** and **D**) of the detected FMO3 signature peptides are shown following product ion screening analysis of a recombinant FMO3 Supersomes tryptic digest (40.5 pmol FMO or 50 µg total protein). FMO3_pep1_L and FMO3_pep4_L eluted at 2.5 and 5.5 min, respectively.

Table 3. Signature peptides for human FMO1, FMO3, FMO5, CYP2C9, and CYP2C19.

Protein	Signature Peptide[a]	Peptide Sequence[b]	Start-End[c]	Average Mass MH^+ (Da)[d]	MRM (m/z)	
					Precursor Ion	Product Ion
FMO1	FMO1_pep1_L	FTEHVEEGR	43-51	1104.2	552.5	589.3 (y5)
	FMO1_pep1_H	FTEHVEEG(R)		1114.2	557.5	599.3 (y5)
	FMO1_pep2_L	VEDGQASLYK	345-354	1110.2	555.5	881.5 (y8)
	FMO1_pep2_H	VEDGQASLY(K)		1118.2	559.6	889.5 (y8)
FMO3	FMO3_pep1_L	FSDHAEEGR	43-51	1048.1	524.5	561.3 (y5)
	FMO3_pep1_H	FSDHAEEG(R)		1058.1	529.5	571.3 (y5)
	FMO3_pep4_L	SNDIGGLWK	34-42	990.1	495.4	560.3 (y5)
	FMO3_pep4_H	SNDIGGLW(K)		998.1	499.4	568.3 (y5)
FMO5	FMO5_pep1_L	FQENPEEGR	44-52	1106.1	553.4	587.3 (y5)
	FMO5_pep1_H	FQENPEEG(R)		1116.1	558.4	597.3 (y5)
	FMO5_pep6_L	WATQVFK	388-394	880	440.5	622.4 (y5)
	FMO5_pep6_H	WATQVF(K)		888	444.5	630.4 (y5)
CYP2C9	CYP2C9_pep1_L	GIFPLAER	98-105	903.2	452.1	585.3
	CYP2C9_pep1_H	GIFPLAE(R)		913.1	456.8	595.3
	CYP2C9_pep2_L	SLVDPK	460-465	656.8	328.9	456.3
	CYP2C9_pep2_H	SLVDP(K)		666.8	333.9	466.3
CYP2C19	CYP2C19_pep1_L	GHFPLAER	98-105	917.2	459.1	585.3
	CYP2C19_pep1_H	GHFPLAE(R)		937.1	469.0	595.3

[a] L and H indicate unlabeled and stable isotope-labeled peptides, respectively.

[b] Stable isotope-labeled amino acid residues are included in parentheses.

[c] Start and end residue positions of peptides in the corresponding full-length protein.

[d] Theoretical average mass of mono-protonated molecular ion.

After identification and verification of the predicted signature peptides, unlabeled signature peptides and corresponding ^{13}C and ^{15}N stable isotope-labeled signature peptides (Table 3) were synthesized and used for the development and optimization of an UPLC-MRM method. This method allows for the multiplexed detection and quantification of FMOs and CYP2Cs in HLM. Representative UPLC-MRM chromatograms of signature peptides in tryptic digests of adult HLM and fetal HLM are shown in Figure 2.

Figure 2.

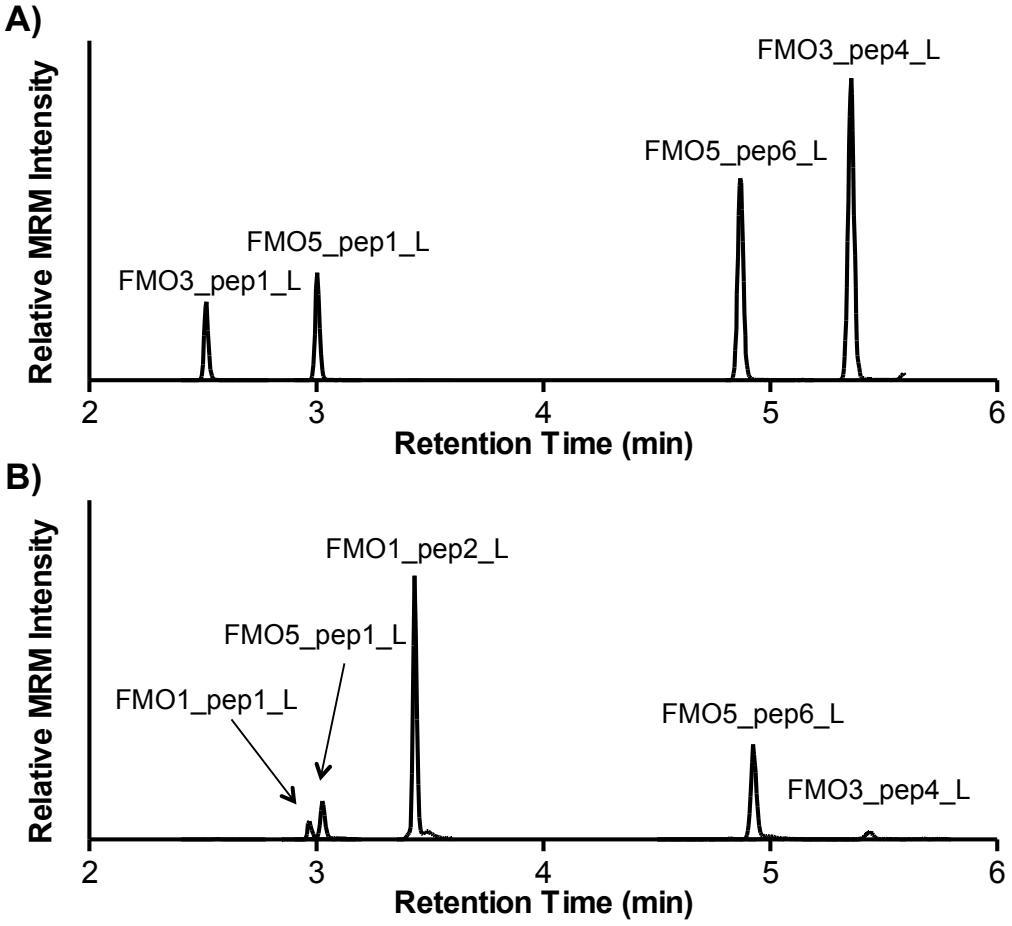

Figure 2. Representative MRM chromatograms of FMO signature peptides in tryptic digests of (A) adult and (B) fetal HLM. Digestion mixtures, containing 30 µg HLM and 1 µg trypsin, were incubated for 4 h at 37°C prior to UPLC-MRM analysis.

2.3.2 Effects of Trypsin Digestion Time and Protein:Trypsin Ratio. To optimize trypsin digestion conditions and determine the dynamic range, the effects of digestion time and protein:trypsin ratio on the absolute quantification of FMOs and CYP2Cs in pooled HLM were evaluated using the developed UPLC-MRM method. The relative UPLC-MRM signals of the signature peptides reached a maximum after 4 h of digestion and plateaued (or decreased slightly in some cases) thereafter (Figures 3A, 3B, and 3C). Due to low expression of FMO1 in pooled HLM, only one of the two FMO1 signature peptides was detected and evaluated (Figure 3B). As a result, tryptic digestion was carried out for 4 h for the remainder of the study. In addition, the relative UPLC-MRM signals of the signature peptides increased linearly with respect to HLM protein loading between 10 μg to 100 μg when 1 μg trypsin was used (Figures 3D, 3E, and 3F); however, a slight downward deviation was noticed above 50 μg of HLM protein. Thus, optimized trypsin digestion conditions, 4 h digestion and 30:1 protein:trypsin ratio, were selected and utilized for the absolute quantification of FMO1, FMO3, FMO5, CYP2C9, and CYP2C19 in HLMs.

Figure 3.

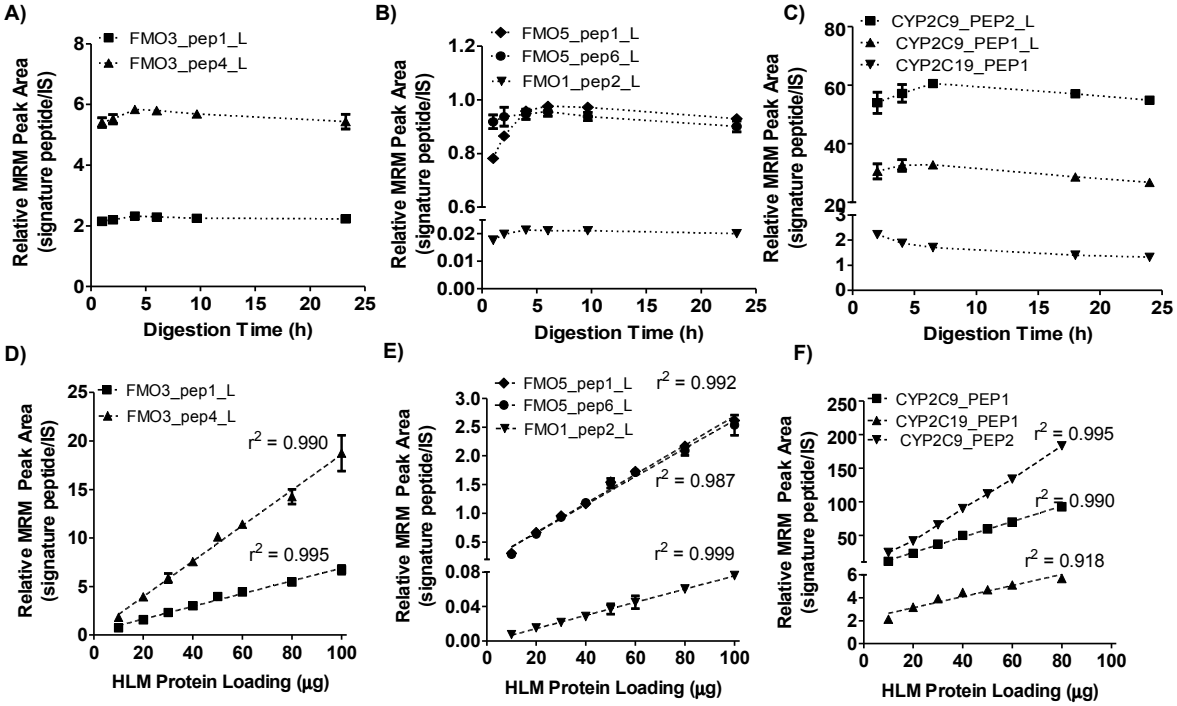

Figure 3. Effects of trypsin digestion time and HLM protein loading on the UPLC-MRM signals of FMO and CYP2C signature peptides derived from pooled HLM. The UPLC-MRM peak areas of FMO and CYP2C signature peptides were normalized by those of corresponding stable isotope-labeled signature peptides spiked in as IS. For the digestion time study (**A** and **B**), each reaction contained 30 µg of pooled HLM and 1 µg of trypsin. For the protein loading study (**C** and **D**), each reaction contained 1 µg of trypsin and varying amounts of HLM proteins. Symbols and error bars represent the mean and standard deviation of triplicate determinations. In many cases, error bars are too small to be seen. Dashed lines (**C** and **D)** represent the best-fit lines of least-square linear regression analysis.

2.3.3 Absolute Quantification of FMO3 and FMO5 in HLM and Correlation to Marker Substrate Activity. Similar to the immunoquantification and targeted proteomic quantification of CYPs (4, 15), recombinant FMO Supersomes of known concentrations were used initially to create calibration standards. The concentrations of the recombinant FMO Supersomes, based on FAD content, were provided by the vendor. The calibration curves for each recombinant FMO Supersome (0.01 to 4 pmol/ digestion; 10-12 concentrations) demonstrated good linearity (r^2 > 0.99). Using 30 μg of HLM, the observed lower limit of quantification for the three FMOs was 0.33 pmol/mg HLM protein. The intraday accuracy (percent deviation) and precision (CV) of the analytical method, based on QC samples, were within 15%.

Method coherence was evaluated by comparing protein quantification results from two different signature peptides of the same protein (*i.e.*, CYP2C9_pep1_L *vs*. CYP2C9_pep2_L; FMO3_pep1_L *vs*. FMO3_pep4_L and FMO5_pep1_L *vs*. FMO5_pep6_L). In each case, a strong correlation, near-unity slope and near-zero Y-intercept were observed (Figures 4B, 4C, and 4D), indicating consistent protein quantification results between the different signature peptides. In addition, good coherence was observed for two FMO1 signature peptides when fetal HLM were analyzed (Figure 4A; described below). As a result, final protein concentrations were calculated as the average of the quantification results from the two signature peptides.

Figure 4.

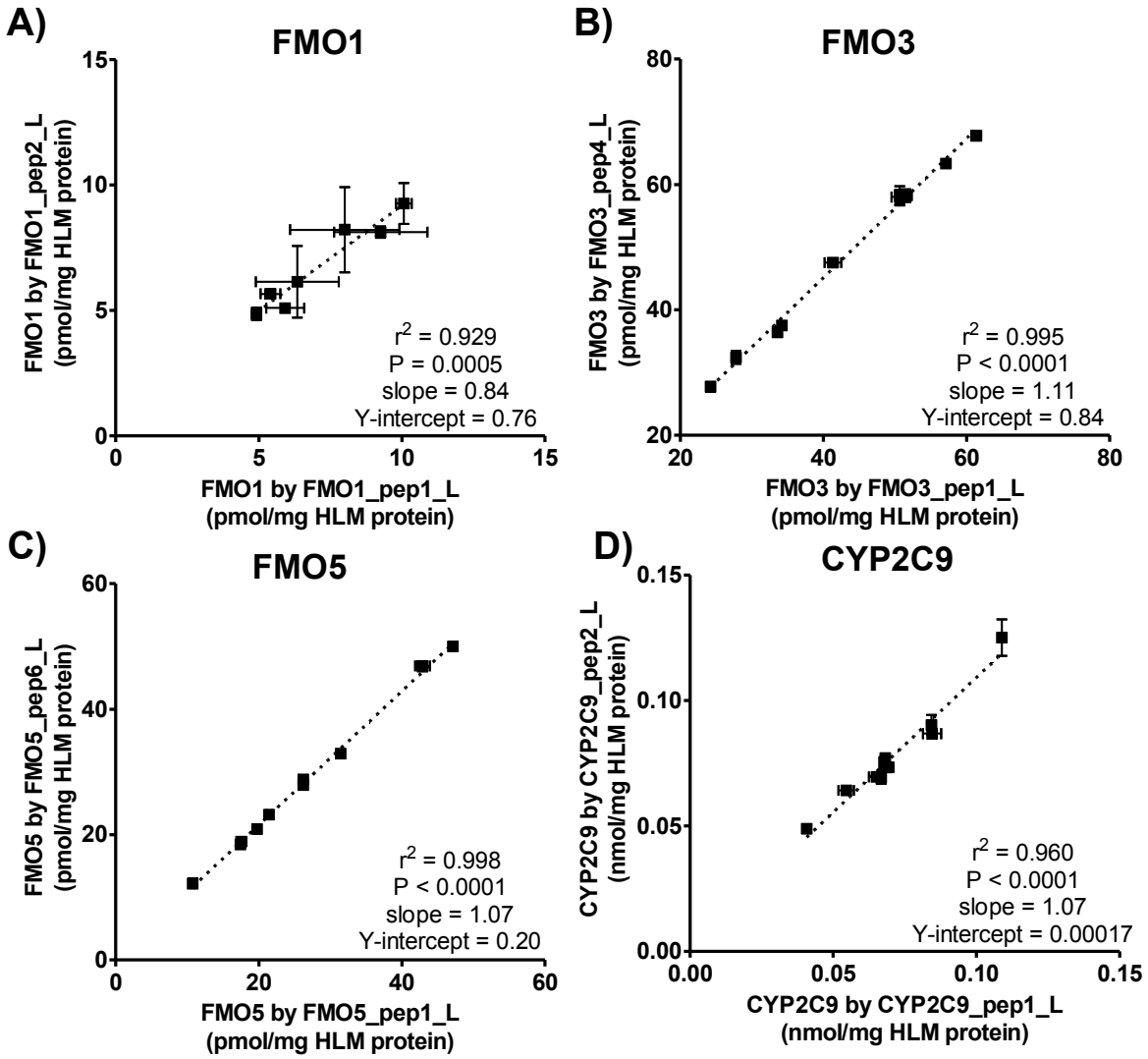

Figure 4. Coherence analysis of FMO and CYP2C9 protein quantification by UPLC-MRM-based targeted proteomic approach using different signature peptides and recombinant FMO Supersomes-generated calibration standards. Quantification of FMO1 was performed using the fetal HLM panel, whereas quantification CYP2C9, FMO3, and FMO5 was performed using the adult HLM panel. Symbols and error bars represent the mean and standard deviation of triplicate determinations for an individual donor HLM. In many cases, error bars are too small to be seen. Dotted lines represent the best-fit lines of least-square linear regression analysis.

Using a panel of adult HLM (n = 9 individual donors and 1 pooled), the protein concentrations of the three FMOs were determined using the developed targeted quantitative proteomic method. The FMO1 concentration in adult HLM was below the lower limit of quantification (<0.33 pmol/mg HLM protein). The final FMO3 and FMO5 average protein concentrations (range and 95% confidence interval [CI]) were 46 (26 – 65 and 36 – 56) and 27 (11.5 – 49 and 18.5 – 36) pmol/mg HLM protein, respectively. The CYP2C9 and CYP2C19 average protein concentrations (range) were 71.0 (41.8-108.8) and 6.4 (1.1- 16.8) pmol/mg HLM. Furthermore, cimetidine sulfoxidation activities were measured in the HLM panel and compared to FMO protein concentrations. A strong correlation was observed between cimetidine sulfoxidation activity and FMO3 protein concentration (r^2 = 0.86, P = 0.0001; Figure 5A), but not FMO5 protein concentration (r^2 = 0.30, P = 0.103; Figure 5B). Specific activities of CYP2C9 and CYP2C19 are provided from the vendor. Strong quantity and activity correlations were also seen in both CYP2C9 (r^2 = 0.96, P < 0.0001; Figure 5D) and CYP2C19 (r^2 = 0.94, P = 0.0001; Figure 5C).

Figure 5.

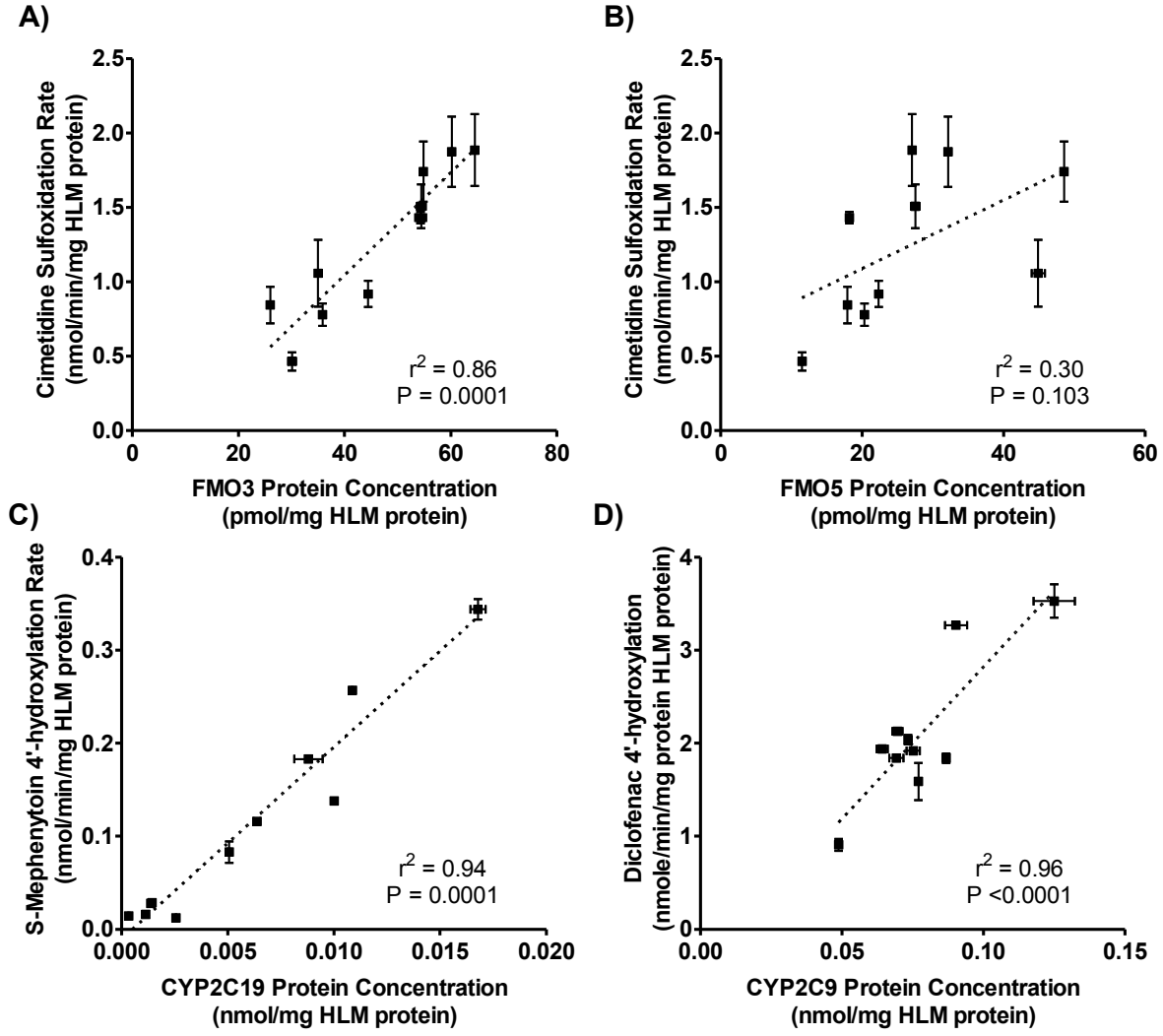

Figure 5. Correlation analysis of FMO and CYP2C protein content and measured marker activity in (A) (C) (D) adult and (B) fetal individual donor HLM panels. Symbols and error bars represent the mean and standard deviation of triplicate determinations for an individual donor HLM. In many cases, error bars for protein concentration are too small to be seen. Dotted lines represent the best-fit lines of least-square linear regression analysis.

2.3.4 Comparison of Recombinant Proteins *vs.* Synthetic Peptides as Calibration Standards for Absolute Quantification. Previously, our laboratory and others have reported signature peptide-dependent absolute quantification of CYPs and drug transporters using synthetic peptides as calibration standards (4, 14, 15, 19, 20). To assess such a scenario for the absolute quantification of FMOs, two signature peptides were selected for each FMO isozyme (Table 1) and quantification coherence between the two peptides was evaluated. When recombinant FMO Supersomes of known concentration were used to generate signature peptide standards, good coherence was observed, as described above (Figure 4). However, when synthetic peptides of known concentrations were used to generate signature peptide standards, good coherence was observed for FMO1, but not for FMO3 or FMO5 (Figure 6).

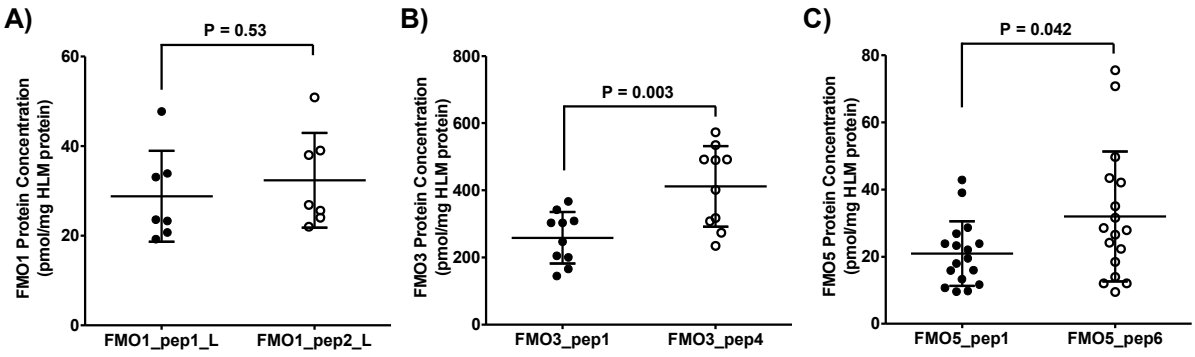

Figure 6. Comparison of FMO protein quantification by UPLC-MRM-based targeted proteomic approach using different signature peptides and synthetic signature peptide-generated calibration standards. Symbols represent the mean of triplicate determinations for an individual donor HLM. Lines and error bars represent the mean and standard deviation for a panel of HLM. Student's *t* tests (two-tailed, unpaired) were used to compare the pairs of signature peptides.

Absolute FMO concentrations measured using synthetic peptide standards were substantially greater than those determined using recombinant protein standards (*i.e.*, Supersomes) (Figure 6 *vs.* Figure 4). For example, the average FMO3 and FMO5 concentrations in adult HLMs were 46 and 27 pmol/mg HLM protein, respectively, with recombinant protein standards. In contrast, they were 259 or 412 pmol/mg HLM protein (5.6- to 9-fold higher) for FMO3 with synthetic FMO3_pep1_L or FMO3_pep4_L standards and 21 or 32 pmol/mg HLM protein (0.8- to 1.2-fold higher) for FMO5 with synthetic FMO5_pep1_L or FMO5_pep6_L standards.

2.3.5 Absolute Quantification of FMOs in Recombinant FMO Supersomes using Synthetic Peptide-generated Calibration Standards. To further investigate discrepancies in the absolute quantification of FMOs when recombinant proteins *vs.* synthetic peptides were used as standards, and determine the ratios of holoprotein *vs.* total protein, total FMO protein was quantified in recombinant FMO Supersomes of different concentrations using synthetic peptides as calibration standards. The measured total FMO protein amount was plotted against the nominal FMO protein amount based on FAD content, which represents the FMO holoprotein (Figure 7). Similar to the previously described signature peptide-dependent quantification, the ratio of total protein *vs*. holoprotein (slopes in Figure 8) for each recombinant FMO Supersomes also was dependent upon the signature peptide used. The ratio ranged from 5.0 to 5.6 for FMO1, 6.0 to 8.4 for FMO3, and 0.9 to 1.5 for FMO5.

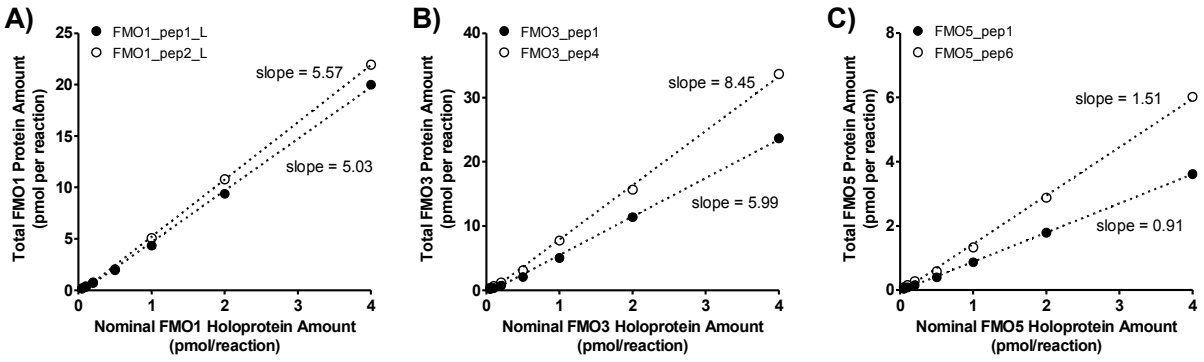

Figure 7. Comparison between total (holoprotein + apoprotein) FMO protein concentration and nominal holoprotein concentration in FMO Supersomes. The total FMO protein concentration was determined using synthetic signature peptides as calibration standards, while the nominal holoprotein concentration was determined based on FAD content (provided by the vendor). Dotted lines represent the best-fit lines of least-square linear regression analysis.

2.4 Discussion

In this study, a UPLC-MRM-based targeted quantitative proteomic method has been developed for the multiplexed absolute quantification of FMOs 1, 3 and 5, and CYP2C9 and 2C19 in HLM. This method has a lower limit of quantification of 0.33 pmol/mg HLM protein for each FMO when 30 μg of HLM is used.

LC-MRM-based targeted quantitative proteomic methods for the absolute quantification of CYPs, UGTs and drug transporters were first reported in the late 2000s (4, 11-13). These methods rely on the identification and detection of signature peptides for each target protein. The selection and verification of suitable signature peptides can be time-consuming and costly, mainly due to peptide synthesis after *in silico* selection. The ability to verify LC-MRM detection of the selected signature peptides in a protein digest prior to committing to peptide synthesis is therefore desirable. As such, we implemented a post-*in silico* product ion screening step to verify the detection of selected signature peptides (Figure 1) prior to their synthesis in order to reduce unnecessary peptide synthesis and costs. For example, only two FMO3 signature peptides (FMO3_pep1_L and FMO3_pep4_L) were synthesized in this study, rather than all eight candidate signature peptides (Table 2).

To achieve absolute quantification using an LC-MRM-based targeted proteomic approach, two types of standards are typically employed, recombinant proteins of known concentration or synthetic signature peptides of known concentration. Due to the poor coherence (*i.e.*, signature peptide-dependent quantification) when synthetic peptides were employed as standards (4, 14, 15, 19, 20), we prefer to use recombinant proteins when available (e.g., CYPs) to generate standards and employ at least two signature peptides for each protein to ensure quantification

coherence. Quantification was coherent between signature peptides for all three FMOs when recombinant FMO Supersomes were used to generate standards (Figure 4). Therefore, we recommend the use of recombinant proteins, when available, to generate standards for LC-MRM-based targeted protein quantification. Moreover, we call for a coordinated effort to produce reference protein standards, especially in the case of drug transporters, for use as calibration standards for targeted quantitative proteomics. It is not completely understood yet what may cause the lack of coherence in signature peptide-dependent quantification when synthetic peptides are used as standards. We have proposed that different digestion efficiencies (e.g., missed cleavage) and/or unexpected post-translational modifications of signature peptides were the underlying causes (14), and warrant future investigation.

FMOs, specifically the holoprotein, require an FAD prosthetic group for catalytic activity. Recombinant FMO Supersomes can be quantified based on their FAD content to give a holoprotein concentration. In contrast, the use of synthetic peptides as standards for targeted proteomic quantification provides a total protein concentration (*i.e.*, holoprotein + apoprotein) for a sample. Such a distinction was seen (Figure 8), as the total FMO protein amount exceeded its nominal holoprotein amount 5- to 6.6-fold for FMO1 and 6- to 8.5-fold for FMO3, while only a small difference (0.9- to 1.5-fold) was seen for FMO5. These results suggest that a large portion of FMO1 and FMO3 proteins in Supersomes are present as apoprotein without the FAD prosthetic group, whereas most FMO5 proteins are holoproteins. This is consistent with a much greater FAD content in FMO5 Supersomes (2700 pmol/mg protein; lot#3154943) relative to those in FMO1 and FMO3 Supersomes (500 and 810 pmol/mg protein, respectively; lot#3098891 and lot#3130681, respectively) reported by the vendor, although differential expression efficiency also could contribute to FAD content differences in FMO Supersomes.

For both conventional immunoquantification and the targeted proteomic quantification described here, an assumption was made that the holoprotein:apoprotein ratio remains the same between a recombinant system (*e.g.*, Supersomes) and HLM. However, this assumption remains to be examined. Deviation from this assumption could result in either underestimation or overestimation of enzymatic activity in HLM, depending on how the ratio in HLM deviates relative to that in the recombinant system. For example, if the ratio deviates upward in HLM (*i.e.*, higher proportion of holoproteins), this will result in an underestimation of HLM holoprotein concentration and the measured HLM activity will exceed the predicted activity calculated as the product of recombinant enzyme activity and HLM protein expression. To test this, one could first determine the rate of a probe substrate reaction, which needs to be catalyzed exclusively by the enzyme of interest, in HLM and then compare the measured HLM activity with the predicted activity based on the measured activity of the recombinant enzyme and measured expression level of the enzyme in HLM. Using FMO3 and cimetidine sulfoxidation as an example, the average measured cimetidine sulfoxidation activity in the adult HLM panel was 1.25 nmol/min/mg HLM (Figure 5A), the measured cimetidine sulfoxidation activity of recombinant FMO3 was 6.0 nmol/min/nmol FMO3 (unpublished data), and the measured FMO3 expression in HLM was 0.046 nmol/mg HLM (Figure 4B). The predicted activity is 0.28 nmol/min/mg HLM, substantially less than the measured activity of 1.25 nmol/min/mg HLM. Thus, an upward deviation of the holoprotein:apoprotein ratio in HLMs could have contributed to the under-prediction, in addition to other possibilities proposed in a companion study (21). The questionable assumption regarding the holoprotein:apoprotein ratio for FMOs, as well as for CYPs, is underappreciated and requires further investigation using newly available analytical tools (*e.g.*, targeted quantitative proteomics).

In summary, a UPLC-MRM-based targeted proteomic assay has been developed for the absolute protein quantification of FMOs 1, 3, 5, CYP2C9 and 2C19 in HLM. The developed FMO and CYP2C assay and other previously developed targeted quantitative proteomic assays are expected to assist in addressing previously unanswered questions in quantitative pharmacology.

2.5 References:

1. Krueger SK, Williams DE. Mammalian flavin-containing monooxygenases: structure/function, genetic polymorphisms and role in drug metabolism. Pharmacology & therapeutics. 2005;106(3):357-87.

2. Cashman JR, Zhang J. Human flavin-containing monooxygenases. Annual review of pharmacology and toxicology. 2006;46:65-100.

3. Mitchell SC. Flavin mono-oxygenase (FMO)--the 'other' oxidase. Curr Drug Metab. 2008;9(4):280-4.

4. Wang MZ, Wu JQ, Dennison JB, Bridges AS, Hall SD, Kornbluth S, et al. A gel-free MS-based quantitative proteomic approach accurately measures cytochrome P450 protein concentrations in human liver microsomes. Proteomics. 2008;8(20):4186-96.

5. Goldstein JA. Clinical relevance of genetic polymorphisms in the human CYP2C subfamily. Br J Clin Pharmacol. 2001;52(4):349-55.

6. Goldstein JA, de Morais SM. Biochemistry and molecular biology of the human CYP2C subfamily. Pharmacogenetics. 1994;4(6):285-99.

7. Lang DH, Yeung CK, Peter RM, Ibarra C, Gasser R, Itagaki K, et al. Isoform specificity of trimethylamine N-oxygenation by human flavin-containing monooxygenase (FMO) and P450 enzymes: selective catalysis by FMO3. Biochemical pharmacology. 1998;56(8):1005-12.

8. Yeung CK, Lang DH, Thummel KE, Rettie AE. Immunoquantitation of FMO1 in human liver, kidney, and intestine. Drug Metab Dispos. 2000;28(9):1107-11.

9. Koukouritaki SB, Simpson P, Yeung CK, Rettie AE, Hines RN. Human hepatic flavin-containing monooxygenases 1 (FMO1) and 3 (FMO3) developmental expression. Pediatric research. 2002;51(2):236-43.

10. Kawakami H, Ohtsuki S, Kamiie J, Suzuki T, Abe T, Terasaki T. Simultaneous absolute quantification of 11 cytochrome P450 isoforms in human liver microsomes by liquid chromatography tandem mass spectrometry with in silico target peptide selection. J Pharm Sci. 2011;100(1):341-52.

11. Fallon JK, Harbourt DE, Maleki SH, Kessler FK, Ritter JK, Smith PC. Absolute quantification of human uridine-diphosphate glucuronosyl transferase (UGT) enzyme isoforms 1A1 and 1A6 by tandem LC-MS. Drug Metab Lett. 2008;2(3):210-22.

12. Kamiie J, Ohtsuki S, Iwase R, Ohmine K, Katsukura Y, Yanai K, et al. Quantitative atlas of membrane transporter proteins: development and application of a highly sensitive simultaneous LC/MS/MS method combined with novel in-silico peptide selection criteria. Pharm Res. 2008;25(6):1469-83.

13. Li N, Nemirovskiy OV, Zhang Y, Yuan H, Mo J, Ji C, et al. Absolute quantification of multidrug resistance-associated protein 2 (MRP2/ABCC2) using liquid chromatography tandem mass spectrometry. Anal Biochem. 2008;380(2):211-22.

14. Peng KW, Bacon J, Zheng M, Guo Y, Wang MZ. Ethnic variability in the expression of hepatic drug transporters: absolute quantification by an optimized targeted quantitative proteomic approach. Drug Metab Dispos. 2015;43(7):1045-55.

15. Michaels S, Wang MZ. The revised human liver cytochrome P450 "Pie": absolute protein quantification of CYP4F and CYP3A enzymes using targeted quantitative proteomics. Drug Metab Dispos. 2014;42(8):1241-51.

16. Omura T, Sato R. The Carbon Monoxide-Binding Pigment of Liver Microsomes. I. Evidence for Its Hemoprotein Nature. J Biol Chem. 1964;239:2370-8.

17. Cashman JR, Park SB, Yang ZC, Washington CB, Gomez DY, Giacomini KM, et al. Chemical, enzymatic, and human enantioselective S-oxygenation of cimetidine. Drug Metab Dispos. 1993;21(4):587-97.

18. Overby LH, Carver GC, Philpot RM. Quantitation and kinetic properties of hepatic microsomal and recombinant flavin-containing monooxygenases 3 and 5 from humans. Chem Biol Interact. 1997;106(1):29-45.

19. Balogh LM, Kimoto E, Chupka J, Zhang H, Lai Y. Membrane Protein Quantification by Peptide-Based Mass Spectrometry Approaches: Studies on the Organic Anion-Transporting Polypeptide Family. J Proteomics Bioinform. 2013;06(10):229-36.

20. Prasad B, Evers R, Gupta A, Hop CE, Salphati L, Shukla S, et al. Interindividual variability in hepatic organic anion-transporting polypeptides and P-glycoprotein (ABCB1) protein expression: quantification by liquid chromatography tandem mass spectroscopy and influence of genotype, age, and sex. Drug Metab Dispos. 2014;42(1):78-88.

21. Zane NR, Chen Y, Wang MZ, Thakker DR. CYP and FMO Families Shows Age-Dependent Differences in Expression and Functional Activity. Drug Metab Dispos (currently under review). the companion paper.

Chapter III: Determination of Human Age-Dependent CYP and FMO Expression using UPLC-MRM-Based Targeted Proteomics

TABLE OF CONTENTS

LIST OF FIGURES

LIST OF TABLES

3.1 Introduction

Human hepatic CYPs and FMOs undergo age-dependent changes in expression, or ontogenetic processes, which affect the pharmacokinetics, toxicity and efficacy of drugs metabolized by these enzymes. Therefore, dose justifications are frequently needed for patients of varying ages. In the past, accurate measurements of CYP and FMO ontogenies were difficult, because of a lack of specific targeting antibodies. For example, there is no antibody available commercially to differentiate between CYP4F2 and CYP4F3B, which share 93% amino acid sequence identity (1). In addition, DMEs also tend to have overlapping activities, making it difficult to differentiate between isoforms. For example, 7-ethoxyresorufin O-deethylation is a widely accepted measurement of CYP1 subfamily activity, but it cannot discriminate between CYP1A1, CYP1A2 and CYP1B1. FMO1 and FMO3 both mediate the sulfoxidation of cimetidine, producing the same metabolite; this activity cannot be used to differentiate between the two isoforms (2). Another difficulty in determining ontogeny is the limited number of proteins that can be assessed at one time. As a result, analytical assays with high specificity and multiplexing are in demand for the study of human hepatic ontogeny.

An MS-based targeted strategy for protein quantification was first published in 2003 by S. A. Gerber *et. al.* (3). It was developed first in 2008 for the absolute quantification of human hepatic CYP3As by M. Z. Wang *et al*. (4). Since then, MS-based targeted protein quantification has been adopted for the measurement of CYPs, FMOs, UGTs and drug transporters, and has been widely accepted for protein quantification (1, 2, 4-7). Before applying targeted proteomics for the discovery of new ontogeny patterns, the known patterns must be confirmed.

The ontogenies of human hepatic CYP3A, CYP2C, and FMO have been studied by Western blot. J. C. Stevens *et. al*. studied CYP3A ontogeny in HLMs from 212 individuals ranging in age

from the 1st trimester up to 9 years (8). He found that CYP3A5 was highly variable and that the variability occurred independent of age; CYP3A7 had extremely high expression at 158-311 pmole/mg fetal liver, but it dropped quickly after birth; CYP3A4 had little expression prior to birth and increased at postnatal ages.

CYP2C ontogeny was reported by S. B. Koukouritaki *et. al.* in 2003. HLM from 237 subjects, ranging from 8 months gestation up to 18 years of age, were analyzed by Western blot and activity assays (9). Hepatic CYP2C9 expression values during the first trimester start at 1-2% of the average adult level. Expression increased during the second and third trimesters to 30% of the adult average. However, CYP2C9 variability is much greater in adult liver, up to 35-fold. CYP2C19 was measurable starting at 8 weeks gestation and was 12-15% of the average adult level. After birth, expression increased rapidly. There was a 25-fold variation in CYP2C19 expression.

Hepatic FMO1 and FMO3 undergo a developmental switch similar to that of CYP3A7 and CYP3A4. FMO1, the major fetal isozyme, peaks early in gestation (first and second trimesters) and decreases gradually to undetectable at birth (10). In contrast, expression of FMO3, the major adult isozyme, turns on after birth and increases over time, reaching an adult level in the early teenage years (10). This differential enzyme expression has garnered much attention, specifically for the dose adjustment of FMO substrate drugs in infants and children (11, 12). FMO5 mRNA expression exceeds that of *FMO3* in adult liver (13); however, earlier reports suggested the opposite (14, 15). Additionally, *FMO5* mRNA expression in fetal livers is approximately one-sixth of that in adult livers (13).

Due to the lack of specificity and poor multiplexing capability of immuno-blotting assays, the ontogenies of many important CYPs remain unknown, especially those of CYP4F2, CYP4F3B and FMO5. CYP4Fs are the third most abundant CYP in the human liver and are responsible for the metabolism of multiple important endogenous molecules (*e.g.*, arachidonic acid, vitamin K1 and vitamin E), drugs (*e.g.* fingolimod), and xenobiotics (*e.g.* DB289 and DB868). The expression, activity and endogenous biological function(s) of FMO5 are unknown.

The multiplexing capabilities and specificity of LC-MRM-based targeted proteomics has allowed the absolute quantifications of CYP2C9, 2C19, 3A4, 3A5, 3A7, 4F2 and 4F3B, and FMO1, 3 and 5 to be completed within a single run needing only 30 ug of HLM protein. The quantification of these enzymes was based on well-validated assays developed in our laboratory (1, 2, 4). The goal of this chapter is to determine the ontogenies of CYP2C9, 2C19, 3A4, 3A5, 3A7, 4F2 and 4F3B, and FMO1, 3 and 5 by LC-MRM-based targeted proteomics using fetal, pediatric and adult livers. This will be the first time CYP4F2 and 4F3B, and FMO5 ontogenies will be examined.

3.2 Materials and Methods

3.2.1 Chemicals, Enzymes, and Liver Tissues. Optima-grade acetonitrile, water, formic acid, and acetic acid were obtained from Fisher Scientific (Pittsburgh, PA). Ammonium bicarbonate, dimethyl sulfoxide, dithiothreitol, and iodoacetamide were purchased from Sigma-Aldrich (Saint Louis, MO). Recombinant human FMO1, FMO3, FMO5, CYP2C9, CYP2C19, CYP3A4, CYP3A5, CYP3A7, CYP4F2 and CYP4F3B Supersomes™, prepared from baculovirus-infected insect cells expressing human FMO and CYP enzymes, were purchased from Corning Gentest (Woburn, MA). The FMO or CYP concentration of each Supersomes (pmol/mL and pmol/mg protein), based on the FAD or heme content determined by an HPLC-fluorescence method or CO difference spectrum assay (16, 17), was provided by the supplier. Synthetic ^{13}C and ^{15}N stable isotope-labeled crude signature peptides were acquired from Thermo Scientific (Ulm, Germany). All synthetic peptide sequences were confirmed by MS/MS fragmentation analysis using a Waters Xevo TQ-S triple-quadrupole MS (Milford, MA). Sequencing-grade modified trypsin was purchased from Promega (Madison, WI). Liver tissues from seven fetal (14-20 weeks gestation), sixteen pediatric (5 months-10 years), and ten adult (22-80 years) donors were obtained from the NICHD Brain and Tissue Bank for Developmental Disorders (Contract #HHSN275200900011C, Ref. No. NO1-HD-9-0011; Baltimore, MD) under an approved UNC-Chapel Hill IRB and were used to prepare fetal, pediatric, and adult HLM (Table 4). The liver samples were kindly shared by our collaborators from UNC-Chapel Hill, Nicole R. Zane Ph.D., Pharm.D. and Dhiren R. Thakker Ph.D.

Table 4. Individual HLM donor information.

Group	Sample	Gender	Age	Race
Adult	A1	54 years	Male	Caucasian
	A2	40 years	Female	Caucasian
	A4	23 years	Male	Hispanic
	A5	23 years	Male	Hispanic
	A7	80 years	Male	Caucasian
	A8	22 years	Female	Caucasian
	A9	32 years	Female	Caucasian
	A10	46 years	Female	Caucasian
	A11	45 years	Female	Caucasian
	A12	32 years	Female	Caucasian
Fetal[c]	F1	Female	18 weeks	African American
	F5	Male	15 weeks	African American
	F6	Female	20 weeks	African American
	F7	Male	16 weeks	African American
	F8	Male	15 weeks	African American
	F9	Male	19 weeks	Caucasian
	F10	Male	16 weeks	African American
Pediatric	P1	Male	6 years	Caucasian
	P2	Male	4 years	Caucasian
	P3	Male	2 years	African American
	P4	unknown	2 years	unknown
	P5	unknown	1 years	unknown
	P6	unknown	4 months	unknown
	P7	Male	4 years	Caucasian
	P8	Male	8 years	Caucasian
	P9	Male	2 years	African American
	P10	Female	9 years	Hispanic
	P11	Female	111 days	Caucasian
	P12	Female	92 days	Caucasian
	P13	Male	63 days	African American
	P14	Female	57 days	African American
	P15	Female	97 days	African American
	P16	Male	71 days	African American

c age for fetal donors is gestational age

3.2.2 Trypsin Digestion. The tryptic digestion of FMO Supersomes and HLM was performed as described previously with minor modifications (1, 4). Briefly, protein samples (30 μg) were reduced in ammonium bicarbonate buffer (pH 8.0, 50 mM final concentration) containing dithiothreitol (4 mM final concentration) and heated at 60°C for 60 min to denature the proteins. After cooling to room temperature, the samples (90 μL total volume) were alkylated with iodoacetamide (10 mM final concentration) for 20 min in the dark prior to digestion with 1 μg trypsin at 37°C for 4 h unless stated otherwise. All reactions were carried out in Eppendorf Protein LoBind microcentrifuge tubes (Hamburg, Germany) to minimize protein and peptide loss due to binding. Solvent evaporation during the incubations was minimized by sealing the capped tubes with parafilm and applying pressure with an aluminum block.

3.2.3 UPLC-MRM Analysis. Lyophilized stable isotope-labeled signature peptides were dissolved in 1 mL of 1:1 (v/v) acetonitrile:water solution. The solution was diluted further to approximately 2-4 μg/mL and then infused into the Xevo TQ-S MS at 5 μL/min with an LC flow of 50% B at 0.4 mL/min. MRM parameters were optimized using IntelliStart (Waters) under positive electrospray ion mode: capillary voltage, 1.5 kV; cone voltage, 40 V; source offset, 40 V; dissolvation temperature, 500°C; dissolvation gas, 1000 L/h; nebulizer gas, 7 bar. The optimum collision energy and precursor/production masses for the signature peptides are summarized in Table 3 or from previous publications (1, 2, 4). UPLC-MRM quantification was performed using the peak area ratios of signature peptides to corresponding stable isotope-labeled signature peptides (internal standards).

3.2.4 Preparation of Calibration Standards. Recombinant FMO1, FMO3, FMO5, CYP2C9, CYP2C19, CYP3A4, CYP3A5, CYP3A7, CYP4F2, and CYP4F3B Supersomes of known concentrations were used to create calibration standards. All recombinant protein standards were

denatured, alkylated and trypsin-digested as described above, prior to UPLC-MRM analysis. Due to the varying amount of total proteins in the standards, additional trypsin (2 μg total) was used to keep the protein:trypsin ratio ≤ 30:1 in the high concentration standards.

3.2.5 Data Analysis. The final protein concentrations were the average value determined using two signature peptides for each protein. All average values were calculated as the mean. The slope and Y-intercept values were determined by least-square linear regression analysis. Student's *t* tests (two-tailed, unpaired) were used to compare the pairs of signature peptides. All data analyses were performed using GraphPad Prism (v. 5.0; San Diego, CA).

3.3 Results

3.3.1 Peptide Separation and Detection. The UPLC-MRM method used in this study was developed by building upon the LC-MRM method described previously by M. Z. Wang *et. al.* 2008 (4). The original LC method was selected for the co-elution of all peptides with a quick 3.5 min gradient to allow for fast analysis, as CYP3A4 and CYP3A5 are expressed quite abundantly in adult human livers. However, the detection and quantification of enzymes for the study of ontogenesis requires a high degree of measurement sensitivity, something that may be compromised by the inhibition of ionization when all peptides are eluted together. Therefore, the current study utilized a UPLC column and 13.5 min gradient with the goals to achieve better peptide separation and minimize ion suppression (Figure 8). The UPLC-MRM settings were detailed previously (2).

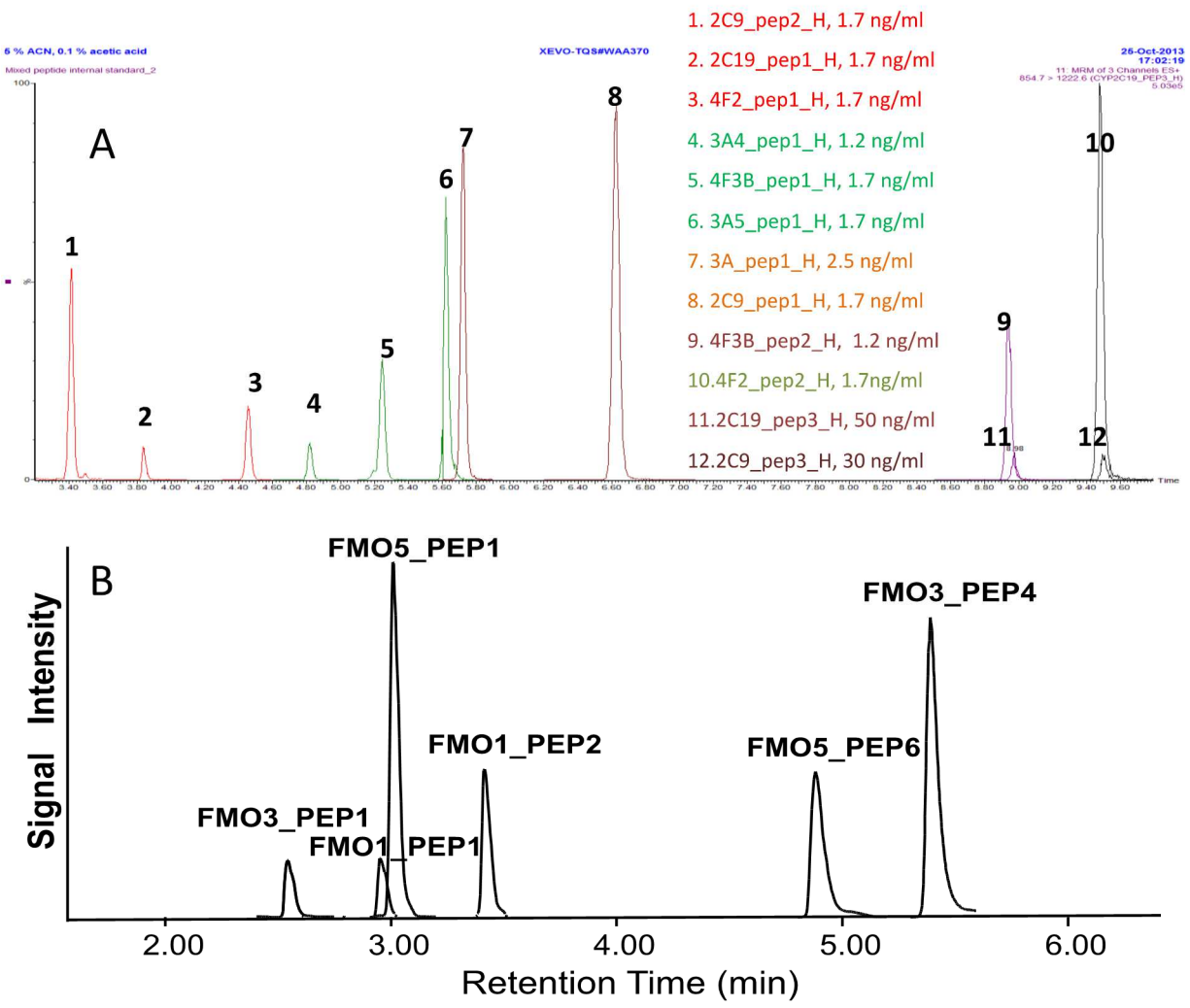

Figure 8. UPLC-MRM chromatograms of stable isotope-labeled signature peptides (internal standards) for quantification of CYPs (**A**) and FMOs (**B**).

3.3.2 Ontogenies of CYPs 3A4, 3A5, and 3A7. A previous study demonstrated the specificity of the LC-MRM-based targeted quantification method for CYP3A4 and CYP3A5, and its strong correlation to Western blots and substrate activity assays (4). A unique CYP3A7 signature peptide has been added in this study to take advantage of the adaptability and multiplexing of the

LC-MRM-based method, while at the same time, cross-validating the ontogenies of CYP3A family members quantified previously.

Fetal hepatic CYP3A4 (Figure 9) and CYP3A5 (Figure 10) averaged (range) 1.2 (0.9-1.3) and 5.0 (0.6-14) pmol/mg HLM protein (n=7 donors), respectively, which are significantly lower than the highly expressed CYP3A7 (Figure 11) average (range) of 536.5 (454.4-645.6) pmol/mg HLM protein. The developmental switch between CYP3A7 and CYP3A4 happened after birth; CYP3A7 slowly decreased during the pediatric stage while CYP3A4 gradually increased (n=16 donors). CYP3A7 and CYP3A4 averaged (range) 51.4 (2.5-163.5) and 64.6 (16.2-177.1) pmol/mg HLM protein, respectively. In adulthood, CYP3A4 reached an average of 76.2 (17.9-123.4) pmol/mg HLM protein (n=10 donors), whereas CYP3A7 dropped to 5.1 (1.3-13.1) pmol/mg HLM protein after removing the 80 year-old subject. This particular subject expressed CYP3A7 at 143.1 pmol/mg HLM protein, 70-fold higher than the average of the other adult donors (<55 years old). In comparison, CYP3A5 expression was independent of age, averaging (range) 3.6 (0.8-15.6) at the pediatric stage and 1.5 (0.4-4.7) at the adult stage.

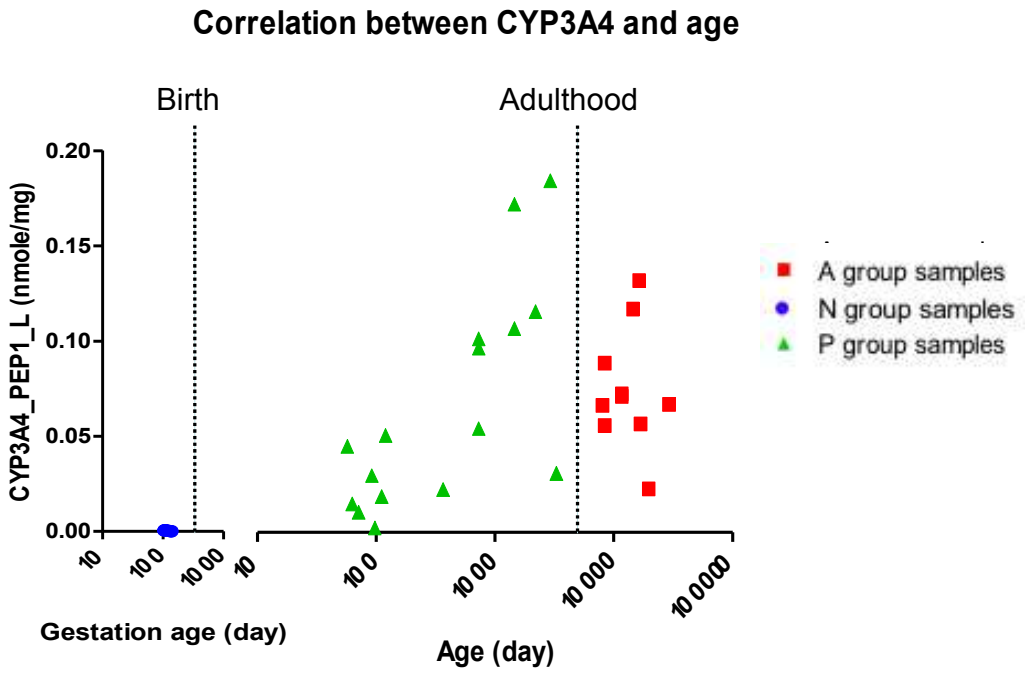

Figure 9. Age-dependent CYP3A4expression in human livers. Fetal (N), pediatric (P), and adult (A) samples were labeled in blue, green, and red symbols respectively.

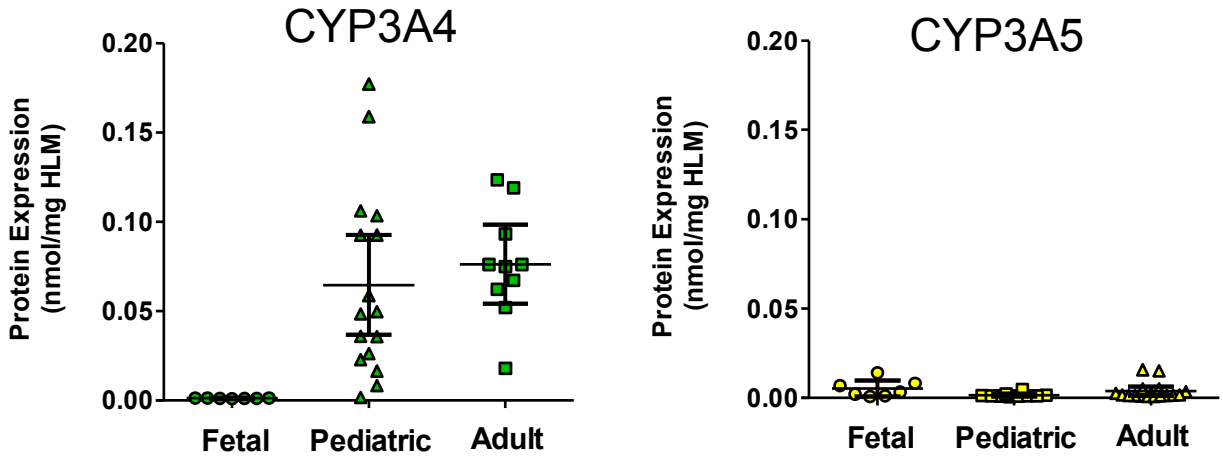

Figure 10. Comparison of age-dependent CYP3A4 and CYP3A5 expression in human livers.

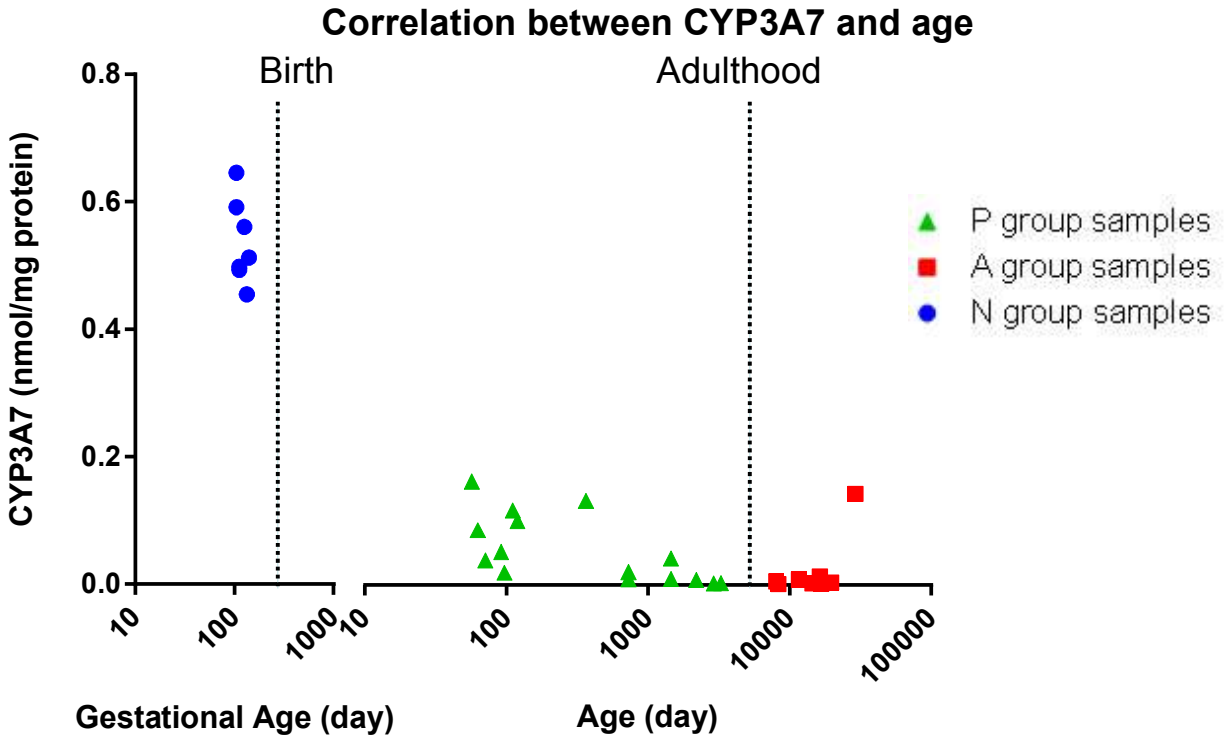

Figure 11. Age-dependent CYP3A7 expression in human livers. Fetal (N), pediatric (P), and adult (A) samples were labeled in blue, green, and red symbols respectively.

3.3.3 Ontogenies of CYPs 2C9 and 2C19. CYP2C9 and CYP2C19 had a similar trend across the age groups (Figure 12). In fetal livers, CYP2C9 and CYP2C19 expression averaged (range) 1.2 (0.9-1.5) and 0.2 (0.1-0.3) pmol/mg HLM protein, respectively. Expression increased to 51.6 (20.8-89.8) and 54.4 (30.0-78.1) pmol/mg HLM protein for CYP2C9 and 9 (0.4-34) and 4.3 (0.1-12.9) pmol/mg HLM protein for CYP2C19 in pediatric and adult tissues, respectively. On average, CYP2C9 expression was higher than that of CYP2C19 at all stages of development. The variability in CYP2C19 expression was higher in pediatric compared to adult livers, whereas CYP2C9 variability was similar.

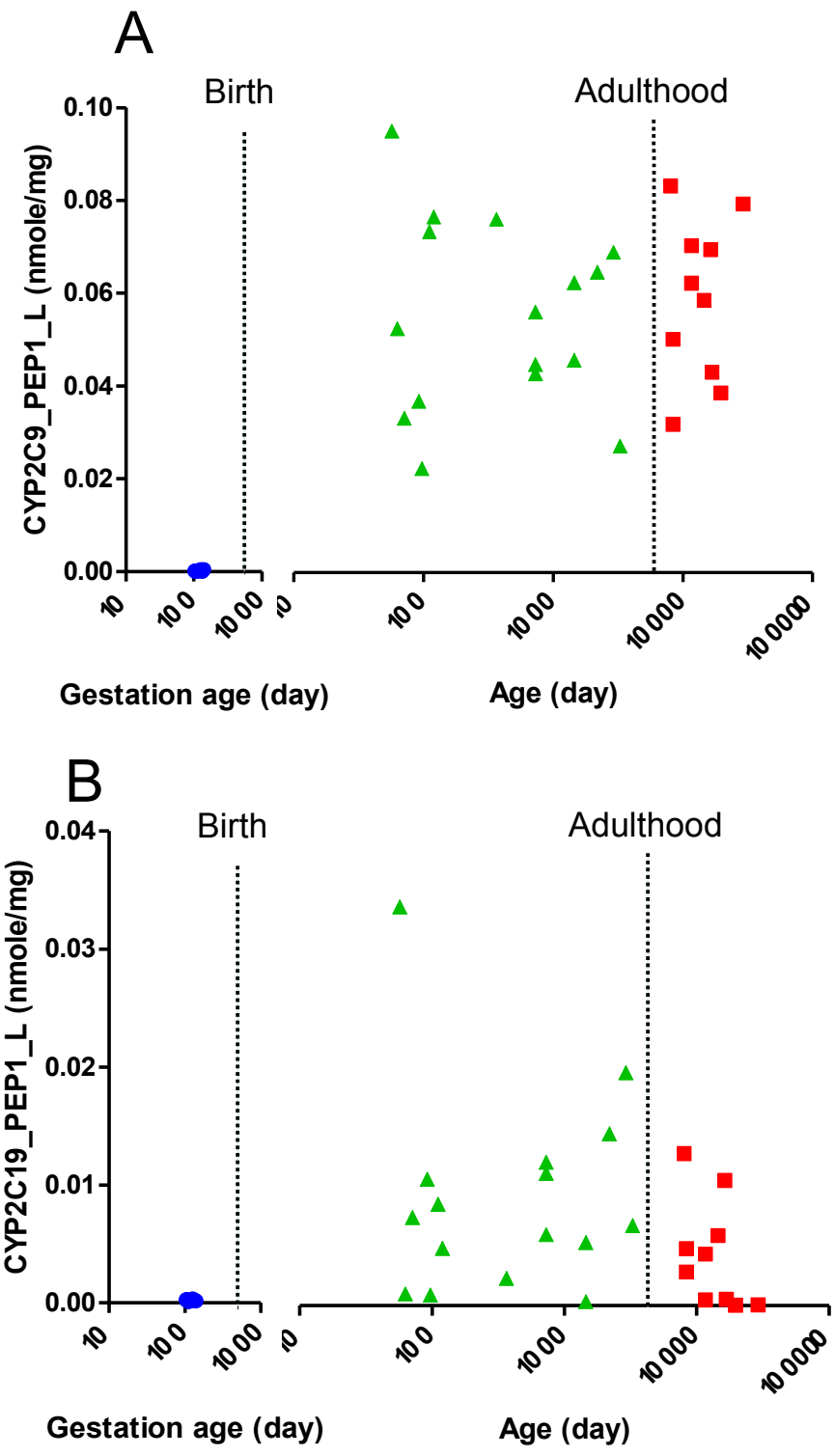

Figure 12. Ontogeny of CYP2C9 and CYP2C19 in human livers. Fetal (N), pediatric (P), and adult (A) samples were labeled in blue, green, and red symbols respectively.

3.3.4 Ontogenies of CYPs 4F2 and 4F3B. The method for targeted analysis of CYP4F2 and 4F3B was established and validated in our laboratory previously (1). The age-dependent expression of these enzymes has not been studied due to a lack of specific antibodies and activity substrate. With UPLC-MRM, the ontogeny of CYP4F2 and CYP4F3B was determined for the first time (Figure 13). CYP4F2 expression followed a pattern/trend similar to that of CYP3A4, CYP2C9, and CYP2C19. Expression started at a low of 2.6 (1.2-4.1) pmol/mg HLM protein in fetal livers, increased to 13.5 (1.2-28.1) in pediatric tissues, and was maintained at 13.0 (4.2-33.8) in adult livers. In comparison, CYP4F3B did not change throughout the ages, ranging from 11.0 (8.5-14.0) to 8.1 (2.2-14.9) to 12.5 (6.3-18.3) for fetal, pediatric, and adult livers, respectively.

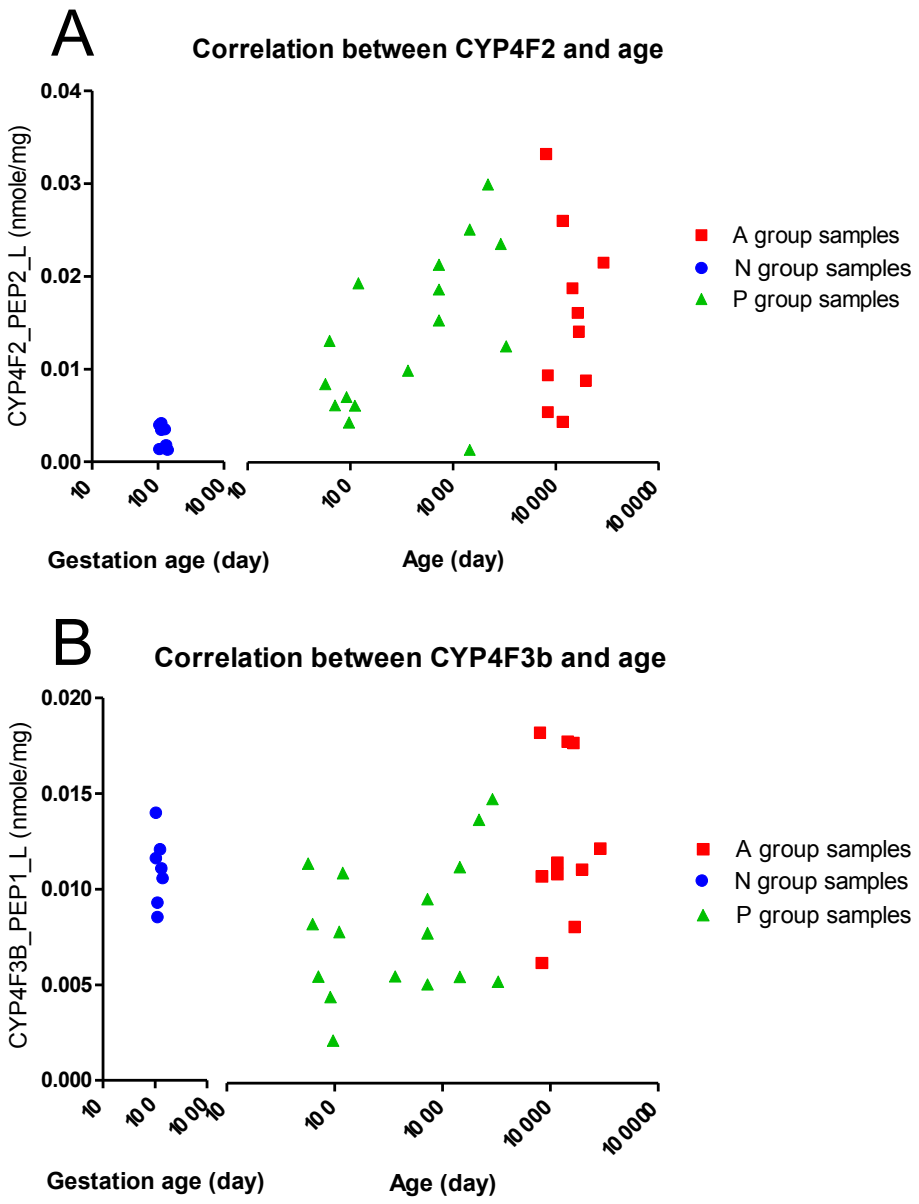

Figure 13. Age-dependent CYP4F2 and CYP4F3B expression in human livers. Fetal (N), pediatric (P), and adult (A) samples were labeled in blue, green, and red symbols respectively.

3.3.5 Ontogenies of FMO1, FMO3, and FMO5. The concentration of FMO1 in adult HLM was below the lower limit of quantification (<0.33 pmol/mg HLM protein). Final FMO3 and

FMO5 average protein concentrations (range and 95% confidence interval [CI]) in adults were 46 (26 – 65 and 36 – 56) and 27 (11.5 – 49 and 18.5 – 36) pmol/mg HLM protein, respectively. In the fetal HLM panel, FMO1 protein concentration averaged (range and 95% CI) 7.0 (4.9 – 9.7 and 5.2 – 8.7) pmol/mg HLM protein. Appreciable amounts of FMO5 also were present, averaging 21 (14 – 32 and 14 – 29) pmol/mg HLM protein (Figure 14A). In contrast to adult HLM, FMO3 in fetal HLM was barely above the lower limit of quantification (0.33 pmol/mg HLM protein), averaging 0.7 pmol/mg HLM protein with a high concentration of 2.2 pmol/mg HLM protein. FMO5 protein concentration averaged (range and 95% CI) was 36.2 (2.9 – 110 and 20.1 – 52.3) pmol/mg HLM protein in the pediatric HLM panel (Figure 14B). There was no statistically significant difference among the three age groups ($P = 0.317$; Figure 14C).

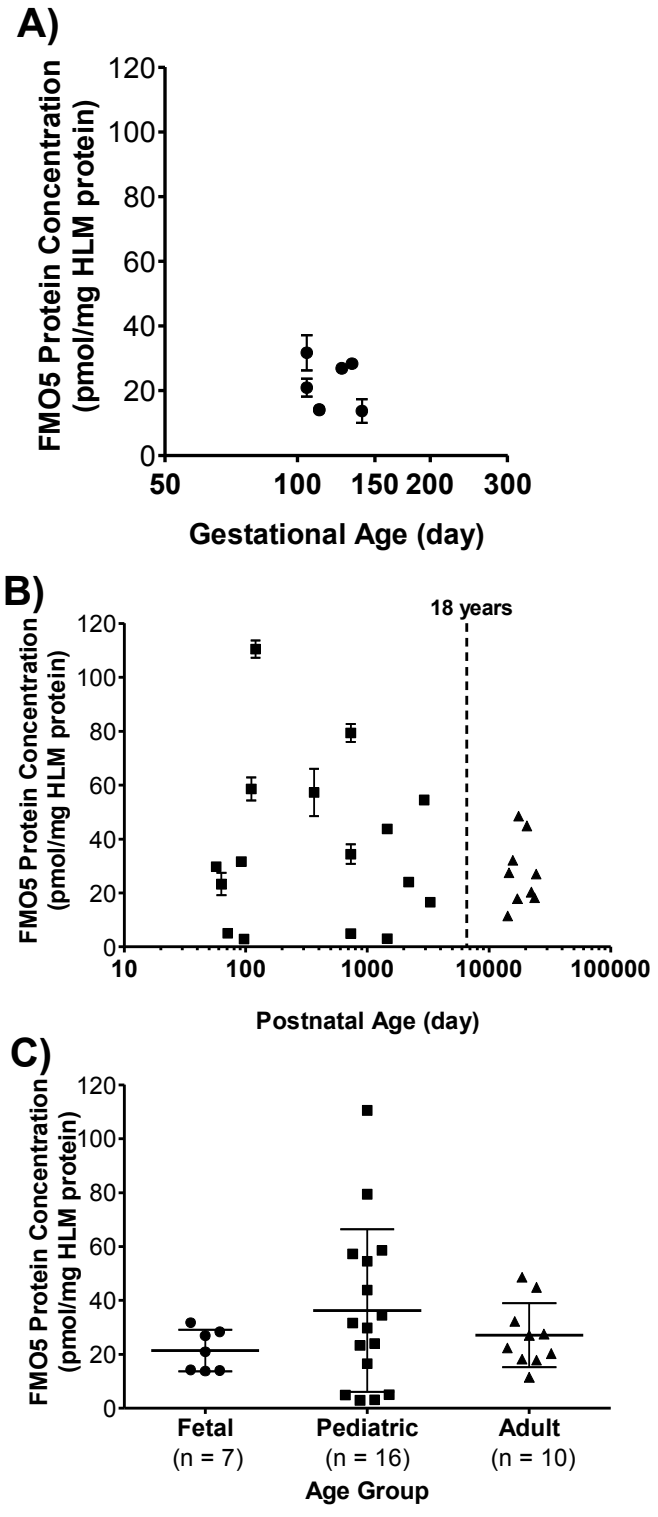

Figure 14. Ontogenies of FMO1, 3, and 5 in human livers.

3.4 Conclusions and Discussions

In this chapter, the ontogenies of human hepatic CYPfCYP2C9, 2C19, 3A4, 3A5, 3A7, 4F2 and 4F3B, and FMO1, 3, and 5 were quantified simultaneously in fetal, pediatric, and adult livers. Each measurement consumed less than 100 μg of HLM protein for biological triplicates of each subject, thanks to the sensitivity, multiplexing capabilities, and selectivity of the UPLC-MRM-based targeted protein quantification method. Among these measured targeted proteins, the ontogenies of CYP4F2, CYP4F3B, and FMO5 were determined for the first time.

3.4.1 CYP3A Ontogeny. CYP3A4 and CYP3A5 account for nearly half of all CYP-mediated drug metabolism and close to 30% of expression in adult liver. The expression of each enzyme is highly inducible; their transcription is controlled by PXR (pregnane X receptor) and CAR (constitutive androstane receptor), both of which respond to a wide range of chemicals. Induction factors, such as diet and drug history, contribute greatly to the inter-individual variability of CYP3A4 and CYP3A5 expression (18). CYP3A7 expression was first found in the fetal liver in 1988 (19). However, due to the lack of specific antibodies, the ontogeny of CYP3A family members remained unexplored. J. C. Stevens *et. al.* studied CYP3A ontogeny using over 200 livers that were donated by subjects ranging in age from the first trimester to 18 years old. Equipped with only a CYP3A5-specific antibody, Stevens had to extrapolate CYP3A7 and CYP3A4 expression based on DHEA oxidation activity (8). CYP3A7 expression in fetal liver was extremely high (158-311 pmol/mg HLM protein). J. S. Leeder *et. al.* examined 51 fetal livers using western blots with a CYP3A4/3A7 cross-reactive antibody and found that CYP3A7 had an average expression of 232 (20.6-434) pmol/mg HLM protein (20). Our UPLC-MRM-based targeted proteomics quantification also showed a much greater level of CYP3A7 in fetal livers compared to CYP3A expression in adult liver. Our measurement was approximately twice

as high, averaging (range) 536.5 (454.4-645.6) pmol/mg HLM protein, compared to that determined by Western blots or activity measurements. This inconsistency could be due to limited dynamic range of Western blot-based immunoquantification, which tends to underestimate highly concentrated samples due to signal saturation. In the current study, we found CYP3A5 expression to be independent of age with large inter-individual variability. CYP3A4 expression was similar to historical data: very little expression in the fetal liver but increases during the pediatric stage until peaking around adulthood. The absolute average was different from activity extrapolations and Western blot measurements, just like CYP3A7. However, good quantitative consistency was found between the current measurements and those done by M. Z. Wang *et. al*. in 2008; CYP3A4 in adult liver was 64.6 (16.2-177.1) compared to 67 (9-322) pmol/mg HLM protein while CYP3A5 was 1.5 (0.4-4.7) compared to 4 (0.3 to 20) pmol/mg HLM protein, respectively (4).

3.4.2 CYP2C ontogeny. CYP2C9 and CYP2C19 are more abundantly expressed than the other two CYP2C family members, CYP2C8 and CYP2C18. Previous reports stated that there were non-detectable CYP2C9 and 2C19 were undetectable in fetal livers (16 to 40 weeks gestation), while CYP2C8 and 2C18 were expressed at 10% of the adult CYP2C9 level, suggesting a developmental switch in expression. CYP2C9 was detectable 24 hours after birth. The same trend was found with the current UPLC-MRM-based quantification method. Unexpectedly, Koukouritaki *et. al*. measured CYP2C9 and CYP2C19 expression to be approximately the same level at all stages of development, however targeted proteomics quantified CYP2C9 to be approximately 5-10-fold higher than CYP2C19. Our CYP2C9/2C19 ratio was consistent with many other reports including those utilizing Western blots (21) and quantitative proteomics (22).

3.4.3 CYP4F ontogeny. An LC-MRM-based CYP4F2 and CYP4F3B specific quantitative method was established quite recently, in 2014 (1). Prior to that, there were no antibodies able to differentiate between the CYP4F isoforms. In addition, even though vitamin K1 ω-oxidation was identified as a specific CYP4F2 activity (23), the reaction is extremely slow and the ω-oxidized vitamin K1 metabolite is not available; we had no luck observing CYP4F2 activity in this way. Because of these combined reasons, CYP4F2 ontogeny had yet to be studied. However, our laboratory demonstrated previously that the CYP4F subfamily is the 3rd highest expressed CYP in human adult livers. McDonald *et. al.* showed that hepatic CYP4F2 expression differences contribute to inter-individual differences in warfarin dosing (23). Thus, it is of great importance to know the absolute quantity of CYP4F enzymes among different age groups.

With no previous CYP4F ontogeny data to compare to, the current adult CYP4F quantification could only be compared to previously quantified CYP4F from a different panel of adult HLMs. Among the 31 adult subjects, Michaels *et. al.* found CYP4F2 to have an average (range) of 14.3 (1.3–27.1) and CYP4F3B to be 11.3 (6.4–20.9) pmol/mg HLM protein (1), both of which are very close to the current averages of 13.0 (4.2-33.8) and 12.5 (6.3-18.3) pmol/mg HLM protein for CYPs 4F2 and 4F3B, respectively.

3.4.4 FMO ontogeny. In adult HLMs, FMO3 was more abundant than FMO5 (46 *vs*. 27 pmol/mg HLM protein), supporting earlier reports (14, 15) but not the most recent report (13), both of which were based on mRNA expression. In the fetal HLMs (14-20 weeks gestation), FMO1 was expressed at relatively high levels (7.0 pmol/mg HLM protein), similar to what was reported previously (7.8 pmol/mg HLM protein; 8-15 weeks gestation) (10). Interestingly, FMO5 was the predominant isozyme in fetal HLM, averaging 3-fold greater protein expression than FMO1 (21 *vs.* 7.0 pmol/mg HLM protein). In the pediatric HLM, FMO5 also appeared to be the

predominant isozyme (36.2 *vs*. 20.0 pmol/mg HLM protein for FMO3), while FMO1 was barely detected. Although FMO5 expression was not significantly different among the three age groups, larger interindividual variability was observed in the pediatric HLM (38- fold vs. 4.3- and 2.3-fold in adult and fetal HLM, respectively). These targeted quantitative proteomic results confirm previous reports that FMO1 and FMO3 expression undergo a developmental transition and also discovered that FMO5 has relatively stable expression throughout development.

3.4.5 Summary. The ontogenies of multiple CYPs and FMOs were studied in human fetal, pediatric, and adult livers. Expression trends observed for CYP3As, CYP2Cs, and FMO1 and 3 confirm historical reports. The ontogenies of CYP4F2 and 4F3B and FMO5 were discovered for the first time. These proteins were quantified together in a single run, owing to the multiplexing capability of the modern UPLC-MRM-based proteomic methods. However, these results should be interpreted with caution, as our study only included a small number of HLM from each age group, fetal samples only represented the second trimester, and neonatal samples (birth to first month) were absent. Future studies employing larger panels of HLM are warranted.

3.5 References

1. Michaels S, Wang MZ. The revised human liver cytochrome P450 "Pie": absolute protein quantification of CYP4F and CYP3A enzymes using targeted quantitative proteomics. Drug Metab Dispos. 2014;42(8):1241-51.

2. Chen Y, Zane NR, Thakker DR, Wang MZ. Quantification of Flavin-containing Monooxygenases 1, 3 and 5 in Human Liver Microsomes by UPLC-MRM-based Targeted Quantitative Proteomics and Its Application to the Study of Ontogeny. Drug Metab Dispos. 2016;44(7):975-83.

3. Gerber SA, Rush J, Stemman O, Kirschner MW, Gygi SP. Absolute quantification of proteins and phosphoproteins from cell lysates by tandem MS. Proc Natl Acad Sci U S A. 2003;100(12):6940-5.

4. Wang MZ, Wu JQ, Dennison JB, Bridges AS, Hall SD, Kornbluth S, et al. A gel-free MS-based quantitative proteomic approach accurately measures cytochrome P450 protein concentrations in human liver microsomes. Proteomics. 2008;8(20):4186-96.

5. Kawakami H, Ohtsuki S, Kamiie J, Suzuki T, Abe T, Terasaki T. Simultaneous absolute quantification of 11 cytochrome P450 isoforms in human liver microsomes by liquid chromatography tandem mass spectrometry with in silico target peptide selection. J Pharm Sci. 2011;100(1):341-52.

6. Sakamoto A, Matsumaru T, Ishiguro N, Schaefer O, Ohtsuki S, Inoue T, et al. Reliability and robustness of simultaneous absolute quantification of drug transporters, cytochrome P450 enzymes, and Udp-glucuronosyltransferases in human liver tissue by multiplexed MRM/selected reaction monitoring mode tandem mass spectrometry with nano-liquid chromatography. J Pharm Sci. 2011;100(9):4037-43.

7. Peng KW, Bacon J, Zheng M, Guo Y, Wang MZ. Ethnic variability in the expression of hepatic drug transporters: absolute quantification by an optimized targeted quantitative proteomic approach. Drug Metab Dispos. 2015;43(7):1045-55.

8. Stevens JC, Hines RN, Gu C, Koukouritaki SB, Manro JR, Tandler PJ, et al. Developmental expression of the major human hepatic CYP3A enzymes. J Pharmacol Exp Ther. 2003;307(2):573-82.

9. Koukouritaki SB, Manro JR, Marsh SA, Stevens JC, Rettie AE, McCarver DG, et al. Developmental expression of human hepatic CYP2C9 and CYP2C19. J Pharmacol Exp Ther. 2004;308(3):965-74.

10. Koukouritaki SB, Simpson P, Yeung CK, Rettie AE, Hines RN. Human hepatic flavin-containing monooxygenases 1 (FMO1) and 3 (FMO3) developmental expression. Pediatric research. 2002;51(2):236-43.

11. Yokoi T. Essentials for starting a pediatric clinical study (1): Pharmacokinetics in children. J Toxicol Sci. 2009;34 Suppl 2:SP307-12.

12. Yanni SB, Annaert PP, Augustijns P, Ibrahim JG, Benjamin DK, Jr., Thakker DR. In vitro hepatic metabolism explains higher clearance of voriconazole in children versus adults: role of CYP2C19 and flavin-containing monooxygenase 3. Drug metabolism and disposition: the biological fate of chemicals. 2010;38(1):25-31.

13. Cashman JR, Zhang J. Human flavin-containing monooxygenases. Annual review of pharmacology and toxicology. 2006;46:65-100.

14. Cashman JR. Human flavin-containing monooxygenase: substrate specificity and role in drug metabolism. Curr Drug Metab. 2000;1(2):181-91.

15. Cashman JR. Structural and catalytic properties of the mammalian flavin-containing monooxygenase. Chem Res Toxicol. 1995;8(2):166-81.

16. Lang DH, Yeung CK, Peter RM, Ibarra C, Gasser R, Itagaki K, et al. Isoform specificity of trimethylamine N-oxygenation by human flavin-containing monooxygenase (FMO) and P450 enzymes: selective catalysis by FMO3. Biochemical pharmacology. 1998;56(8):1005-12.

17. Omura T, Sato R. The Carbon Monoxide-Binding Pigment of Liver Microsomes. I. Evidence for Its Hemoprotein Nature. J Biol Chem. 1964;239:2370-8.

18. Hines RN, McCarver DG. The ontogeny of human drug-metabolizing enzymes: phase I oxidative enzymes. J Pharmacol Exp Ther. 2002;300(2):355-60.

19. Wrighton SA, Molowa DT, Guzelian PS. Identification of a cytochrome P-450 in human fetal liver related to glucocorticoid-inducible cytochrome P-450HLp in the adult. Biochem Pharmacol. 1988;37(15):3053-5.

20. Leeder JS, Gaedigk R, Marcucci KA, Gaedigk A, Vyhlidal CA, Schindel BP, et al. Variability of CYP3A7 expression in human fetal liver. J Pharmacol Exp Ther. 2005;314(2):626-35.

21. Lapple F, von Richter O, Fromm MF, Richter T, Thon KP, Wisser H, et al. Differential expression and function of CYP2C isoforms in human intestine and liver. Pharmacogenetics. 2003;13(9):565-75.

22. Ohtsuki S, Schaefer O, Kawakami H, Inoue T, Liehner S, Saito A, et al. Simultaneous absolute protein quantification of transporters, cytochromes P450, and UDP-glucuronosyltransferases as a novel approach for the characterization of individual human liver: comparison with mRNA levels and activities. Drug Metab Dispos. 2012;40(1):83-92.

23. McDonald MG, Rieder MJ, Nakano M, Hsia CK, Rettie AE. CYP4F2 is a vitamin K1 oxidase: An explanation for altered warfarin dose in carriers of the V433M variant. Mol Pharmacol. 2009;75(6):1337-46.

Chapter IV: Expression of CYP1 Enzymes in KLE Endometrial Cancer Cell Line and Normal Tissues

TABLE OF CONTENTS

TABLE OF FIGURES

4.1 Introduction

CYP1B1metabolizes many polycyclic aromatic hydrocarbon-containing procarcinogens, such as benzo(a)pyrene and 7,12-dimethylbenz[a]anthracene (1). This enzyme is expressed in many types of human cancers, including breast (2), colon (3), prostate (4), endometrium (5) and ovary (6). Steroid hormone-related cancers, such as breast, ovarian, uterine and endometrial (7-9), were found to have high levels of CYP1B1(10). The capability of CYPs to activate toxins has been exploited to treat cancers. Chemotherapy drugs like ifosfamide, cyclophosphamide, and dacarbazine are specifically activated by CYP enzymes in tumor tissues (11). CYP1B1 either is absent or at very low levels in corresponding normal tissues, making it an ideal target for anticancer prodrug therapies (12-14).

CYP1B1 shares more than 40% amino acid sequence identity with two closely related enzymes, CYP1A1 and CYP1A2. CYP1A2 is expressed at high levels in the liver, while CYP1A1 is expressed in extrahepatic organs/tissues. These three enzymes have overlapping substrates, but sometimes generate different products. For example, the hormone 17β-estradiol (E2) is oxidized by CYP1A1 and CYP1A2 to form primarily 2-OH-estradiol (2E2) (15), which is harmless; CYP1B1 converts E2 to 4-OH-estradiol (4E2), which is carcinogenic (16).

An ideal CYP1B1-dependent anticancer prodrug should not show toxicity following metabolism by CYP1A1/1A2, in order to prevent collateral damage to normal tissues. Based on this principle, *in vitro* cell-based screenings of chemical libraries for new CYP1B1-dependent prodrugs should include, but not be limited to, two stages: first, prodrug toxicity should be demonstrated in *in vitro* cell models that overexpress CYP1B1 only, and second, qualified

compounds need to be screened in normal *in vitro* cell models that express CYP1A1 and/or CYP1A2, displaying a lack of toxicity.

Presently, compound library screens are hindered by the lack of well-characterized cell lines for first stage screening. The human uterus adenocarcinoma cell line KLE, derived from a poorly differentiated endometrial cancer, possesses tumorigenic activity in nude mice (17) and has been shown to overexpress CYP1B1 (5). However, no absolute activity or protein quantification data showing the KLE cell line to solely express CYP1B1 is available. Previous attempts in the laboratory to characterize CYP1A and CYP1B1 expression in the cell line using enzymatic activity, with estradiol as the substrate, have been unsuccessful, due to the slow enzymatic conversion rate and high background of the E2 chemical stock, although new efforts are ongoing to improve metabolite extraction using methyl tert-butyl ether (MTBE). This left absolute and specific UPLC-MRM-targeted quantification as the only means by which CYP1A1, CYP1A2, and CYP1B1 expression in KLE cells could be determined. The goal of this chapter is to characterize CYP1A1, CYP1A2, and CYP1B1 expression in the KLE cell line and normal human tissues using a UPLC-MRM-based targeted proteomic approach.

4.2 Materials and Methods

4.2.1 Chemicals, Enzymes, Tissues, and Cells. Dulbecco's modified Eagle's medium (DMEM), DMEM/F-12 (1:1), and fetal bovine serum (FBS) were purchased from Life Technologies (Carlsbad, CA). A BCA protein assay kit was purchased from Pierce Biotechnology (Rockford, IL). Optima-grade acetonitrile, water, formic acid, and acetic acid were obtained from Fisher Scientific (Pittsburgh, PA). Ammonium bicarbonate, dimethyl sulfoxide, dithiothreitol, and iodoacetamide were purchased from Sigma-Aldrich (Saint Louis, MO). Recombinant human CYP1A1, CYP1A2, and CYP1B1 Supersomes, prepared from baculovirus-infected insect cells expressing human CYP enzymes, were purchased from Corning Gentest (Woburn, MA). Synthetic ^{13}C and ^{15}N stable isotope-labeled crude signature peptides were acquired from Thermo Scientific (Ulm, Germany). All synthetic peptide sequences were confirmed by MS/MS fragmentation analysis using a Waters Xevo TQ-S triple-quadrupole MS (Milford, MA). Sequencing-grade modified trypsin was purchased from Promega (Madison, WI). Human kidney, liver, and intestinal microsomes were purchased from XenoTech, LLC (Lenexa, KS). A slice of human brain frontal cortex was kindly provided by the University of Kansas Medical Center (Kansas City, MO). KLE cells were purchased from American Type Culture Collection (Manassas, VA). Blank human plasma (collected in K_2-EDTA tubes) was purchased from Innovative Research (Novi, MI).

4.2.2 Cell Culture. KLE cells were cultured in DMEM/F-12 (1:1) medium without phenol red and supplemented with 10% (v/v) FBS, and were maintained at 37°C with 5% CO_2 and 95% humidity. The medium was refreshed twice a week. Cells were harvested on different days post-seeding using TrypLETM Express for the absolute measurement of CYP1B1 quantity.

4.2.3 Microsome Isolation from Cell Culture and Human Brain Frontal Cortex Tissues. Microsomes from human brain and KLE cells were prepared as reported previously (18) with minor modifications. Briefly, cells and brain frontal cortex tissue were homogenized in a buffer (pH 7.4) containing 50 mM Tris-HCl, 1 mM EDTA, and a protease inhibitor cocktail (Roche, Indianapolis, IN),. Following homogenization, the samples were centrifuged at 10,000 x *g* for 30 minutes and the supernatant collected. The supernatant then was centrifuged at 150,000 x *g* for 60 minutes. The resulting pellet was resuspended in a buffer (pH 7.4) containing 10 mM potassium phosphate and 20% sucrose. Microsomal protein concentration was determined using a BCA assay. The microsomes were stored at -80^{o}C.

4.2.4 Targeted quantitative proteomic method for protein quantification. Targeted proteomic quantification of CYP1B1, CYP1A1, and CYP1A2 protein levels in microsomes was performed as described previously for other CYP enzymes with minor modifications (19, 20). Briefly, protein samples (30 µg) were reduced in an ammonium bicarbonate buffer (pH 8.0; 50 mM final concentration) containing dithiothreitol (4 mM final concentration) and heated at 60°C for 60 min to denature the proteins. After cooling to room temperature, the samples (90 µl total volume) were alkylated with iodoacetamide (10 mM final concentration) for 20 min in the dark before digestion with 1 µg trypsin at 37°C for 4 h. Recombinant human CYP1A1, CYP1A2, and CYP1B1 Supersomes of known concentrations were used to create calibration standards (0.002 to 5 pmol/digestion). All reactions were carried out in Protein LoBind microcentrifuge tubes (Eppendorf, Hamburg, Germany) to minimize protein or peptide loss due to binding. Reactions were cold-quenched with storage at -80°C. The signature peptide sequences used were ELVALLVR for CYP1B1, GFYIPK for CYP1A1, and YLPNPALQR for CYP1A2. A mixture of stable isotope-labeled signature peptides (1 µl; internal standards) were spiked into thawed

samples prior to loading into an autosampler (6°C) for UPLC-MRM analysis as described previously (19, 20). The mass transitions used during UPLC-MRM analysis were m/z 456.8→571.4 for ELVALLVR, m/z 362.7→357.3 for GFYIPK, and m/z 536.6→584.4 for YLPNPALQR. The lower limit of quantification was 0.07 pmol CYP/mg microsomal protein for CYP1B1, CYP1A1 and CYP1A2.

4.2.5 Data Analysis. All measurements were done in triplicate. Student's *t* tests (two-tailed, unpaired) were used to compare the pairs of measurements. All data analyses were performed using GraphPad Prism.

4.3 Results and Discussion

4.3.1 CYP1B1 expression in human brain, plasma, kidney, liver, and intestine. CYP1A1 and CYP1A2 are known to be expressed in the human liver and intestines, but not CYP1B1 (19, 21-23). CYP levels in the human brain, plasma, and kidney are much lower, making these atypical sites for drug metabolism. Microsomes isolated from each of these tissues were tested by CYP1B1-targeted UPLC-MRM-based absolute quantification for confirmation of historical observations, as well as for examining the specificity of the targeted assay in different matrices. As shown in Figure 15, the chromatographic peak that eluted at 8.42 min, indicating the presence of CYP1B1, was not observed in any of the human tissue samples. Despite the high level of sensitivity (LLOQ = 0.07 pmol/mg microsomal protein), the negative CYP1B1 signal from different tissue microsomes showed that our absolute protein quantification assay had very good target selectivity in different tissue matrices. These results also confirm previous reports that normal human tissues express very little or no CYP1B1. Some publications, however, have shown an appreciable or dominant amount of CYP1B1 mRNA in human small intestine and kidney (21, 22). The lack of correlation between mRNA and protein expression indicates that relative mRNA level may not directly translate to corresponding protein expression. This also demonstrates the importance of looking at absolute protein quantity when characterizing enzyme expression.

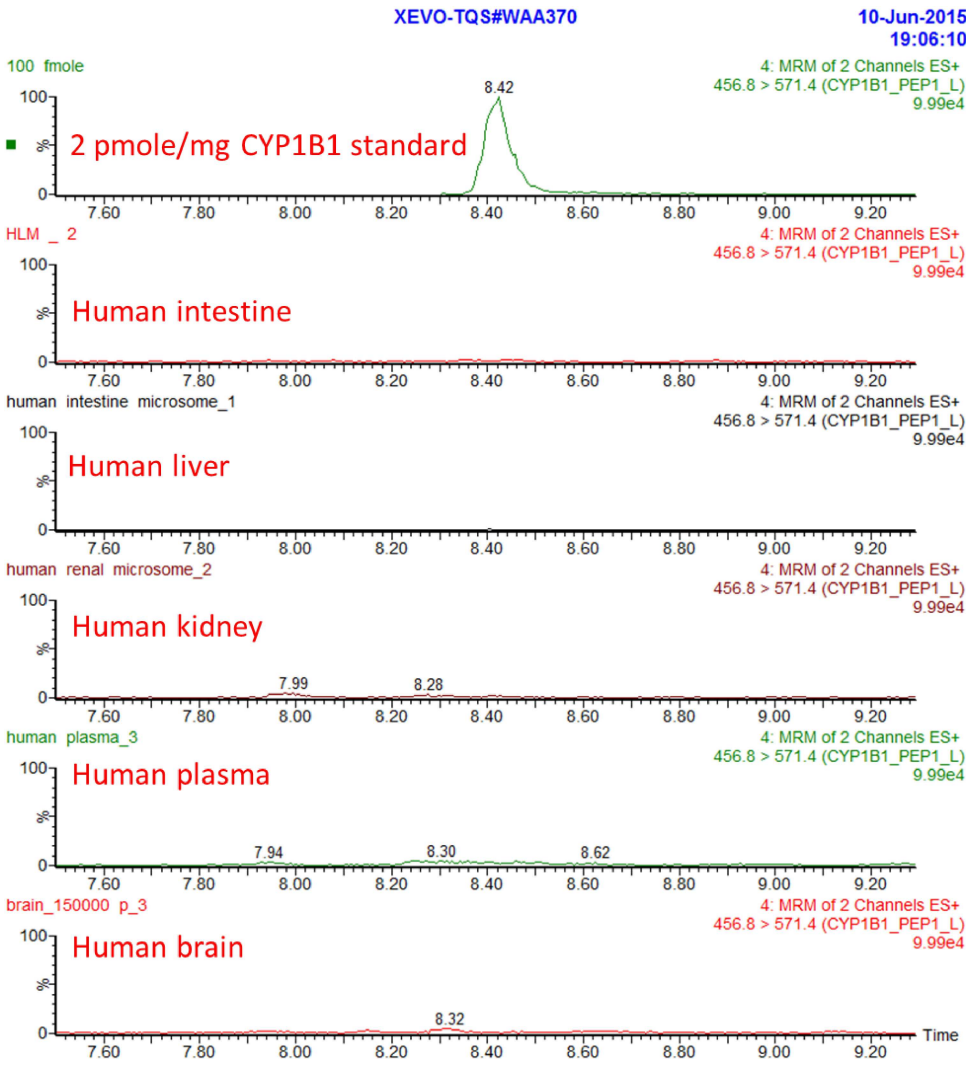

Figure 15. CYP1B1 expression in different human tissues. CYP1B1 signature peptide signals from CYP1B1 recombinant protein standards and human intestinal, hepatic, renal, plasma, and brain frontal cortex microsomes detected by UPLC-MRM targeted proteomics**.** Digests from each sample, equivalent to 3 µg of protein, were loaded onto the column for separation and MS quantification.

4.3.2 CYP1A1, CYP1A2, and CYP1B1 expression in KLE cell microsomes. KLE cells cultured for 9 days post-seeding were harvested and processed for microsome isolation. UPLC-MRM signals for CYP1B1, CYP1A1, and CYP1A2 recombinant proteins, which serve as positive controls, (Figure 16, upper chromatograms) were compared to the signals from KLE microsomes (Figure 16, lower chromatograms). CYP1B1 was present in KLE cell microsomes. No detectable expression of CYP1A1 or CYP1A2 was found.

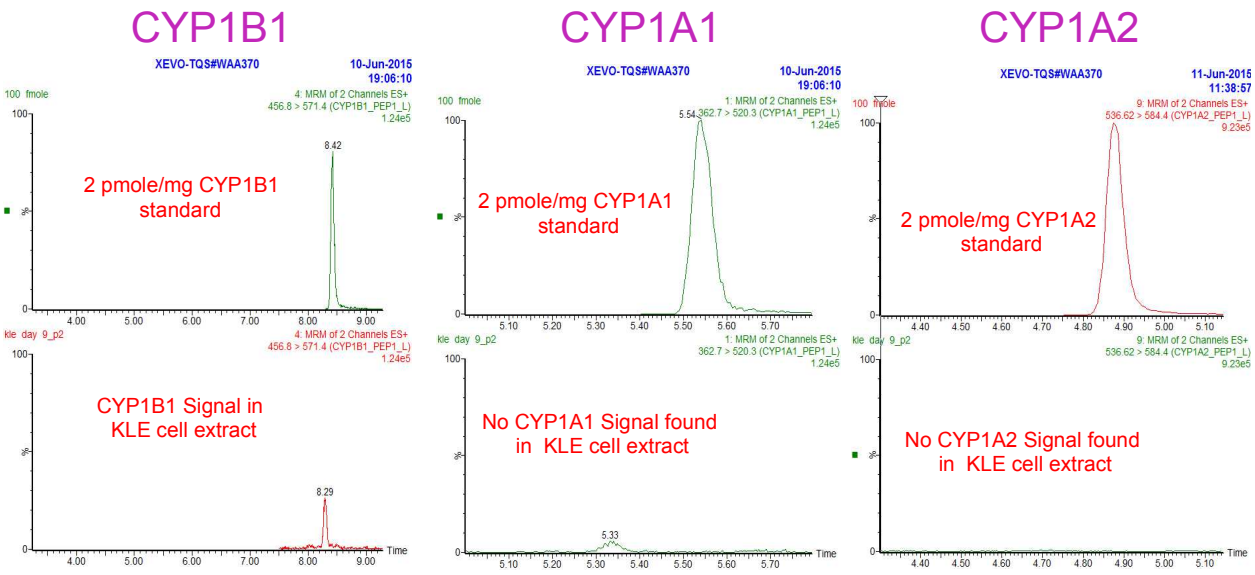

Figure 16. CYP1B1, CYP1A1, and CYP1A2 expression in KLE microsomes. Digests from each sample, equivalent to 3 µg of protein, were loaded onto the column for separation and MS quantification.

As discussed in the introduction, at least two stages of selection should be used when screening for CYP1B1-dependent anticancer prodrugs: 1) positive toxicity demonstrated in cell lines solely expressing CYP1B1, and 2) a lack of toxicity in normal human cells. Figure 16 clearly shows that the KLE cell line fits the first criteria for prodrug screening.

4.3.3 Expression of CYP1B1 in KLE cells at different days post-seeding. CYP1B1 protein expression increased from day 3 to day 9 post-seeding (0.31 vs. 0.68 pmol/mg microsomes) and remained at a similar level on day 14 post-seeding (0.41 pmol/mg microsomes) (Figure 17A). Protein expression tracked quite well with mRNA expression in the KLE cells at different days post-seeding (Figure 17B; generated and kindly provided by Zhiying Wang, Ph.D.).

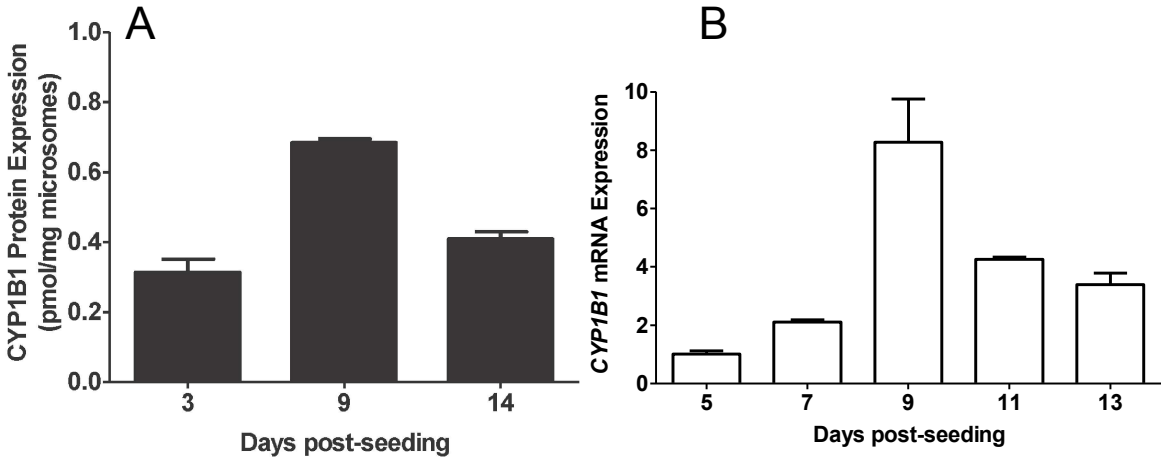

Figure 17. CYP1B1 expression in KLE cells at different days post-seeding. CYP1B1 protein expression (**A**) was quantified by UPLC-MRM-targeted proteomics. Chromatographic peak areas of KLE microsomal digest were compared to those from serial concentrations of CYP1B1 recombinant protein digests, allowing the CYP1B1 concentration in KLE microsomes to be extrapolated. CYP1B1 mRNA expression (**B**) on days 5-13 post-seeding were measured by RT-PCR.

These results show that the best window for CYP1B1-dependent prodrug screening using KLE cells would be approximately 9 days post-seeding, when CYP1B1 protein expression is the highest. However, an appreciable amount of CYP1B1 expression did last for at least two weeks. Dr. Zhiying Wang also transiently transfected CYP1B1 into human HEK293 cells and measured CYP1B1 mRNA expression at different days post-transfection (Wang, Z., Chen, Y., and Wang.

M. Z.; J Biomol Screen (under 3rd review)). Her results showed that KLE cells were superior to transiently transfected HEK293T cells as CYP1B1 expression quickly diminished in the transfected cells.

4.3.4 Summary. Absolute CYP1 expression in KLE cells was quantified for the first time using a UPLC-MRM-targeted proteomic approach. Quantification showed that KLE cells lack CYP1A1 and CYP1A2 expression, which are found in normal human organs/tissues. An appreciable amount of CYP1B1, which is usually found in many steroid-related human tumor tissues, was expressed. The highest CYP1B1 expression in KLE cells occurred around day 9 post-seeding, but an appreciable amount was seen for at least two weeks. In conclusion, KLE cells will be a good fit for CYP1B1-dependent anticancer prodrug screening.

4.4 References

1. Shimada T, Hayes CL, Yamazaki H, Amin S, Hecht SS, Guengerich FP, et al. Activation of chemically diverse procarcinogens by human cytochrome P-450 1B1. Cancer Res. 1996;56(13):2979-84.

2. McKay JA, Melvin WT, Ah-See AK, Ewen SW, Greenlee WF, Marcus CB, et al. Expression of cytochrome P450 CYP1B1 in breast cancer. FEBS Lett. 1995;374(2):270-2.

3. Gibson P, Gill JH, Khan PA, Seargent JM, Martin SW, Batman PA, et al. Cytochrome P450 1B1 (CYP1B1) is overexpressed in human colon adenocarcinomas relative to normal colon: implications for drug development. Mol Cancer Ther. 2003;2(6):527-34.

4. Tokizane T, Shiina H, Igawa M, Enokida H, Urakami S, Kawakami T, et al. Cytochrome P450 1B1 is overexpressed and regulated by hypomethylation in prostate cancer. Clin Cancer Res. 2005;11(16):5793-801.

5. Saini S, Hirata H, Majid S, Dahiya R. Functional significance of cytochrome P450 1B1 in endometrial carcinogenesis. Cancer Res. 2009;69(17):7038-45.

6. McFadyen MC, Cruickshank ME, Miller ID, McLeod HL, Melvin WT, Haites NE, et al. Cytochrome P450 CYP1B1 over-expression in primary and metastatic ovarian cancer. Br J Cancer. 2001;85(2):242-6.

7. Liu JY, Yang Y, Liu ZZ, Xie JJ, Du YP, Wang W. Association between the CYP1B1 polymorphisms and risk of cancer: a meta-analysis. Mol Genet Genomics. 2015;290(2):739-65.

8. Li C, Long B, Qin X, Li W, Zhou Y. Cytochrome P1B1 (CYP1B1) polymorphisms and cancer risk: a meta-analysis of 52 studies. Toxicology. 2015;327:77-86.

9. Zhang H, Li L, Xu Y. CYP1B1 polymorphisms and susceptibility to prostate cancer: a meta-analysis. PloS one. 2013;8(7):e68634.

10. Gajjar K, Martin-Hirsch PL, Martin FL. CYP1B1 and hormone-induced cancer. Cancer Lett. 2012;324(1):13-30.

11. Patterson LH, Murray GI. Tumour cytochrome P450 and drug activation. Curr Pharm Des. 2002;8(15):1335-47.

12. McFadyen MC, Murray GI. Cytochrome P450 1B1: a novel anticancer therapeutic target. Future Oncol. 2005;1(2):259-63.

13. Guengerich PF, Chun YJ, Kim D, Gillam EM, Shimada T. Cytochrome P450 1B1: a target for inhibition in anticarcinogenesis strategies. Mutat Res. 2003;523-524:173-82.

14. Swanson HI, Njar VC, Yu Z, Castro DJ, Gonzalez FJ, Williams DE, et al. Targeting drug-metabolizing enzymes for effective chemoprevention and chemotherapy. Drug Metab Dispos. 2010;38(4):539-44.

15. Spink DC, Eugster HP, Lincoln DW, 2nd, Schuetz JD, Schuetz EG, Johnson JA, et al. 17 beta-estradiol hydroxylation catalyzed by human cytochrome P450 1A1: a comparison of the activities induced by 2,3,7,8-tetrachlorodibenzo-p-dioxin in MCF-7 cells with those from heterologous expression of the cDNA. Arch Biochem Biophys. 1992;293(2):342-8.

16. Hayes CL, Spink DC, Spink BC, Cao JQ, Walker NJ, Sutter TR. 17 beta-estradiol hydroxylation catalyzed by human cytochrome P450 1B1. Proc Natl Acad Sci U S A. 1996;93(18):9776-81.

17. Richardson GS, Dickersin GR, Atkins L, MacLaughlin DT, Raam S, Merk LP, et al. KLE: a cell line with defective estrogen receptor derived from undifferentiated endometrial cancer. Gynecol Oncol. 1984;17(2):213-30.

18. Fisher CD, Lickteig AJ, Augustine LM, Ranger-Moore J, Jackson JP, Ferguson SS, et al. Hepatic cytochrome P450 enzyme alterations in humans with progressive stages of nonalcoholic fatty liver disease. Drug Metab Dispos. 2009;37(10):2087-94.

19. Michaels S, Wang MZ. The revised human liver cytochrome P450 "Pie": absolute protein quantification of CYP4F and CYP3A enzymes using targeted quantitative proteomics. Drug Metab Dispos. 2014;42(8):1241-51.

20. Wang MZ, Wu JQ, Dennison JB, Bridges AS, Hall SD, Kornbluth S, et al. A gel-free MS-based quantitative proteomic approach accurately measures cytochrome P450 protein concentrations in human liver microsomes. Proteomics. 2008;8(20):4186-96.

21. Shi Z, Dragin N, Galvez-Peralta M, Jorge-Nebert LF, Miller ML, Wang B, et al. Organ-specific roles of CYP1A1 during detoxication of dietary benzo[a]pyrene. Mol Pharmacol. 2010;78(1):46-57.

22. Bieche I, Narjoz C, Asselah T, Vacher S, Marcellin P, Lidereau R, et al. Reverse transcriptase-PCR quantification of mRNA levels from cytochrome (CYP)1, CYP2 and CYP3 families in 22 different human tissues. Pharmacogenet Genomics. 2007;17(9):731-42.

23. Paine MF, Hart HL, Ludington SS, Haining RL, Rettie AE, Zeldin DC. The human intestinal cytochrome P450 "pie". Drug metabolism and disposition: the biological fate of chemicals. 2006;34(5):880-6.

Chapter V: Induction of CYP4F2 in HepaRG and Sandwich-Cultured Hepatocytes (SCH) with Lovastatin for the Study of Drug-Drug Interactions between Warfarin and Lovastatin

TABLE OF CONTENTS

TABLE OF FIGURES

5.1 Introduction

Warfarin is one of the most commonly administered anti-coagulant drugs (1, 2). In the United States, two million people take warfarin annually for the treatment of blood clots, stroke, myocardial infarction, and other diseases (2, 3). However, this drug is responsible for the second highest number of emergency room visits, behind insulin, because of its adverse effects, mainly the risk of a lethal hemorrhage (4). Among the ten thousand reported cases of warfarin-induced hemorrhages in the United States from 1993 to 2006, a thousand were fatal (5). Additionally, the narrow therapeutic window of this drug has considerable inter-patient variability. The most important factors influencing this are co-administered drugs (6) and genetic polymorphisms (7-13).

Warfarin is metabolized by multiple CYP enzymes in the human liver, including CYP2C9 (14), CYP3A4 and CYP1A2 (15, 16). Polymorphisms in CYP2C9 and VKORC1, a target of warfarin, account for up to 25% of warfarin dose variance (12, 17). Another 20-30% of the variability could be explained by pharmacokinetic or pharmacodynamic interactions between warfarin and other drugs (6). Approximately 144 drugs have been reported to interact with warfarin (18). However, after the consideration of all known factors influencing dose variance, only about half of the clinical cases have been accounted for (4, 7). The unknown underlying reasons for dose variance require additional investigation at the molecular level.

Warfarin reduces the circulating blood level of vitamin K1 (VK1), which functions as a blood clotting factor. In 2009, McDonald *et. al.* discovered that CYP4F2 genetic polymorphisms underlie warfarin dose variance. They demonstrated that VK1 was metabolized almost

exclusively by this enzyme. A CYP4F2 mutant allele caused an approximate 25% reduction in enzymatic expression, leading to decreased VK1 depletion; therefore, CYP4F2 mutant carriers need additional warfarin to reach the same drug potency as wild-type carriers. (19)

In 2007, Hsu *et. al.* provided the first evidence that CYP4F2 expression was induced by lovastatin (1μM), a drug used in the treatment of hypercholesterolemia, in both HepG2 (human liver carcinoma) cells and primary human hepatocytes (20). They found both CYP4F2 mRNA and protein expression levels were elevated following lovastatin treatment. We hypothesize that lovastatin may interact with warfarin through the induction of hepatic CYP4F2. Consequently, patients who take lovastatin may require a lower dose of warfarin in order to avoid warfarin's dangerous adverse effects.

This hypothesis could be tested in different *in vitro* hepatic cell models, including differentiated HepaRG (human hepatoma) cells and primary human hepatocytes. The post-oral maximum human plasma lovastatin level that occurred four hours after lovastatin administration (40 mg) was determined previously in our lab to be less than 100 nM (21); therefore, the lovastatin concentrations used in *in vitro* cell cultures to study induction should be around 100 nM. Subtle changes in CYP4F2 expression due to lovastatin may require a highly sensitive assay. Western blots do not have adequate sensitivity. In addition, there is no commercially available CYP4F2 specific antibody; CYP4F2 and CYP4F3B share greater than 93% amino acid sequence identity. However, Michaels *et. al.* established a highly specific and sensitive LC-MRM-based targeted method for the absolute quantification of CYP4F2, which potentially could be applied to measure CYP4F2 induction in *in vitro* hepatic cell models following lovastatin treatment.

The goal of this chapter was to perform induction studies in differentiated HepaRG cells and primary human hepatocytes with lovastatin at various concentrations. CYP4F2 protein and mRNA expression were quantified by a UPLC-MRM-based targeted proteomic approach and RT-PCR, respectively. If obvious, or statistically significant, CYP4F2 induction were measured following treatment with clinically significant lovastatin concentrations (lower than 100 nM), the observation may support the hypothesis. If lovastatin does not induce CYP4F2, the hypothesis will be rejected.

5.2 Materials and Methods

5.2.1 Chemicals and Reagents. Lovastatin was purchased from U.S. Pharmacopeia (Rockville, MD). DMSO, ammonium bicarbonate, dithiothreitol, iodoacetamide, and D-glucose were purchased from Sigma-Aldrich (St. Louis, MO). Recombinant human CYP3A4, CYP4F2 and CYP4F3B Supersomes, prepared from baculovirus-infected insect cells expressing human CYP enzymes, were obtained from Corning Gentest (Woburn, MA). Williams's E medium (WME), TrypLE™ Express, FBS, GlutaMax™, SYTO® 82 orange fluorescent nucleic acid stain, ROX reference dye, and TRIzol® reagent were from Life Technologies (Carlsbad, CA). GoTaq® G2 Hot Start Colorless Master Mix was acquired from Promega (Madison, WI). A BCA protein assay kit was purchased from Pierce Biotechnology (Rockford, IL).

5.2.2 Cell Cultures. HepaRG cells and additives for HepaRG Growth and Differentiation Mediums were purchased from Biopredic International (Overland Park, KS). Primary human hepatocytes and OptIncubate hepatocyte medium was provided by XenoTech, LLC. (Lenexa, KS). HepaRG cells were cultured in Growth medium (WME supplemented with GlutaMax and HepaRG Growth Medium Supplement) for 2 weeks, followed by 2 weeks of Differentiation medium (WME supplemented with GlutaMax and HepaRG Differentiation Medium Supplement). The medium was refreshed every other day. Primary human hepatocytes were isolated and plated by the vendor. The medium was changed daily. All cells were maintained at 37°C in 5% CO_2 and 95% humidity. Induction experiments were carried out less than 72 hours after plating in primary human hepatocytes.

5.2.3 Lovastatin Induction. Lovastatin stocks were prepared with DMSO, aliquoted and stored at -20°C prior to use. Lovastatin stocks or DMSO (vehicle) were added to HepaRG

differentiation medium to give final concentrations of 0, 0.01, 0.1, 1 and 25 μM, or to OptIncubate hepatocyte medium to give 0, 0.1, 1 and 10 μM; vehicle concentrations were equal to or less than 0.1% (v/v). The experiment was initiated by replacing the culture medium with lovastatin- or vehicle-containing medium. Cells were harvested at 24 hours with TRIzol for mRNA isolation and at 48 hours for cell microsomal protein extraction.

5.2.4 Reverse transcription and real-time PCR. Total RNA was isolated from HepaRG cells and primary human hepatocytes using TRIzol reagent according to the manufacturer's protocol. RNA concentration and purity were determined using a Nanodrop® ND1000 spectrophotometer (Nanodrop Technologies, Wilmington, DE). One μg RNA was reverse transcribed to cDNA using a High Capacity cDNA Reverse Transcription kit. Following first strand cDNA synthesis, 12.5 ng cDNA, primer mix (1uM final), water and homemade RT-PCR reagent were mixed to give a final volume of 25 μL. The homemade RT-PCR reagent recipe was kindly provided by Dr. Dongwei Hui in the Department of Pharmacology and Toxicology at the University of Kansas; briefly, SYTO® 82 orange fluorescent nucleic acid stain (10 μM) and ROX reference dye (5 nM) were mixed with GoTaq® G2 Hot Start Colorless Master Mix (2x). PCR amplification and real-time monitoring were performed with an Applied Biosystems 7500 Fast real-time PCR system to evaluate CYP3A4, CYP4F2, LDL-receptor, HMG-CoA reductase, and TATA-box binding protein (TBP; housekeeping gene) expression. The primer sequences used were: 5'- TTCCAACTCACAGGATGAAGTAAG -3' (forward) and 5'-GGACACACAAGCTGGGAAGA -3' (reverse) for HMC-CoA reductase; 5'-GATCCTGTTCATGGCTTCATGTA -3' (forward) and 5'- GGCCAGCCTCTTTTCATCCT -3' (reverse) for LDL-receptor; 5'- CTTCACAAACCGGAGGCCTTTTGGT -3' (forward) and 5'-TCCTTGAGTTTTCCACTGGTGAAGG -3' (reverse) for CYP3A4; 5'-

CCTGACAGAAGGATGTCCCAG-3' (forward) and 5'- CCCCAAAACCAGTTCCGTCT -3' (reverse) for CYP4F2; 5'- CATCTTCCCCGTCATCCGTTTT-3' (forward) and 5'- TTTTGTCACAAGGGCACTGAGC -3' (reverse) for CYP4F3B; 5'- ATCTTTGCAGTGACCCAGCA -3' (forward) and 5'- GTAAGGTGGCAGGCTGTTGT -3' (reverse) for TBP. Amplification was performed with an initial denaturation of 95°C for 10 min followed by 40 cycles of 95°C for 10 s and 60°C for 35 s. The comparative threshold method was used to calculate the relative amount of mRNA in a sample compared to other samples.

5.2.5 Microsome isolation and LC-MRM-targeted method for protein quantification. Microsomes were prepared from HepaRG cells and primary human hepatocytes as reported previously (22), with minor modifications. Briefly, harvested cells were homogenized in a buffer (pH 7.4) containing 50 mM Tris-HCl, 1 mM EDTA, and protease inhibitor cocktail (Roche, Indianapolis, IN) with a Dounce homogenizer. After homogenization, the samples were centrifuged at 10,000 x g for 30 min. The supernatants were collected and centrifuged again at 150,000 x *g* for 60 min. The resulting pellet was resuspended in a buffer (pH 7.4) containing 10 mM potassium phosphate and 20% (w/v) sucrose. Microsomal protein concentrations were measured using a BCA assay. The microsomes were stored at -80ºC.

Targeted proteomic quantification of CYP3A4, CYP4F2 and CYP4F3B protein levels in microsomal fractions was performed as described previously for other CYP enzymes with minor modifications (23, 24). Briefly, protein samples (30 µg) were reduced in an ammonium bicarbonate buffer (pH 8.0; 50 mM final concentration) containing dithiothreitol (4 mM final concentration) and heated at 60°C for 60 min to denature the proteins. After cooling to room temperature, the samples (90 µl total volume) were alkylated with iodoacetamide (10 mM final concentration) for 20 min in the dark and then digested with 1 µg trypsin at 37°C for 4 h.

Recombinant human CYP3A4, CYP4F2, and CYP4F3B Supersomes of known concentrations were used to create calibration standards (ranged from 0.002 to 5 pmol/digestion). All reactions were carried out in Protein LoBind microcentrifuge tubes (Eppendorf, Hamburg, Germany) to minimize protein or peptide loss due to binding. Reactions were quenched with storage at -80°C. A mixture of stable isotope-labeled signature peptides (1 µl; Thermo Scientific, Ulm, Germany) were spiked into thawed samples as internal standards prior to loading onto the autosampler (6°C) for ultra-high pressure liquid chromatography-tandem mass spectrometry (UPLC-MS/MS) analysis as described previously.(23, 24)

5.2.6 Statistical analysis. All experiments were conducted in triplicate or quadruplicate, unless noted otherwise. Student's t tests (two-tailed, unpaired) were used to compare pairs of measurements. All statistical analyses were performed using Prism 5.0. $P < 0.05$ was considered significant.

5.3 Results

5.3.1 Induction of HepaRG cells by lovastatin. HepaRG cells were grown in growth medium for a minimum of two weeks prior to switching to differentiation medium. Minor toxicity was observed upon the switch; many attached HepaRG cells detached. The number of suspended cells decreased with each medium change and by the end of the first week of differentiation, no suspended cells remained. At the end of the second week, a mixed population of two cell morphology types were observed: hepatocyte-like colonies surrounded by epithelium-like monolayers. These two morphologies are commonly observed in differentiated HepaRG cell cultures (25, 26).

In our previous induction study, CYP4F2 mRNA expression and DB289 *O*-demethylation activity peaked around 24 hours and 48 hours following treatment with the highest lovastatin concentration, 25 μM, respectively (data not shown). Therefore, these time points were used for the current induction study. Our lab reported previously that the peak lovastatin plasma concentration occurred 4 hours after oral administration and was lower than 100 nM (personal communication; Dr. Michael Zhuo Wang, University of Kansas). Differentiated HepaRG cells were incubated with 0 (vehicle control), 10, 100 and 1000 nM lovastatin to mimic the plasma concentration. Lovastatin is a known inducer of HMG-CoA reductase, LDL-receptor, and CYP3A4; these genes were monitored as positive controls. No statistically significant inductions were observed in any of the positive control gene or CYP4F2 mRNA levels with 10 or 100 nM lovastatin (Figure 18). Small but significant CYP4F2, HMG-CoA and LDL-receptor mRNA increases were observed with 1 μM lovastatin; there was no change in CYP3A4. At 25 μM lovastatin, all mRNA expression levels were significantly increased, with CYP3A4 increased approximately 3.5-fold compared to vehicle control.

Protein expression of CYP3A4, CYP4F2, and CYP4F3B also were monitored (Figure 18). No statistically significant difference was observed for either enzyme at any lovastatin concentration. However, in general, CYP expression per mg of cell microsomes decreased with increasing lovastatin concentration.

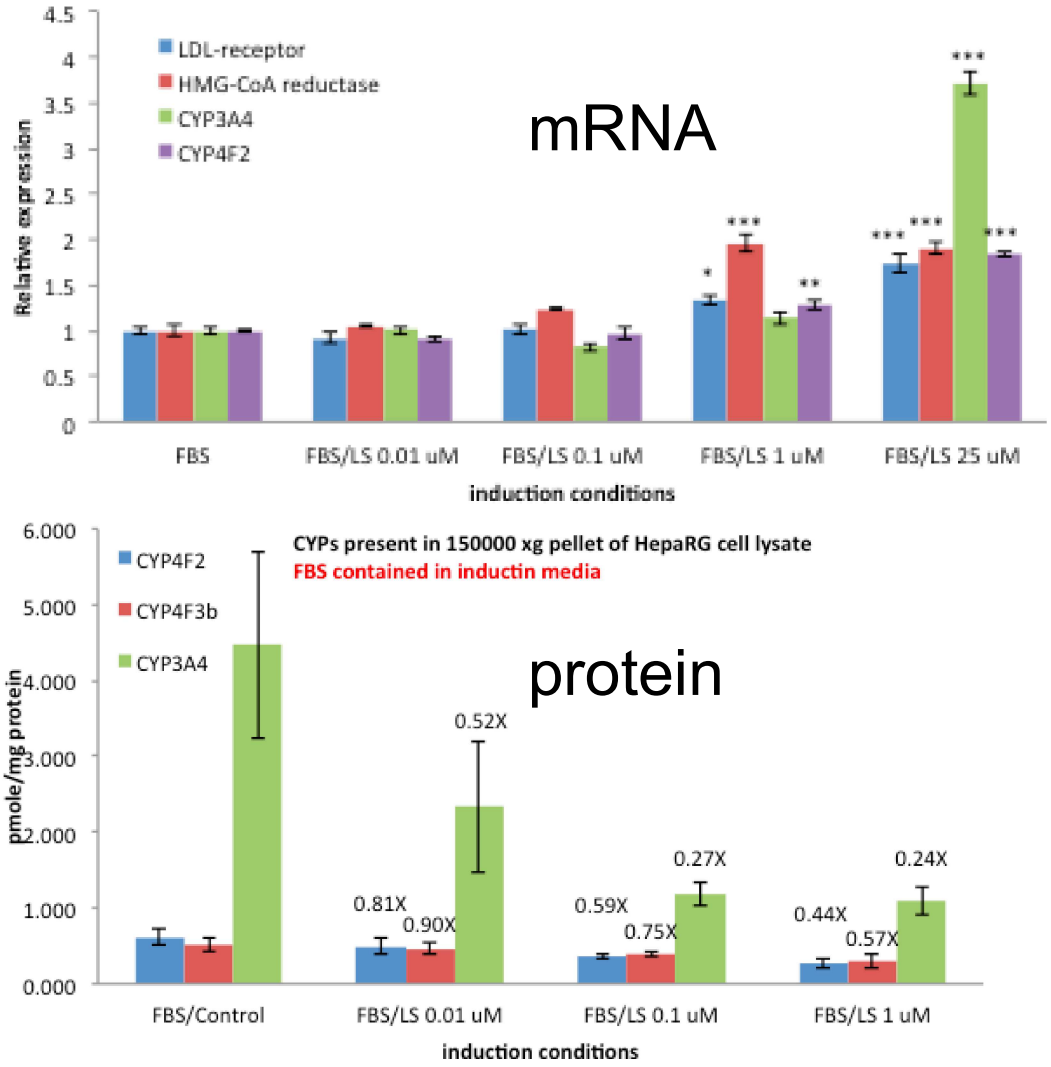

Figure 18. mRNA and protein expression of CYP4F2 and other targets in differentiated HepaRG cells following treated by lovastatin. HepaRG cells were grown in growth medium for two weeks, followed by differentiation medium for another two weeks prior to treatment. Lovastatin was administered at 0, 10, 100, 1000, and 25,000 nM. mRNA expression at 24 hour post-lovastatin addition was measured by RT-PCR. Protein expression at 48 hour post-treatment was measured by UPLC-MRM-based quantitative proteomics.

5.3.2 Induction of primary human hepatocytes by lovastatin. Primary human hepatocytes were plated fresh by the vendor and cultured for less than 48 hours prior to the start of the experiment. Since lovastatin concentrations lower than 1 μM did not change CYP4F2 expression in differentiated HepaRG cells, the concentrations used in primary human hepatocytes were adjusted to 0, 0.1, 1, and 10 μM. At 0.1 μM lovastatin, two positive control genes, LDL-receptor and HMG-CoA reductase, showed a significant induction of 3.2- and 6.0-fold compared to vehicle control, respectively (Figure 19). Even though CYP4F2 mRNA increased 1.6-fold, the change was not statistically significant. At 1 μM lovastatin, CYP4F2, LDL-receptor and HMG-CoA were increased significantly, 1.8-, 4.9- and 7.4-fold, respectively. All positive control genes showed a significant increase at 10 μM lovastatin. CYP4F2 expression, surprisingly, stayed at the same level as the vehicle control.

No significant differences were measured in CYP protein expression at any lovastatin concentration (Figure 19). Compared to vehicle control, mean expression decreased with the addition of lovastatin; however, the decrease was not statistically significant, nor did it follow a dose response.

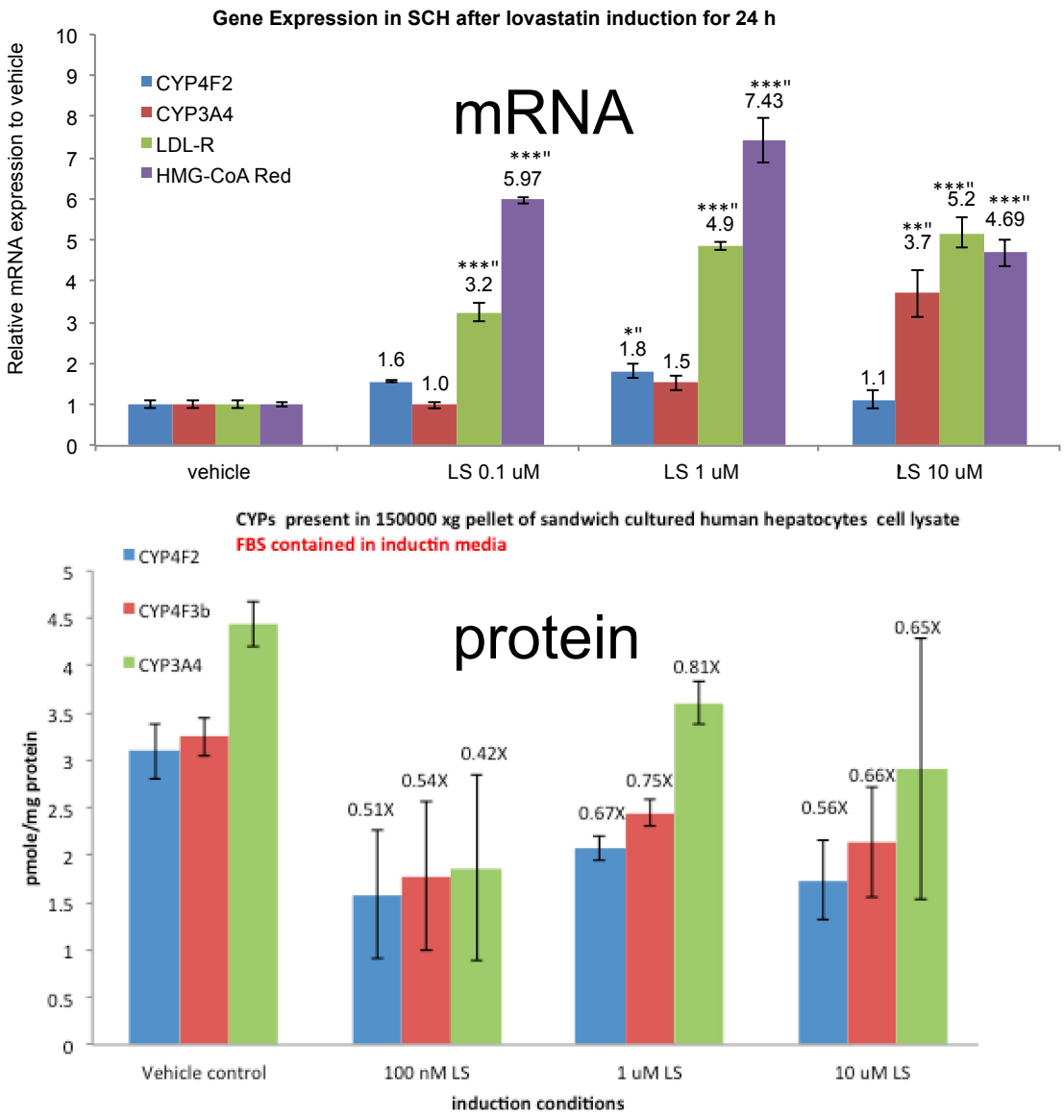

Figure 19. mRNA and protein expression in lovastatin treated primary human hepatocytes. Fresh primary human hepatocytes were treated with 0, 0.1, 1, and 10 µM lovastatin for 24 hours (mRNA) and 48 hours (protein). mRNA expression was measured by RT-PCR. Protein expression was measured by UPLC-MRM-based quantitative proteomics.

5.4 Discussion

Primary human hepatocytes are the golden standard for induction studies; however, they are expensive, lack a regular supply, not amenable to long-term studies and demonstrate large inter-individual variability. Hepatic cell lines are an inexpensive substitution. Two such surrogates that are used often are HepaRG and HepG2 cells. HepG2 cells grow quickly, but lack DME and drug transporter expression. HepaRG cells have been used in several recent studies (27-30). This cell line possesses the ability to differentiate. Following differentiation, DME, including CYPs (especially CYP3A4), and drug transporter expression levels are increased significantly (25, 31). In the current study, we compared absolute protein expression and the ability of lovastatin to induce target genes in differentiated HepaRG cells to primary human hepatocytes from a single donor. Our data showed comparable CYP3A4 expression in the two *in vitro* models; however, differentiated HepaRG cells were inferior in CYP4F2 and CYP4F3B expression. Also, HepaRG cells were less sensitive to induction by lovastatin; LDL-receptor (3.2-fold) and HMG-CoA reductase (6.0-fold) mRNA levels were increased significantly in primary human hepatocytes with 100 nM lovastatin treatment (Figure 19), while no significant increase was observed in HepaRG cells.

The *in vitro* induction experiments were successful, as the expression of the positive control genes were increased quite obviously with various lovastatin concentrations. Despite this, a significant CYP4F2 increase was not observed until 1 μM of lovastatin in both HepaRG cells and primary human hepatocytes. This concentration is at least ten times higher than the highest lovastatin plasma concentration measured in our lab (21). Therefore, the minimum CYP4F2 concentration needed *in vitro* for induction, 1uM lovastatin, is likely not attainable *in vivo*. Hsu *et. al.* first demonstrated that 1 μM lovastatin induced CYP4F2 mRNA and protein levels in

HepG2 and primary human hepatocytes (20). Increased CYP4F2 protein was not observed in the current study. However, our protein quantification varied greatly, most likely due to protein loss during mechanical cell homogenization and microsome preparation. The Dounce homogenizer used in the current study may cause reduced cellular protein levels due to adhesion. Microsome preparation by differential centrifugation is known to result in the loss of a significant amount of microsomal protein across the various steps (data not shown). These technical issues may be resolved by lysing the cells with different cell lysis techniques (*e.g.*, detergent) and/or measuring whole cell instead of microsomal CYP4F2.

Although this short-term experiment failed to support our hypothesis, there is no guarantee that long-term lovastatin users would not experience drug-drug interactions with warfarin. Current *in vitro* induction studies only last for 48 hours, whereas patients are on lovastatin for months or years. It is difficult to carry out long-term induction studies in *in vitro* models because of declining cell viability/health over time. Additional experiments are warranted before ruling out completely the potential risk of lovastatin and warfarin co-administration.

5.5 References

1. Rettie AE, Tai GY. The pharmacogenomics of Warfarin - Closing in on personalized medicine. Mol Interv. 2006;6(4):223-7.

2. Kudzma EC, Carey ET. Pharmacogenomics: personalizing drug therapy. The American journal of nursing. 2009;109(10):50-7; quiz 8.

3. Hirsh J, Dalen JE, Anderson DR, Poller L, Bussey H, Ansell J, et al. Oral anticoagulants: Mechanism of action, clinical effectiveness, and optimal therapeutic range. Chest. 2001;119(1):8S-21S.

4. Rettie AE, Tai G. The pharmocogenomics of warfarin: closing in on personalized medicine. Mol Interv. 2006;6(4):223-7.

5. Wysowski DK, Nourjah P, Swartz L. Bleeding complications with warfarin use - A prevalent adverse effect resulting in regulatory action. Archives of internal medicine. 2007;167(13):1414-9.

6. Marsh S, McLeod HL. Pharmacogenomics: from bedside to clinical practice. Human molecular genetics. 2006;15 Spec No 1:R89-93.

7. Caldwell MD, Berg RL, Zhang KQ, Glurich I, Schmelzer JR, Yale SH, et al. Evaluation of genetic factors for warfarin dose prediction. Clinical medicine & research. 2007;5(1):8-16.

8. Cavallari LH, Langaee TY, Momary KM, Shapiro NL, Nutescu EA, Coty WA, et al. Genetic and clinical predictors of warfarin dose requirements in African Americans. Clinical pharmacology and therapeutics. 2010;87(4):459-64.

9. Paola Borgiani CC, Vittorio Forte3Elisabetta Sirianni, Lucia Novelli, Placido Bramanti, Giuseppe Novelli. CYP4F2 genetic variant (rs2108622) significantly contributes to warfarin dosing variability in the Italian population. Pharmacogenomics. 2009;10(2):261-6.

10. Fava C MM, Almgren P, Rosberg L, Lippi G, Hedblad B, Engström G, Berglund G, Minuz P, Melander O. The V433M variant of the CYP4F2 is associated with ischemic stroke in male Swedes beyond its effect on blood pressure. Hypertension. 2008;52(2):373-80.

11. Cen HJ, Zeng WT, Leng XY, Huang M, Chen X, Li JL, et al. CYP4F2 rs2108622: a minor significant genetic factor of warfarin dose in Han Chinese patients with mechanical heart valve replacement. Br J Clin Pharmacol. 2010;70(2):234-40.

12. Schwarz UI, Stein CM. Genetic determinants of dose and clinical outcomes in patients receiving oral anticoagulants. Clinical pharmacology and therapeutics. 2006;80(1):7-12.

13. Cha PC, Mushiroda T, Takahashi A, Kubo M, Minami S, Kamatani N, et al. Genome-wide association study identifies genetic determinants of warfarin responsiveness for Japanese. Human molecular genetics. 2010;19(23):4735-44.

14. O'Reilly RA. Studies on the optical enantiomorphs of warfarin in man. Clinical pharmacology and therapeutics. 1974;16(2):348-54.

15. Rettie AE, Korzekwa KR, Kunze KL, Lawrence RF, Eddy AC, Aoyama T, et al. Hydroxylation of warfarin by human cDNA-expressed cytochrome P-450: a role for P-4502C9 in the etiology of (S)-warfarin-drug interactions. Chem Res Toxicol. 1992;5(1):54-9.

16. Kaminsky LS, Zhang ZY. Human P450 metabolism of warfarin. Pharmacol Ther. 1997;73(1):67-74.

17. Rieder MJ, Reiner AP, Gage BF, Nickerson DA, Eby CS, McLeod HL, et al. Effect of VKORC1 haplotypes on transcriptional regulation and warfarin dose. N Engl J Med. 2005;352(22):2285-93.

18. Company B-MSP. COUMADIN (warfarin sodium) tablet Dayly med: current medical information; 2011 [updated 10/2011. Available from: http://dailymed.nlm.nih.gov/dailymed/drugInfo.cfm?id=54115.

19. Matthew G. McDonald MJR, Mariko Nakano, Clara K. Hsia, and Allan E. Rettie. CYP4F2 is a vitamin K1 oxidase: An explanation for altered warfarin dose in carriers of the V433M variant. Molecular Pharmacology. 2009;75(6):1337-46.

20. Hsu MH, Savas U, Griffin KJ, Johnson EF. Regulation of human cytochrome P450 4F2 expression by sterol regulatory element-binding protein and lovastatin. J Biol Chem. 2007;282(8):5225-36.

21. Wujian J, Kuan-Wei P, Sihyung Y, Huijing S, Mario S, Zhuo WM. A Simple Protein Precipitation-based Simultaneous Quantification of Lovastatin and Its Active Metabolite Lovastatin Acid in Human Plasma by Ultra-Performance Liquid Chromatography-Tandem Mass Spectrometry using Polarity Switching. J Chromatogr Sep Tech. 2015;6(3):268.

22. Fisher CD, Lickteig AJ, Augustine LM, Ranger-Moore J, Jackson JP, Ferguson SS, et al. Hepatic cytochrome P450 enzyme alterations in humans with progressive stages of nonalcoholic fatty liver disease. Drug Metab Dispos. 2009;37(10):2087-94.

23. Michaels S, Wang MZ. The revised human liver cytochrome P450 "Pie": absolute protein quantification of CYP4F and CYP3A enzymes using targeted quantitative proteomics. Drug Metab Dispos. 2014;42(8):1241-51.

24. Wang MZ, Wu JQ, Dennison JB, Bridges AS, Hall SD, Kornbluth S, et al. A gel-free MS-based quantitative proteomic approach accurately measures cytochrome P450 protein concentrations in human liver microsomes. Proteomics. 2008;8(20):4186-96.

25. Kanebratt KP, Andersson TB. Evaluation of HepaRG cells as an in vitro model for human drug metabolism studies. Drug metabolism and disposition: the biological fate of chemicals. 2008;36(7):1444-52.

26. Josse R, Aninat C, Glaise D, Dumont J, Fessard V, Morel F, et al. Long-term functional stability of human HepaRG hepatocytes and use for chronic toxicity and genotoxicity studies. Drug metabolism and disposition: the biological fate of chemicals. 2008;36(6):1111-8.

27. Bucher S, Jalili P, Le Guillou D, Begriche K, Rondel K, Martinais S, et al. Bisphenol a induces steatosis in HepaRG cells using a model of perinatal exposure. Environ Toxicol. 2016.

28. Nelson LJ, Morgan K, Treskes P, Samuel K, Henderson CJ, LeBled C, et al. Human Hepatic HepaRG Cells Maintain an Organotypic Phenotype with High Intrinsic CYP450 Activity/Metabolism and Significantly Outperform Standard HepG2/C3A Cells for Pharmaceutical and Therapeutic Applications. Basic Clin Pharmacol Toxicol. 2016.

29. Jackson JP, Li L, Chamberlain ED, Wang H, Ferguson SS. Contextualizing Hepatocyte Functionality of Cryopreserved HepaRG(R) Cell Cultures. Drug metabolism and disposition: the biological fate of chemicals. 2016.

30. Nunn AD, Scopigno T, Pediconi N, Levrero M, Hagman H, Kiskis J, et al. The histone deacetylase inhibiting drug Entinostat induces lipid accumulation in differentiated HepaRG cells. Sci Rep. 2016;6:28025.

31. Gerets HH, Tilmant K, Gerin B, Chanteux H, Depelchin BO, Dhalluin S, et al. Characterization of primary human hepatocytes, HepG2 cells, and HepaRG cells at the mRNA level and CYP activity in response to inducers and their predictivity for the detection of human hepatotoxins. Cell Biol Toxicol. 2012;28(2):69-87.

Chapter VI: Quantitative Filter-Assisted Sample Preparation (qFASP) and Evaluation for Label-Free MS^E Data Independent Acquisition(DIA)-Based Global Quantification of Liver DME

TABLE OF CONTENTS

LIST OF FIGURES

LIST OF TABLES

6.1 Introduction

DME expression has an important role in the determination of drug pharmacokinetics, pharmacodynamics, and toxicity (32-34). The quantification of DMEs in the microsomal portion of various human organs using MS-based targeted proteomics has become a common practice in the field of drug metabolism and disposition (35-37). Targeted proteomics on a liquid chromatography-multiple reaction monitoring (LC-MRM) platform is an accurate and specific protein quantification tool, and can be multiplexed (23, 24, 36-39). However, the cost and time for method development/validation rises linearly with an increase in the amount of protein(s) to be quantified (38, 40). In 2006, Silva *et. al*. discovered that the intensity of the top three ionizing peptides of a protein correlates directly to the protein concentration within complex biological matrices when the label-free data independent acquisition strategy (DIA; MS^E technique is the Waters version of DIA) of the quadrupole-time of flight (Q-TOF) MS platform is applied (41). Since then, label-free Q-TOF MS^E-based protein quantification has been adopted in some studies, due to its low cost and greater multiplexing capabilities (hundreds of proteins can be quantified simultaneously) (42-46).

Label-free MS^E quantification can be hampered by many factors. First, the proteomic analysis tools, especially nano-UPLC systems, have very low tolerance to biological contaminants, such as phospholipids, nucleic acids or undigested proteins. As a result, extensive sample cleanup, such as polyacrylamide gel electrophoresis (PAGE), filter-assisted sample preparation (FASP) or immunocapture, must be performed prior to the introduction of biological samples. However, PAGE suffers from incomplete digestion and peptide adsorption to the gel (47-49). FASP is troubled by low digestion reproducibility and poor peptide recovery (50). Immunocapture allows a limited number of proteins to be analyzed, therefore quantification throughput suffers.

Besides the sample preparation/cleanup process, digested peptides are lost to adsorption to glass or plastic vials (51, 52). In addition, trap columns, which are used for nano-UPLC systems to guard, de-salt and speed-up sample run-time usually, were found to lose polar peptides during the trapping process due to the column having low retention and a shorter length compared to analytical columns and particle sizes being larger (53).

Finally, work done by Harwood, Achour *et. al.*, and Wegler *et. al.* (presented at a roundtable session at the 2015 AAPS annual meeting) revealed large inconsistencies between label-free MS^E protein quantification and targeted proteomics for the quantification of DMEs in HLMs (54-56). However, little attempt was made in explaining these inconsistencies. Regardless of peptide loss and varying digestion efficiency, DIA searches have an intrinsic false discovery rate (FDR) for peptide identification and protein searching. We hypothesize that the peptide or protein false positive discoveries (FPDs) occurring during data processing by the Waters® ProteinLynx Global Server (PLGS) also contribute to the inconsistencies between the two quantification techniques.

In the current work, we sought to address the challenges above, which trouble label-free MS^E proteomic quantifications. A quantitative FASP (qFASP) protocol that offers reproducible tryptic digestion, close to complete recovery of digested peptides, and sample cleanliness in terms of phospholipid removal comparable to that of the original FASP, was developed. An albumin-masking protocol was evaluated and adopted to prevent peptide adsorption to sample vials. A sample loading/direct injection scheme was utilized to ensure complete peptide recovery prior to MS analysis. Recombinant DMEs at various concentrations were digested and analyzed by label-free MS^E quantification to assess the impact of FPDs on the linearity of protein quantification. Finally, ten individual HLMs (iHLMs) were processed with the qFASP protocol and the

abundance of various DMEs quantified using a nano-UPLC-Q-TOF-based label-free MS^E and UPLC-MRM targeted proteomics. The resulting correlations were examined to determine the consistency between the two MS-based methods with the newly developed qFASP protocol.

6.2 Materials and Methods

6.2.1 **CHEMICALS, ENZYMES, AND LIVER TISSUES**

Optima-grade acetonitrile, water, formic acid, and acetic acid were obtained from Fisher Scientific (Pittsburgh, PA). Protein LoBind Tubes were acquired from Eppendorf (Hamburg, Germany). Certified screw top 250 uL polypropylene sample vials were from Agilent (Santa Clara, CA). Ammonium bicarbonate (ABC), dithiothreitol (DTT), and iodoacetamide (IAM) were purchased from Sigma-Aldrich (Saint Louis, MO). Recombinant human FMO1, FMO3, FMO5, CYP1A2, CYP3A4, CYP3A5, CYP2C9, CYP2C19, and CYP4F2 were obtained from Corning Gentest (Woburn, MA). Pooled HLM (XTreme 200) and nine individual adult donor HLM (Table 1) were purchased from XenoTech, LLC (Lenexa, KS). Synthetic 13C and 15N stable isotope-labeled crude signature peptides were acquired from Thermo Scientific. The synthetic peptides, used previously as internal standards for the absolute quantifications of CYPs, FMOs and drug transporters (23, 24, 38, 39), were used in the current study as reference peptides to assess peptide recovery in FASP, qFASP, digested sample storage, and nano-UPLC sample loading methods (Table 5). These peptides span a wide range of the HPLC index spectrum, therefore offering a good representation for the proteome digests. All synthetic peptide sequences were confirmed by MS/MS fragmentation analysis using a Waters Xevo TQ-S triple-quadrupole MS (Milford, MA). Sequencing-grade modified trypsin was purchased from Promega (Madison, WI). Hi3 Ecoli Standard and MassPREP Enolase Digestion Standard were acquired from Waters (Milford, MA). Both standards were dissolved in 20% (v/v) ACN to give a final concentration of 1 μM, aliquoted in protein LoBind vials, and stored at -80ºC.

6.2.2 IN-SOLUTION DIGESTION

The in-solution digestion of HLMs and recombinant DMEs was performed as described previously (23, 24, 38). Stable isotope-labeled peptides that had been used for the absolute quantifications of CYPs, FMOs, and various drug transporters in previous studies were combined and served as internal standards in the current study (Table 5) (23, 24, 38, 39).

Table 5. Stable isotope-labeled peptides used in the current study.

peptide Sequenceb[a]	Compound Code	Average Mass MH^+ (Da)	MRM (m/z)	
			Precursor Ion	Product Ion
NVTGFFQS(F)K	OATP1B1_pep1_H	1185.3	593.0	971.7
TYNSTS(F)SR	OATP1B1_pep3_H	1073.1	537.0	808.5
SSIIHIE(R)	OATP1B1_pep9_H	965.1	482.7	564.3
NVTGF(F)QSLK	OATP1B3_pep1_H	1151.3	575.8	937.5
IYNSVFFG(R)	OATP1B3_pep2_H	1113.3	556.8	836.4
GIIDSTVGEH(R)	PMCA4_pep4_H	1194.3	398.7	508.2
GFYIP(K)	CYP1A1_pep1_H	732.8	366.7	528.3
YLPNPSLNAF(K)	CYP1A1_pep2_H	1272.5	636.3	784.4
YLPNPALQ(R)	CYP1A2_pep1_H	1082.3	541.3	594.4
TVQEHYQDFD(K)	CYP1A2_pep2_H	1418.5	473.5	609.3
ELVALLV(R)	CYP1B1_pep1_H	923.2	462.1	581.4
NPHLALS(R)	CYP1A_pep1_H	918.1	459.5	569.4
GIFPLAE(R)	CYP2C9_pep1_H	913.1	456.8	595.3
SLVDP(K)	CYP2C9_pep2_H	666.8	333.9	466.3
GHFPLAE(R)	CYP2C19_pep1_H	937.1	469.0	595.3
SLLSPT(F)TSGK	CYP3A_pep1_H	1147.6	574.6	834.5
EVTN(F)LR	CYP3A4_pep1_H	888.5	445.0	660.5
DTIN(F)LSK	CYP3A5_pep1_H	947.5	474.5	618.5
VIS(F)LTK	CYP3A7_pep1_H	817.5	409.3	605.3
AEGG(L)WLR	CYP4F_pep1_H	908.9	454.96	708.4
SV(I)NASAAIAPK	CYP4F2_pep1_H	1149.3	575.0	962.6
VV(L)ALTLLR	CYP4F2_pep2_H	1005.3	503.0	806.7
SV(**I**)NASAAIVPK	CYP4F3B_pep1_H	1177.4	589.0	870.6
VV(**L**)GLTLLR	CYP4F3B_pep2_H	991.3	496.0	792.6
VVLALTLLH(F)R	CYP4F11_pep1_H	1292.6	431.6	547.6
SITNASAA(I)APK	CYP4F12_pep1_H	1150.9	576.0	950.5
FTEHVEEG(R)	FMO1_pep1_H	1114.2	557.5	599.3
VEDGQASLY(K)	FMO1_pep2_H	1118.2	559.6	889.5
FSDHAEEG(R)	FMO3_pep1_H	1058.1	529.5	571.3
SNDIGGLW(K)	FMO3_pep4_H	998.1	499.4	568.3
FQENPEEG(R)	FMO5_pep1_H	1116.1	558.4	597.3
WATQVF(K)	FMO5_pep6_H	888.0	444.5	630.4
AG(F)AGDDAPR	Actin_pep1_h	986.4	493.7	630.3

[a] amino acids in () are labeled with ^{13}C OR ^{15}N

6.2.3 ORIGINAL FASP DIGESTION & ASSESSMENTS

The FASP protocol was performed as described by Wisniewski *et. al*. in 2009 (57), with minor modifications. Briefly, 30-60 ug of pooled HLM protein was denatured in a 100 mM Tris/HCl solution (pH 7.5) containing 0.4% (w/v) sodium dodecyl sulfate (SDS) and 100 mM DTT at 95°C for 3 min. The denatured protein was washed twice with 200 uL of UA solution (8 M urea, 0.1 M Tris-HCl; pH 8.5) on Microcon 10kD filters (Merck Millipore Ltd., Ireland) equilibrated with LC-MS grade water, and centrifuged at 14,000 x *g* for 40 min. The addition of 50 mM IAM in UA solution (100 uL) to the samples was followed by shaking at 600 RPM for 1 min, incubation in the dark for 20 min, and centrifugation at 14,000 x *g* for 30 min. A wash with UA solution (100 uL) was performed again, followed by two washes with 50 mM ABC (100 uL; 14,000 x *g* for 30 min). Trypsin (a ratio of 1 ug trypsin: 30 ug sample), in 50 uL of 50 mM ABC, was added to the filters, and the samples shaken at 600 RPM for 1 min and incubated at 37°C for 4 hours. Stable isotope-labeled reference peptides were spiked into the digest solutions. The filters then were put on top of a protein LoBind vial and centrifuged at 14,000 x *g* for 20 min. NaCl solution (0.5 M; 200 uL) was added to each filter, centrifuged, and combined with the first filtrate. Desalting of the filtrate was carried out on Pierce PepClean C-18 spin columns (Rockford, IL) according to the vendor's protocol.

Contributions of SDS and urea on the digestion of DMEs. FASP was performed as described above, with both SDS and urea, with SDS only, with urea only, or without either. In the SDS only digestion, UA solution was replaced by 20 mM ABC. In urea only samples, SDS was absent during the protein denaturation step. In 2012, Cunningham *et. al.* showed that a high NaCl concentration (1M) was basically ineffective in the recovery of digested peptides from cellulose made molecular weight cut-off (MWCO) filters (58). HLM tryptic digests were eluted by adding

100 uL of 50 mM ABC, centrifuged as above, and eluted again with two additional rounds of 50 uL 50 mM ABC. The three eluents were combined and injected for UPLC-MRM peptide quantification.

Recovery of digested peptides from MWCO filter. MWCO filters were equilibrated with LC-MS grade water and positioned on top of protein LoBind tubes. Concentrated reference peptide stocks dissolved in 50 uL of 50 mM ABC were added to each filter (peptide elution groups) or directly to the LoBind tubes below the empty filter ("full recovery" control groups). The filters of each group were eluted with either four rounds of 100 uL of 50 mM ABC or four rounds of 100 uL of 20% (v/v), 50% (v/v) or 60% (v/v) ACN and centrifugation at 14,000 x *g* for 30 min. Following the fourth elution, the centrifugation step was increased to 60 min. The eluents were collected in protein LoBind vials and subjected to UPLC-MRM analysis. Peptide recoveries in each elution condition were presented as the peptide peak area ratio between the "peptide elution groups" divided by the "full recovery control groups".

6.2.4 qFASP DIGESTION AND ASSESSMENTS

The qFASP digestion protocol is detailed in **6.5 qFASP** protocol. The protocol is compared to the well-established, in-solution digestion protocol for quantification of DMEs in pooled HLM. The removal of phospholipids is compared to the original FASP protocol.

HLM digestion by qFASP vs. in-solution. Recombinant CYP3A4, CYP1A2, or FMO5 at 0, 1, 2, and 4 pmole were spiked into 40 ug of pooled HLM (XTreme 200), and underwent both qFASP and in-solution digestion. Samples (4 uL) were subjected to UPLC-MRM for signature peptide quantification. The lower limits of quantification (LLOQ) of qFASP were evaluated by

processing a mixture of recombinant CYP1A2, CYP2C9, CYP3A4, CYP4F2 and FMO3, ranging from 1 fmole to 4000 fmole/digestion, and analysis by UPLC-MRM.

Sample vial binding site masking & evaluation. Reference peptides dissolved in LC-MS grade H_2O, 15% (v/v) ACN, or 50% (v/v) ACN were added to un-masked, certified polypropylene sample vials. To mask hot spots in the sample vials, 200 uL of 2mg/mL bovine serum albumin (Thermo Scientific, Rockford, IL) were added and the vials incubated overnight. The albumin was removed from the sample vials and stored for another masking later. The masked vials were rinsed twice with 200 uL LC-MS grade water by gently pipetting up and down. Reference peptides dissolved in water then were loaded into the masked vials for analysis. To examine potential signal interferences that may be introduced by remaining free albumin, nine consecutive injections of 10 uL of 20 mM ABC solution that was stored in albumin masked vials were analyzed by UPLC-MS scan. Chromatography and instrument settings were the same as in a previous report (38). MS scan was set so that the third quad of Waters XEVO TQ-S was scanning between 100-2000 m/z every two seconds while the collision energy remained at 4 eV throughout the LC run. The presence of free albumin also was checked with the Pierce BCA protein assay (Thermo Scientific). The sample loading volume was five times that suggested in the vendor's protocol, in order to increase the BCA sensitivity.

Evaluation of phospholipid remaining in qFASP vs. FASP digest. In-source fragmentation of phospholipids generate choline or phospho-choline ions, which can be monitored at 104 or 184 m/z (59). Two sets of LC conditions were used to examine phospholipid content in the HLM digests. The first set was the same as the UPLC conditions for analysis of the digested peptides. The second set was run on an Agilent Zorbax Bonus-RP column (2.1 x 50 mm, 3.5 um) with a 0.5 mL/min flow rate. Elution started at 20% (v/v) B for 1 min, followed by a 7 min gradient

linearly raised to 100% B, maintained for an additional min, and returned to 20% B. The two LC conditions shared the same mobile phase. The MS settings also were the same as those used for peptide monitoring, except that the cone voltage was set at 90 V to encourage in-source fragmentation. Both quad one and quad three were set at 104 or 184 m/z throughout the entire chromatographic run.

6.2.5 UPLC-MRM AND NANO-UPLC MS^E SETTINGS

UPLC-MRM settings were the same as those reported previously. Parameters needed for the targeted quantification of stable isotope-labeled peptides and the corresponding signature peptides were published previously and summarized briefly in Table 5.

The nano-UPLC systems used consisted of a Waters nano Acquity Binary Solvent Manager and nano Acquity Sample Manager. Mobile phases A and B were water and acetonitrile containing 0.1% (v/v) formic acid, respectively. Table 6 contains details of the LC columns, sample loadings, and separation gradients.

Table 6. Liquid chromatography conditions used for peptide separation.

Gradient Code	LC-MS type	trap / direct injection	Pre-column	Analytical column	Sample loading				Peptide Elution				function
					Loop loading type	Injection volume	Loop online (min)	Single pump Trapping	Flow rate	Elution Gradient	Column wash	Column equilibration	
A	UPLC-MRM	direct injection	inline filter; BEH300 C18 1.7 um guard column	BEH C18, 2.1x150 mm, 1.7 um		10 uL	13.5 (flow through needle)		0.4 mL/min	2% B 1 min, 2-15% for 2 min, 15-30% B for 7 min	95% B 1.5 min	2% B, 1 min	validate qFASP; validate peptide storage conditions
B	nano UPLC-Q-TOF	Single pump trapping	Symmetry C18, 180 umx20 mm, 5 um trap column	CSH C18, 75 um x 250 mm, 1.7 um	partial loop	4.5 uL	only online during 5 min trapping	3 uL/min, 5 min, 0.5% B	300 nL/min	3-45% B, for 70 or 90 min	95% B 10 min	3% B, 20 min	fast loading; measure mass accuracy; LC optimization
C	nano UPLC-Q-TOF	direct injection	Symmetry C18, 180 umx20 mm, 5 um trap column	CSH C18, 75 um x 250 mm, 1.7 um	full loop (1x loop overfill)	5 uL	30 min, 13 uL 3% B push sample to the head of column		300 nL/min	3-45% B, for 90 min	95% B 10 min	3% B, 20 min	Quantification of DMEs in iHLM with MS^E

Prior to data acquisition, the Waters Xevo-G2 Q-TOF was run for over a week with other samples in order to prime the detector, ensuring it is suitable for quantification analysis. The Q-TOF detector was setup with the infusion of a leucine encephalin peptide and a mass calibration profile created using glu-fibrinopeptide. Sample eluent was introduced to the Q-TOF by a nano flow sprayer equipped with a Thermo stainless steel emitter (50 mm length, 360 um O.D.), which is glued to a 1 cm, 380 um I.D. silica capillary at the inlet end. The emitter position was fine tuned for optimal signal intensity. The Q-TOF was run under positive mode with a 2.8 kV capillary voltage, 30 V sampling cone voltage, 0.2 extraction cone, 100^{o}C source temperature, 350^{o}C desolvation temperature, 50 L/H cone gas flow, 0.5 bar nano-flow gas pressure, and 800 L/H desolvation gas flow; scanning occurred at 100-1800 m/z every second with a 0.014 s inter-scan delay. Precursor ions were collected under 4 eV collision energy (CE), and the product ions produced with a 10-38 eV CE ramp.

6.2.6 LABEL-FREE NANO UPLC MS^{E} DATA QUALITY & IMPACT OF FPDs ON MS^{E} PROTEIN QUANTIFICATION

Equal amounts of recombinant CYP3A4, CYP3A5, CYP2C9, CYP2C19, FMO1, FMO3, and FMO5 were combined and processed following the in-solution digestion protocol with an increasing pmol of recombinant protein. The digests were subjected to nano UPLC-MS^{E} analysis. Each digested recombinant protein was loaded onto the column at 1, 5, 10, or 40 fmole per loading.

6.2.7 LABEL-FREE NANO-UPLC MS^{E} AND TARGETED UPLC-MRM QUANTIFICATION OF DMEs IN iHLMs

Digestions of 40 ug iHLMs were carried out according to the qFASP digestion protocol (6.5 qFASP protocol). Prior to drying with the speedvac, peptides recovered from the MWCO filters with 60% (v/v) ACN were divided; one part was spiked with 2.5 pmole of Hi3 Ecoli Standard for label-free nano UPLC-Q-TOF MS^E quantification, while the other part was spiked with stable isotope-labeled peptides for UPLC-MRM targeted quantification. The targeted quantification of iHLMs was calibrated using a mix of recombinant DMEs,CYP1A2, CYP2C9, CYP3A4, CYP4F2 and FMO3, each between 1 and 4000 fmole/qFASP digestion and processed in a manner similar to that of the iHLMs. An equivalent amount of HLM digest (1.28 ug; 5 uL) was injected onto the nanoUPLC column for each sample; 2.56 ug was loaded into the UPLC column. During MS^E data collection, lock-spray mass calibration was not used due to a previous observation that sample-probe nano-spray was often disturbed during lock-spray collection. All post-data collection masses were calibrated manually through adjustment of the "calibration gain" by matching the recorded m/z of the doubly charged VIGQNEAVDAVSNAIR peptide (one of the six Hi3 standard peptides) to its theoretical doubly charged m/z of 828.4392.

6.2.8 DATA ANALYSIS

Both Xevo TQ-S triple quadrupole MS and Xevo G2 Q-TOF were operated under Masslynx 4.1 (Waters, Milford, MA). Data analysis for targeted UPLC-MRM protein quantification has been reported previously (38). MS^E data were analyzed by PLGS 2.5.1 with the following settings: lock mass, 785.8426 Da/e (not applied for the iHLM analysis); low and high energy threshold, 250 counts and 100 counts; intensity threshold, 500 counts; 3 minimum peptide match required per protein; 3 minimum ions required per peptide; false positive rate (FDR), 1%; carbamidomethyl cysteine and oxidation methionine set as fixed and variable modifications; and 1 tryptic missed cleavage. All spectrums were searched against the reviewed human proteome

FASTA databank that was downloaded from Uniprot.org (June-24-2015). Sequences of *E. coli* Chaperone protein ClpB (P63284) and *S. cerevisiae* enolase 1 (P00924) were added manually to the databank. PLGS output were analyzed further by Synatper (v 1.12.0), according to the author's manual-script (60) and reference manual (http://lgatto.github.com/synapter/), for the calculations of nano UPLC retention time reproducibility, Q-TOF mass accuracies, number of significant peptides under 1% FDR, and PLGS score distribution for PLGS pass 1 and pass 2 searches. All correlations and additional statistics were performed with GraphPad Prism Software (version 5.0; San Diego, CA).

6.3 Results and Discussion

6.3.1 qFAPS DIGESTION OF HLM

qFASP optimizations and assessments. The original FASP is known to have dramatic peptide loss as acknowledged by Wisniewski *et. al.* in 2009 (57). In addition, Hustof *et. al*. showed that FASP was unable to completely remove the added denaturant, SDS, and potential issues such as SDS co-eluting with the peptide(s) during LC-MS analysis may occur (61). Either of these two problems would affect label-free nano-UPLC analysis adversely. Therefore, it is vital to assess peptide loss in each step of the FASP protocol and the role of additives, like SDS and urea, in the digestion and analysis of DMEs.

FASP were performed for the digestion of HLM with or without SDS or urea (Figure 20). Quantitative UPLC-MRM analysis of the digested signature peptides revealed that both SDS and urea caused large digestion variability, as demonstrated by the error bars (range) (Figure 1 A, B, C). Although each digestion group was performed in duplicate only, the large variability of the FASP protocol was consistent with previous reports. In 2014, An *et. al.* described a 14.1-29.6% CV when monoclonal antibodies were digested by FASP and quantified by targeted LC-MRM with stable isotope-labeled peptides as internal standards (62). In the current study, the variability was significantly smaller when SDS and urea were not present in the digestion (Figure 1D). The low variability was confirmed by UPLC-MRM in all subsequent HLM digestions performed without either of the denaturants. The roles of SDS and urea were probed further by correlation of the mean of the duplicated peak areas from digested signature peptides in different digestion groups, using urea only, SDS only or neither, giving near unity slopes and a correlation coefficient close to 1 (Figure 21). These results suggested that the digestions of the signature

peptides in the targeted proteins, CYPs, FMOs, OATPs or OCT1, did not benefit from the addition of SDS or urea.

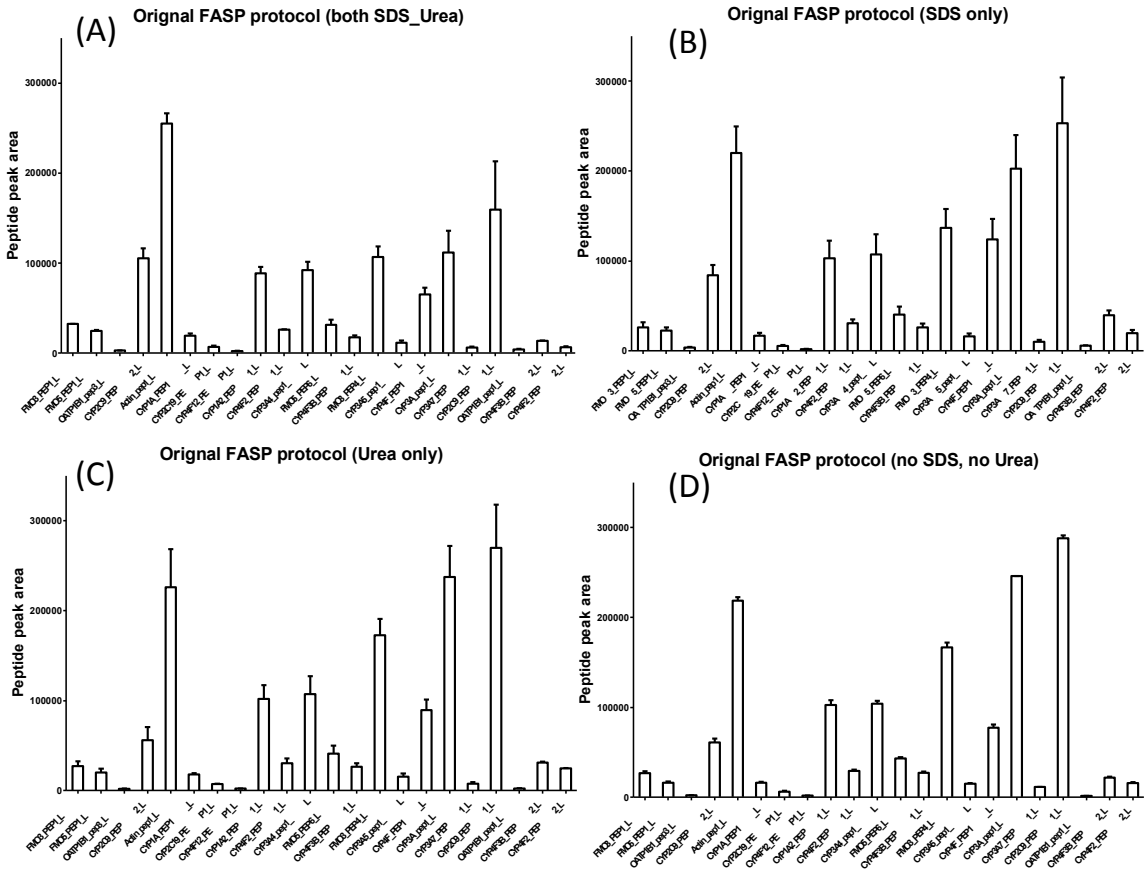

Figure 21. Assessing SDS and urea in the digestion of DMEs in pooled HLM with the FASP protocol. FASP digestion of 30 ug of pooled HLM was performed with both SDS and urea (A), SDS only (B), urea only (C), or without either (D). Peptide peak areas were results of quantitative targeted UPLC-MRM analysis of the HLM digests. Duplicate digestions were performed in each group. Bars and error bars represent mean and range.

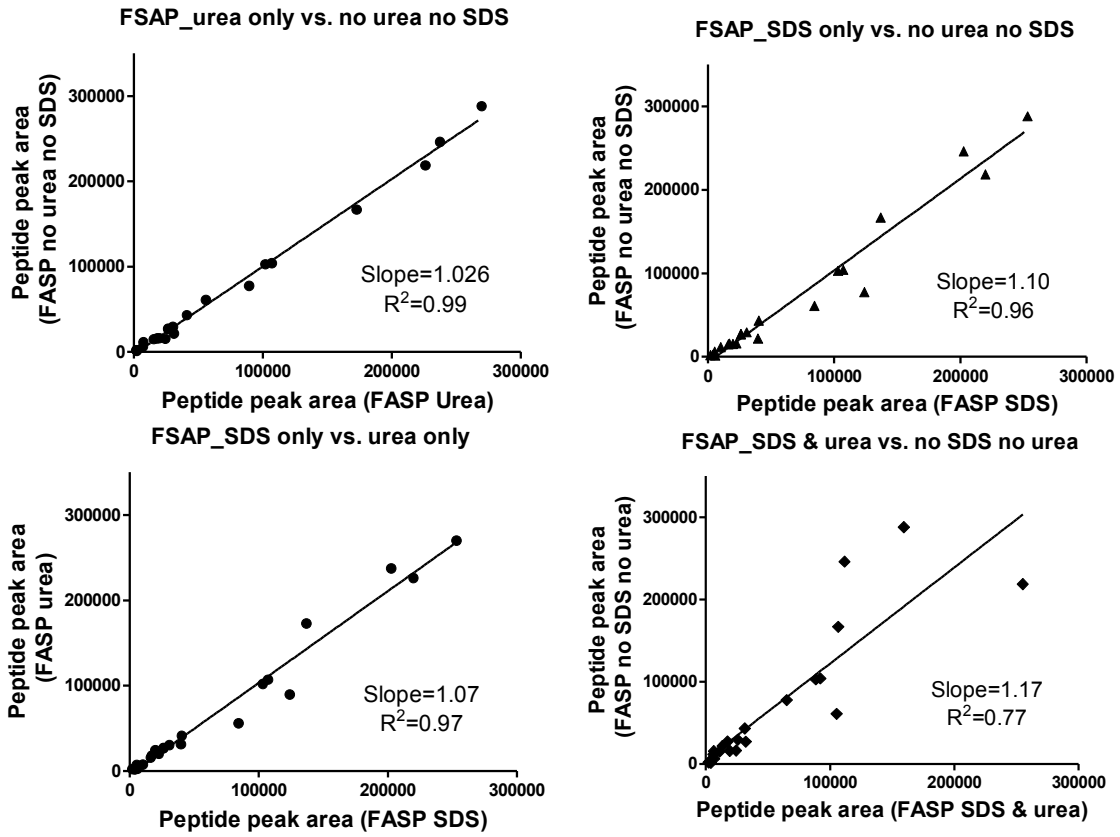

Figure 22. Correlation of signature peptides digested by FASP performed with or without SDS or urea. Each data point is the mean peptide peak area from the targeted UPLC-MRM analysis of duplicate 30 ug HLM tryptic digestions.

The original FASP protocol used 0.5 M NaCl for the recovery of digested peptides from the 10 kDa MWCO filter and subsequently desalted with C18 solid-phase extractions for LC-MS analysis. Cuninngham *et. al.* showed that a high concentration of NaCl (1M) was basically ineffective in eluting digested peptides from the MWCO filters. We observed that a significant amount of peptides remained on the filter following the 5th or 6th filter elution with water or 50 mM ABC (data not shown). These results indicate that aqueous or aqueous salt solutions will not

allow for full peptide recovery from the filters. In addition, high salt elution requires an extra downstream desalting step, which also causes peptide loss. Current experiments examined the use of 20, 50, or 60% (v/v) ACN for peptide recovery. Increased peptide recovery was observed with increased ACN concentration (Figure 23). An almost complete recovery of all hydrophilic (lower retention time) and hydrophobic (high retention time) reference peptides was achieved using four rounds of elution with 60% (v/v) ACN. In fact, three rounds of elution with 60% (v/v) ACN was found to give comparable recovery (data not shown); the fourth round was performed in the hope of recovering potential long chain, more hydrophobic peptides. Elution with 60% (v/v) ACN also eliminates the SPE desalting step. Assessments of the C18 desalting cartridges showed loss of hydrophilic peptides and increased variability (Supplemental Figure 1), and therefore are bad for quantification.

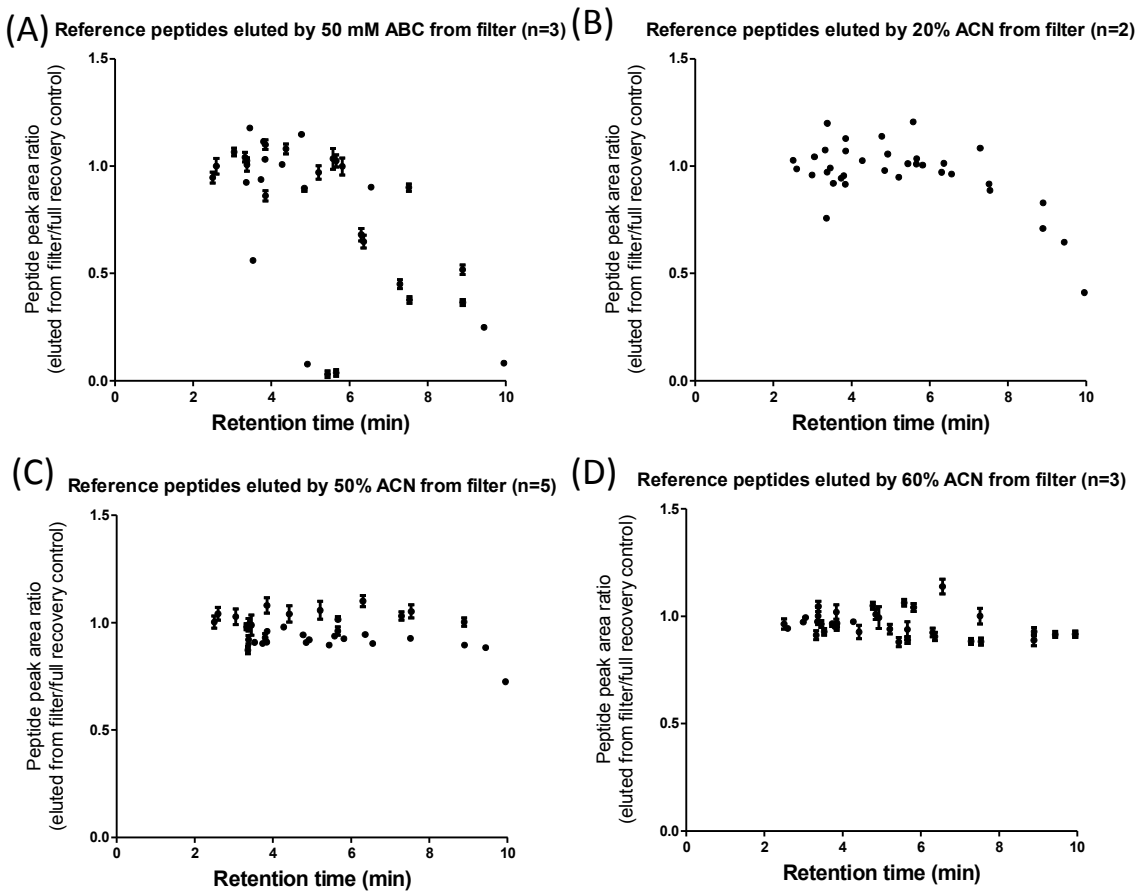

Figure 23. Recovering synthetic stable isotope-labeled reference peptides from YM-10 Microcon filters. Synthetic peptides were recovered by elution with water or 20%, 50% or 60% (v/v) ACN (see Materials and Methods). Peptides were analyzed by UPLC-MRM and retention times were results of BEH C18 analytical column separation. Error bars represent standard deviations or ranges (20% ACN elution).

Sample vial masking and validations. Peptides can easily bind to plastic or glass surfaces due to their amphipathic nature. Untreated polypropylene sample vials were used in the current study. Digested samples dissolved in water were found to experience major signal loss for

hydrophobic peptides. When 2%, 5%, 10%, 15%, 20% or 50% (v/v) ACN were used to dissolve reference peptides, the hydrophobic peptide signal increased proportionally to the percentage of ACN (peptides in 0, 15, and 50% (v/v) ACN are shown in Figure 4 A and B). Hydrophobic peptide peak areas plateaued at 15% (v/v) can, whereas hydrophilic peptides were retained less and less on the BEH C18 column (2.1 mm I.D.) (Figure 24 B) during UPLC-MRM analysis. However, when peptides dissolved in 15% (v/v) ACN were loaded onto a Symmetry C18 nano trap column (180 um I.D.; intended for MS^E analysis), many hydrophilic peptides suffered major signal loss. Although the use of ACN to dissolve the peptides solved the issue of peptide binding to polypropylene sample vials, it caused peptide loss at the nano-UPLC column due to pre-elution. This dilemma indicates that all digested peptides should remain in an aqueous solution while not binding to polypropylene vials. In 1976, Felgner *et. al.* discovered that artificial hexokinase activity loss in polypropylene vials can be reversed by masking the vials with albumin, likely due to albumin competitively inhibiting the binding of enzyme to the vial (63). Therefore in the current study, sample vials were incubated with albumin (2 mg/mL) overnight and rinsed twice with water. Reference peptides dissolved in water and stored in albumin-masked vials had almost the same UPLC-MRM peak area as that of the peptides dissolved in 15% (v/v) ACN and stored in un-masked vials (Figure 24C). Concerns arising from vial-masking include the introduction of free albumin to the nano UPLC-Q-TOF system causing background interference in peptide analysis or increased back pressure in the nano column (75 um i.d.). Up to nine consecutive injections of water in albumin masked vials were analyzed by MS scans from UPLC-triple quadrupole or nano UPLC-Q-TOF. No identifiable albumin signal was observed in the background of any of the consecutive injections. Following the primary over-night coating, the vials were rinsed twice with water. Only sodium formate polymer or protonated formic acid

polymer signals were observed in the solvent front after the first vial wash. These interferences disappeared after the second wash.

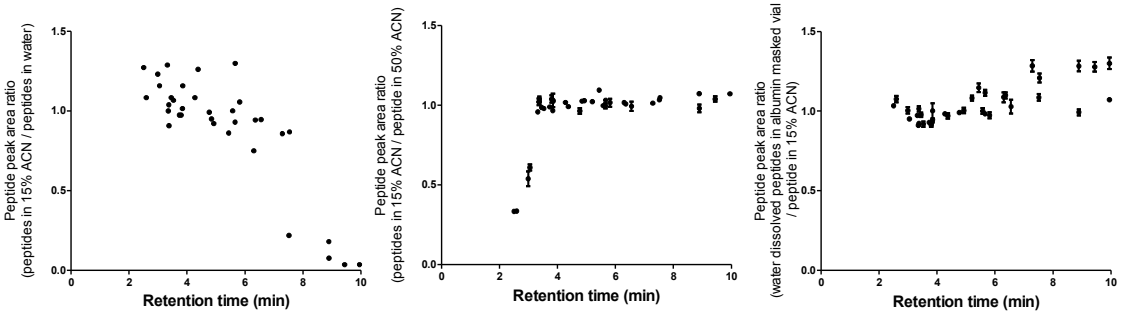

Figure 24. Preventing peptide adsorption to polypropylene sample vials. Synthetic isotope-labeled peptides were dissolved in water or 15% or 50% (v/v) ACN, and stored in un-masked sample vials were compared to the same concentrations of peptides dissolved in water and stored in albumin masked vials. Peptides were measured by UPLC-MRM. Error bars represent standard deviations.

Phospholipid remaining in qFASP vs. FASP digest. Phospholipid contamination from human tissue samples pose detrimental consequences in nano UPLC-Q-TOF label-free analysis, as it can cause large interferences in the current, carry over to many subsequent injections, inhibition of peptide signal due to its preferential ionization (64), and ion-pairing with nano column bedding, greatly reducing its separation efficiency and life time. As a result, a majority of phospholipids must be expelled from biological samples before the digests can enter the nano scale analytical column. Phospholipid removal is one key feature of qFASP, which was assessed and compared with the original FASP protocol in the current study.

An in-source fragmentation method that measures fragmented phospholipid products of choline and phospho-choline, which have unique signature masses at 104 and 184, was used for the detection of phospholipids in HLM digestion samples.(59) HLM digestions prepared by different methods were injected on two columns using different elution gradients to provide additional confirmation (Figure 25). A mix of synthetic peptides was injected to both columns and served as the "no phospholipid" negative control. Injections of in-solution digested HLM were the positive control. Peaks present in the positive control chromatogram but not in the negative control indicate elution of phospholipids. On the BEH-C18 column (same column and gradient for targeted protein quantification) (Figure 25 A and B), qFASP digested HLM showed similar cleanliness as the negative control. On the Zorbax bonus-RP C18 column, qFASP reached comparable cleanliness as the original FASP digestion (Figure 25 C and D).

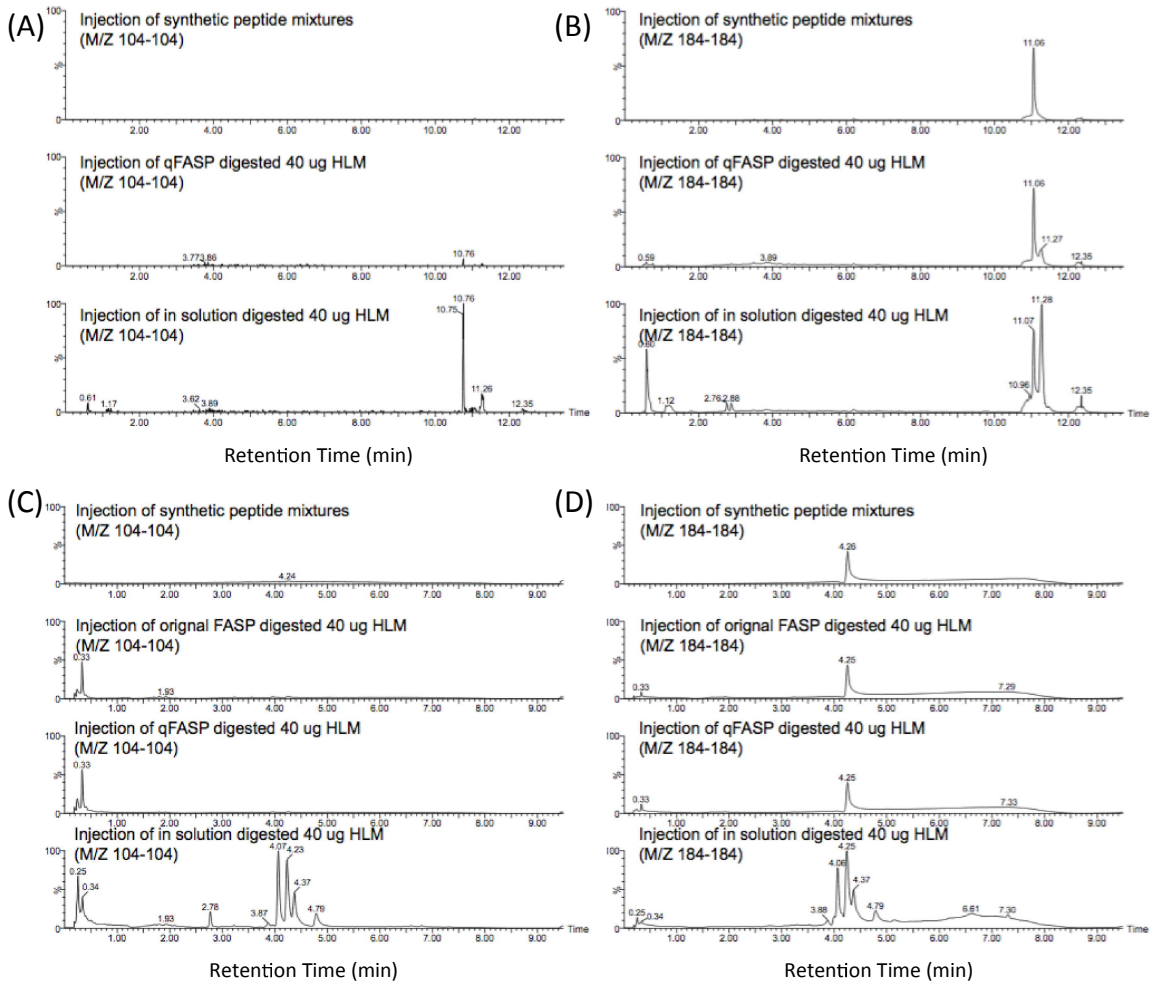

Figure 5. Chromatograms of in-source fragmented phospholipid that remained in qFASP, FASP, or in-solution digested HLM solutions. The digestion products of 40 ug pooled HLM were eluted on a BEH C18 UPLC column (A, B) or a Zorbax Bonus RP column (C, D) with the elution gradient used for peptide analysis or polar lipid analysis. See detailed LC conditions in Materials and Methods.

qFASP quantification limits and quantification coherence compared to in-solution digestion. In-solution digestion is a quick yet unclean process for absolute protein quantification on the LC-MRM platform, and has been well established and adopted widely (23, 24, 36-39). To

determine whether qFASP maintains the quantitative nature of sample processing, a thorough comparison to in-solution digestion must be performed.

The lower limit of quantification (LLOQ) was determined by the digestion of mixed recombinant CYP1A2, CYP2C9, CYP3A4, CYP4F2, and FMO3 at various concentrations (1-4000 fmole) by qFASP. Very sensitive quantifications were achieved with qFASP digestion (Table 2). The LLOQ of some peptides reached 1 fmole per digestion, CYP3A_PEP1_L and CYP1A2_PEP2_L. The detection limits of many signature peptides are comparable or superior to those obtained previously with in-solution digestion. Two peptides of CYP4F2 reached LLOQs of 5 fmole/digestion in qFASP, 10 times more sensitive than the 50 fmole/digestion LLOQ achieved with in-solution digestion (23). Two signature peptides of CYP3A4 also reached lower LLOQs, 2-20 times lower than those achieved with in-solution digestion (24). The improvement in quantification sensitivity may be due to reduced background noise or ionization inhibition resulting from the qFASP sample cleaning procedure, or reduction/elimination in peptide adhesion to sample vials due to albumin vial masking. At a minimum, this experiment demonstrated that qFASP was able to recover very small amounts of digested peptides with great linearity, as demonstrated by the R^2 values close to 1 with each calibration curve (Table 7).

Table 7. Dynamic ranges of qFASP digested recombinant CYPs and FMO3 analyzed by UPLC-MRM targeted proteomic approach

Signature peptide code	Lower Limit of Quantification (LLOQ)[3]		Highest amount within a linear calibration curve		R^2	LLOQ
	amount digested by qFASP (fmole)	amount loaded on UPLC column (fmole)	amount digested by qFASP (fmole)	amount loaded on UPLC column (fmole)		Amount in in-solution digesiton (fmole)
CYP1A_PEP1_L	50	2.94	4000	235.20	0.9959	
CYP1A2_PEP1_L[1]	2	0.12	4000	235.20	0.9971	
CYP1A2_PEP2_L[2]	1	0.06	4000	235.20	0.9972	
CYP2C9_PEP1_L	50	2.94	4000	235.20	0.9991	
CYP2C9_PEP2_L	50	2.94	4000	235.20	0.9982	
CYP3A_pep1_L	1	0.06	4000	235.20	0.9995	20 (M.Z.Wang *et. al.* 2008)
CYP3A4_pep1_L	10	0.59	4000	235.20	0.9985	20 (M.Z.Wang *et. al.* 2008)
CYP4F_PEP1_L	100	5.88	4000	235.20	0.9968	
CYP4F2_PEP1_L	5	0.29	4000	235.20	0.9995	50 (S. Michaels *et. al.* 2008)
CYP4F2_PEP2_L	5	0.29	4000	235.20	0.9994	50 (S. Michaels *et. al.* 2008)
FMO3_PEP1_L	100	5.88	4000	235.20	0.993	10 (Y. Chen *et. al.* 2016)
FMO3_PEP4_L	10	0.59	4000	235.20	0.9978	10 (Y. Chen *et. al.* 2016)

1. excluding 50 fmole data point, the calibration curve have 10 concentrations left
2. excluding 20 and 50 fmole data point, the calibration curve have 10 concentrations left
3. Calibration standards were built by recombinant proteins. LLOQs were within 20% CV%, all other data points were within 15% CV%.

Recombinant DMEs at different concentrations were spiked into pooled HLM to make artificial individual HLMs (AiHLMs). UPLC –MRM analysis of AiHLMs prepared by both qFASP and in-solution digestion revealed quantification similarities (Figure 26). Chromatographic peak areas of signature peptides digested from spiked in recombinant enzymes tracked closely between methods (Figure 26 A-G). Four replicates of all qFASP digestions showed excellent reproducibility (narrow error bars), which confirmed previous observations that removing SDS and urea increases digestion reproducibility (Figure 21D). The correlation of all recorded signature peptides from both methods showed a near unity slope and close to zero y-intercept at all ranges (Figure 26H). Signature peptides resulting from both digestion methods reach ratios close to one (Figure 26I). This again confirms that 60% (v/v) ACN recovers almost all peptides, whether they are hydrophilic or hydrophobic, from the MWCO membrane. Although the peptide peak area ratio in the hydrophilic region deviated more from one. This might be caused by insufficient evaporation of ACN in the qFASP procedure (30 min speed-vac). Later qFASP digestions were performed with a longer speed-vac time (1 hour but varied depending on the speed-vac system) for better chromatographic peak shape. Overall, these two experiments demonstrated that qFASP preserved the quantification nature of HLMs and achieved similar or better LLOQs compared to in-solution digestion.

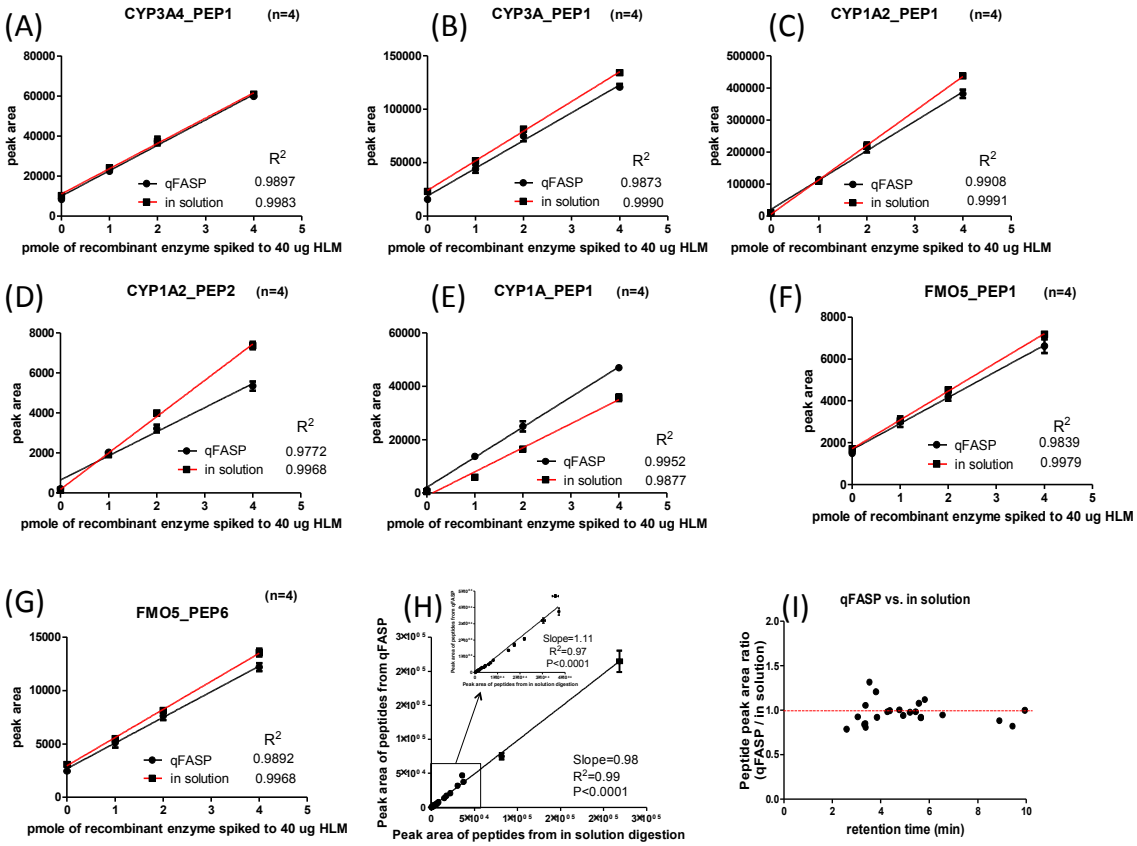

Figure 26. Comparison of quantitative FASP (qFASP) to in-solution digestion of HLM. Recombinant CYP3A4, CYP1A2, and FMO5 of 0, 1, 2, and 4 pmoles were spiked into 40 ug pooled HLM to make artificial individual HLMs (AiHLMs). These AiHLMs were digested by both qFASP and in-solution digestion. The y-axis is the UPLC-MRM chromatographic peak area of the monitored signature peptides digested from AiHLMs. Error bars represent standard deviations.

6.3.2 LAB-FREE DIA DATA QUALITY, FPD EVALUATION, AND NANO-UPLC OTIMIZATION

NanoUPLC Q-TOF MS^E data quality. Poor data quality leads to misidentification or even

uninterpretable data for PLGS. Therefore, data quality should be checked first hand. Here, mixed recombinant DME proteins were subjected to in-solution digestion and analyzed by nanoUPLC-Q-TOF MS^E. Synapter (60) on R Script was used for data quality assessments. Figure 27A shows overlaid chromatograms of digestion mixtures of recombinant enzymes loaded onto a nano UPLC column from 1 to 40 fmole per species. Although online-trapping mode (Table 22, LC gradient B) was used for quick sample loading, good chromatographic reproducibility could still be seen in Figure 27A, and statistically confirmed (Figure 27B). Close to 100% of the m/z used by PLGS for significant peptide identification had an error less than 10 ppm mass error (Figure 27 C and D); the same was seen with 1 and 5 fmole loading (data not shown). Additionally, the majority of significant peptide identification was within a 1% false positive rate, further confirmation of good mass accuracy in the data collection (Figure 28A). A comparison between searching the raw data against the human proteome to searching against the randomized decoy human proteome showed that very little recorded masses came from peptides of recombinant proteins (Figure 28 B and C). Most recorded masses (the large overlapped region on the lower PLGS scores on the x-axis) that poorly matches the regular human proteome may came from host insect cells, small-molecule contaminants in recombinant protein isolations, or sample preparation processes.

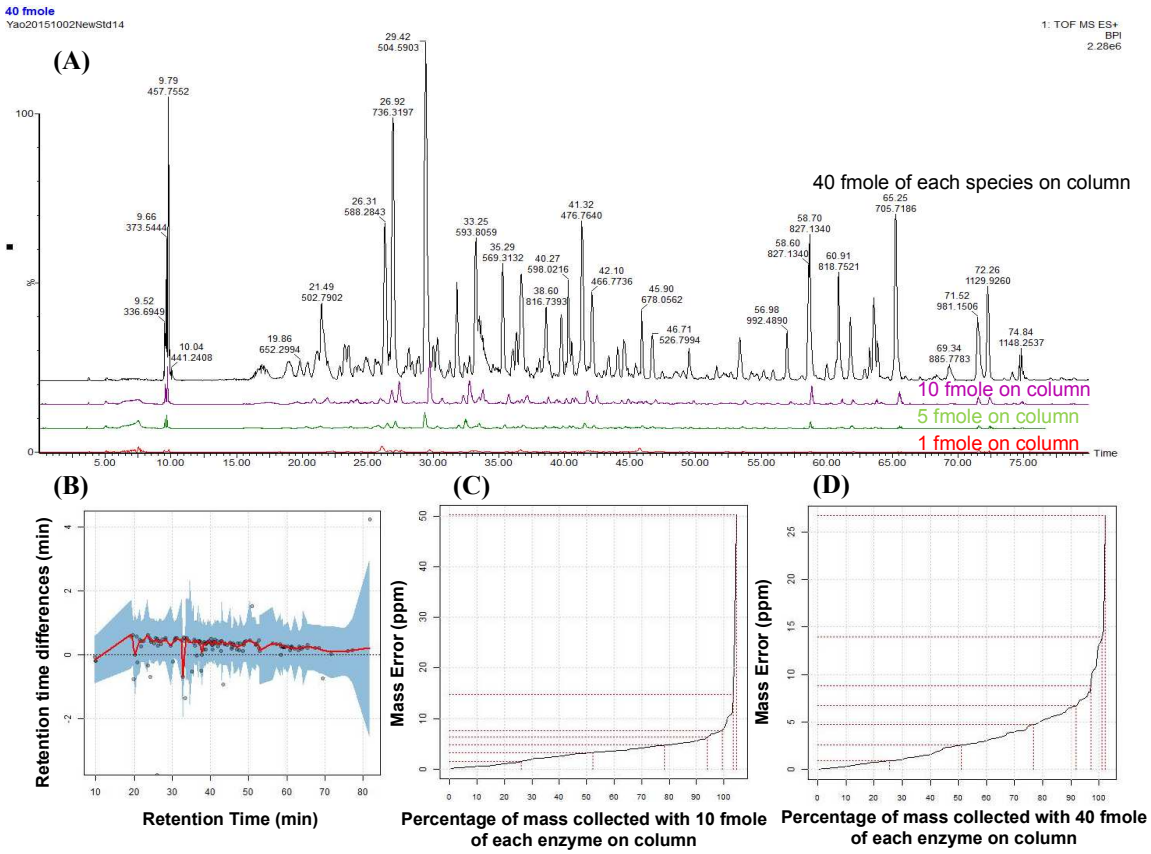

Figure 27. Mixture of digested recombinant DMEs (CYPs & FMOs) were analyzed by DIA (MSE) proteomic strategies. A mixture of recombinant CYP2C9, CYP2C19, CYP3A4, CYP3A5, FMO1, FMO3, and FMO5 were serially diluted, digested, and analyzed by nanoUPLC-Q-TOF. Data were processed by PLGS and Synapter. The figure above shows stacked chromatograms (BPI) of digested enzymes at different concentrations (A); retention time differences between two separate injections with 10 and 40 fmole of each enzyme on the column (B); and mass accuracies in the two samples (C and D). The red solid line and blue shadow region in B represent mean and 95% confidence range of the difference in retention times.

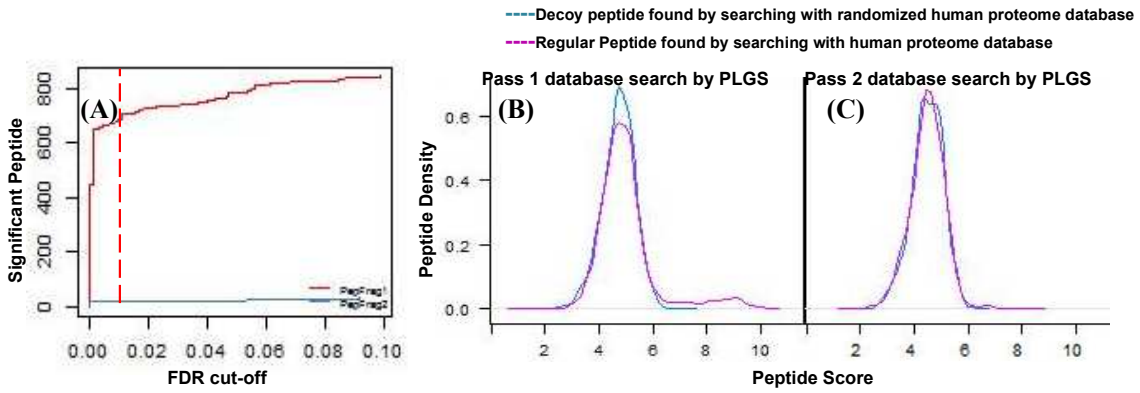

Figure 28. Cumulative plot of false discovery rate (FDR). Data generated by injection of 10 fmole of each digested recombinant enzyme (CYP2C9, CYP2C19, CYP3A4, CYP3A5, FMO1, FMO3 and FMO5) on column (A). Dash line marks 1% FDR. Distribution of PLGS scores for pass 1 and pass 2 unmodified fully tryptic peptides. Blue, decoy peptides; purple, regular peptides (B and C).

Impact of FPD on LFDI protein quantifications Many DMEs are homologs that share large portions of amino acid sequences. For example, CYP3A4 and CYP3A5 share 84% amino acid sequence identity; CYP4F2 and CYP4F3B have 93% sequence identity (24). Although a 1% false discovery rate (FDR) is applied to all data deconvolutions, it is still necessary to assess how falsely identified homologs might impact the quantification of true positive enzymes. Table 8 shows the sum signal of the top three most intense peptides in each PLGS identified protein. The enzymes are not present in the digestion but "identified" by PLGS is considered false positive, which is denoted by red font (Table 8). As the on-column loading amount increased, more FPDs appeared with increasing "intensities". Figure 29 shows the correlations of the top-three peptide intensities of quantified proteins and their loading amount. CYP2C9, CYP3A5, and FMO1, 3 and 5 were not affected by FPDs in the tested range. However, CYP3A4, and especially

CYP2C19, had curves bending downward. Surprisingly, when the intensities of the homologous FPDs were added back to the true positives (CYP2C18 and CYP2C8 added to CYP2C19; CYP3A43 and CYP3A7 added to CYP3A4), the linearity had a greater recovery. This data indicated that PLGS assigned intensities from true positive proteins to their highly similar false homologs. But only occasionally, the false intensity assignment would badly distort the true quantity (Figrue 29, CYP2C19).

Table 8 . Signal intensities of PLGS identified proteins

	Summed intensity of top three ionizing peptides of each PLGS deduced protein											
Loading ^	CYP2C8*	CYP2C9	CYP2C18*	CYP2C19	CYP3A4	CYP3A5	CYP3A7*	CYP3A43*	FMO1	FMO3	FMO4*	FMO5
1 fmoe		15395		29808	63745	57119			92772	141479		
5 fmole		101066	2392	149709	118460	435684	3333	12419	237622	289122		68763
10 fmole		194750	8716	407653	277522.7	1117658	15067	4014	497965	592150	5793	159255
40 fmole	1559	819020	652035	684160	2802715	4933256	88852	61862	2512481	1910182	46143	645234

CYP2C9, CYP2C19, CYP3A4, CYP3A5, FMO1, FMO3, and FMO5 were mixed in equal molar by the vendor provided norminal concentration;
^ amount of each protein loaded on to the column
* false positive dedused by PLGS

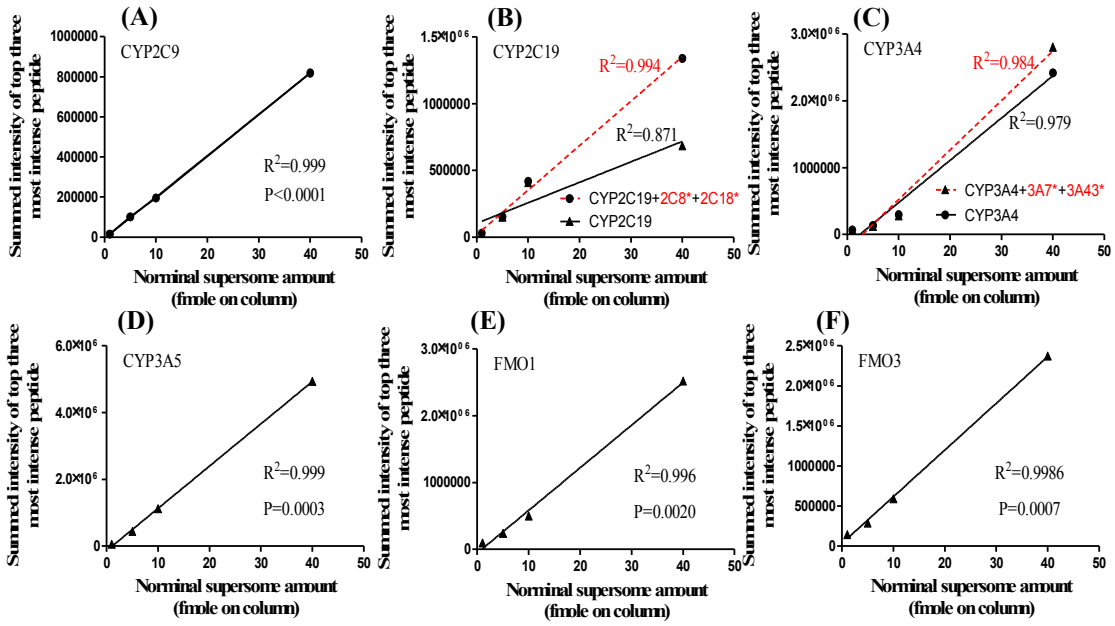

Figure 29. Impact of FPDs on protein quantifications using the "top three" rule applied by PLGS. The amount of enzyme digest loaded onto the column correlated with the intensity sum of the top three peptides calculated by PLGS. Red highlighted (*) enzymes were not present in the tryptic digestion, and therefore could be considered as FPDs. Red highlighted correlation coefficients and extrapolated dash lines are reconstitutions by adding the top three peptide intensities of the true positive enzymes to that of its FPD isoforms.

Thus FPD might be an explanation for the inconsistencies between LFDI protein quantification and targeted proteomic quantification presented by Harwood, Achour *et. al.,* and Wegler *et. al.* (54-56).

NanoUPLC sample loading optimization. Peptide online trapping is typically used in nano UPLC separation for MS^E proteomic analysis, taking advantage of its de-salting, analytical column-guarding, and fast sample loading (41, 42, 45, 60). The disadvantage of online trapping is that great amounts of hydrophilic peptides are lost. When mixed stable isotope-labeled

peptides (Table I) where injected with online trapping mode, NTEA(I)K, FSDHAEEG(R), and FQENPEEG(R) were completely lost, while other hydrophilic peptides were reduced to a varying extent in the chromatogram (data not shown). The same phenomenon was reported by the column manufacture as well (Waters Application Note 720005047EN).

Loss of peptides undermines quantification by label-free methods. Table 2 gradient C describes an optimized direct injection approach that ensures no peptide is lost during nano UPLC sample loading. After 5 uL of sample was centered in the injection loop, around 2.5-times the loop volume (13uL) of 3% mobile phase B pushed the sample from the loop to the column head; the sample loop was switched off-line and the elution gradient started to separate the proteomic peptides. The trapping column was still in tandem connection to the analytical column without diverging to the waste (no trapping occurred). The trapping column only functions as a guard column. This loading method is slower than trapping, but fully reserves all tryptic peptides for nano analytical column separation. It was used in subsequent label-free MS^E quantification of qFASP processed iHLM samples.

6.3.3 CORRELATING LABEL-FREE NANO-UPLC MS^E TO TARGETED UPLC-MRM ON QUANTIFICATIONS OF DMEs IN qFASP PROCESSED iHLMs

UPLC-MRM targeted quantification coherence of qFASP processed iHLMs. Ten iHLMs processed by qFASP were each divided into two parts, one spiked with stable isotope-labeled synthetic peptides for UPLC-MRM targeted quantification and the other part spiked with Hi3 E *coli* ClpB standards for LFDI nano UPLC-Q-TOF analysis. UPLC-MRM analyzed samples were calibrated with standard curves built by recombinant proteins processed in parallel with iHLMs.

At least two signature peptides of each targeted protein were monitored by UPLC-MRM targeted

proteomics. The quantities of two signature peptides were correlated to examine quantification coherence. Almost all correlations revealed strong correlation coefficients, close to unity slope, and near zero y-intercept in all targeted proteins (Figure 30), indicating consistent quantification results between the different signature peptides. As a result, two signature peptide quantities were averaged for correlation to the label-free nano UPLC MS^E measured results.

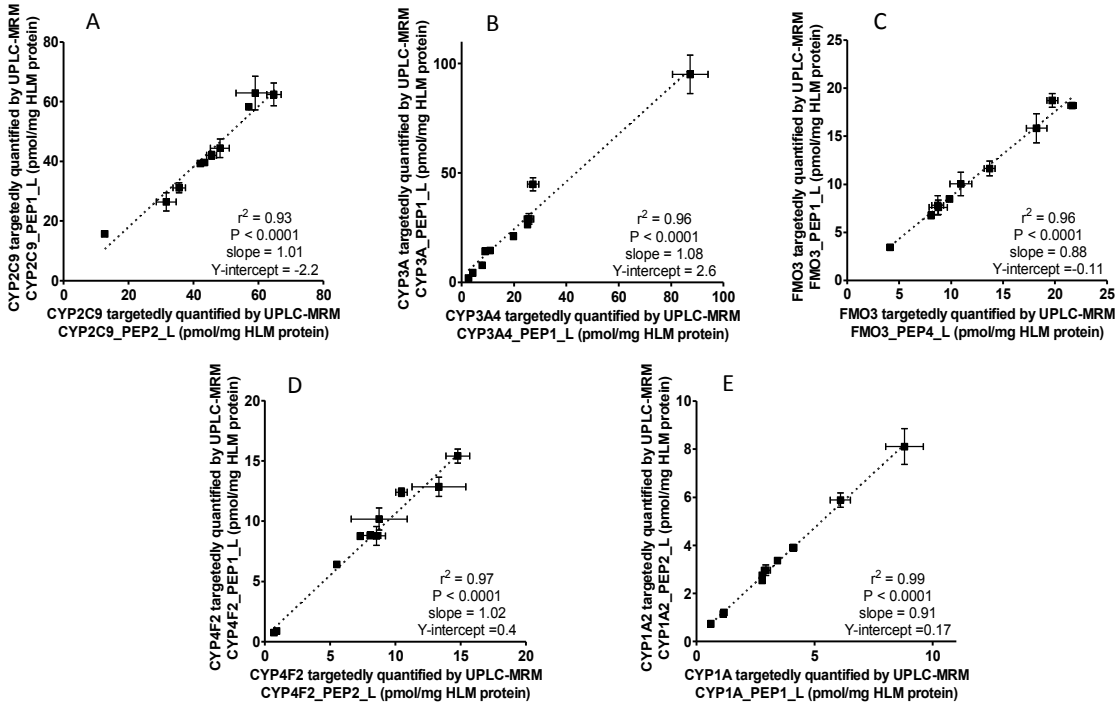

Figure 30. Quantification coherence of UPLC-MRM targeted approach quantified CYPs and FMO3 in qFASP digested individual HLMs (iHLM) and pooled HLM. Quantities of two signature peptides from each protein were correlated. Equivalent of 2.67 ug HLM digests were loaded onto the UPLC column. CYP3A_PEP1_L (SLLSPTFTSGK) is shared by CYP3A4, CYP3A5 and CYP3A7 (B). CYP1A_PEP1_L (NPHLALSR) is shared by CYP1A1 and CYP1A2 (E).

Label-free nanoUPLC MS^E quantification of iHLM and its correlation to targeted

approach. The lock-spray were found to interfere with sample signal stability, therefore it was turned off during analysis. Collected masses were manually calibrated according to the doubly charged M/Z of VIGQNEAVDAVSNAIR (one of the six Hi 3 standard peptides) 828.4392. Due to time constraints of the shared instrument, triplicate digests of 8 iHLMs were analyzed on the Q-TOF instrument. After 24 injections (each 150 min) of qFASP cleaned HLM samples onto the nano UPLC systems, no increase in column back-pressure, nor any raise of mass spectrum background noise, was observed, indicating a high level of sample cleanliness.

PLGS was used for protein search and quantity calculation. For all injections, 241 proteins were resolved on average, with a minimum of 143 and a maximum of 305. An average (range) of 11 (4—15) CYPs and 17 (14-18) UGTs were identified or quantified.

Correlation between the two mass spectrometry based quantification methods revealed very strong correlations. CYP3A4 quantified by the two methods showed a R^2=0.97 (Figure 31C); the sum of CYP3A4, 3A5, and 3A7 quantified by MSE correlated with CYP3A_PEP1 (peptide shared by the CYP3A4, 5, 7, quantified by UPLC-MRM) with a R^2=0.97 (Figure 31D). Correlation of CYP4F2 showed the worst R^2 of 0.73. MSE failed to identify CYP4F2 in one of the iHLM, therefore only 7 data points are shown in Figure 11 E and F. CYP1A2 was only quantified in 5 out of the 8 iHLMs analyzed by MSE, and not shown in the figure. Interestingly, FPD did not greatly bend any of the correlations in this study, unlike the measurement of recombinant CYP2C19 in Figure 9B. What's more intriguing, is that the sum of CYP2C9 and 2C8 quantified by MS^E correlated well with CYP2C9 measured by the targeted MS method (Figure 31B), which may be explained by FPD as it could distort CYP2C8 quantification. However, studies showed that CYP2C9 and CYP2C8 are coherently expressed (35, 65) in human liver, which also could be an explanation for the good correlation observed in Figure 31B.

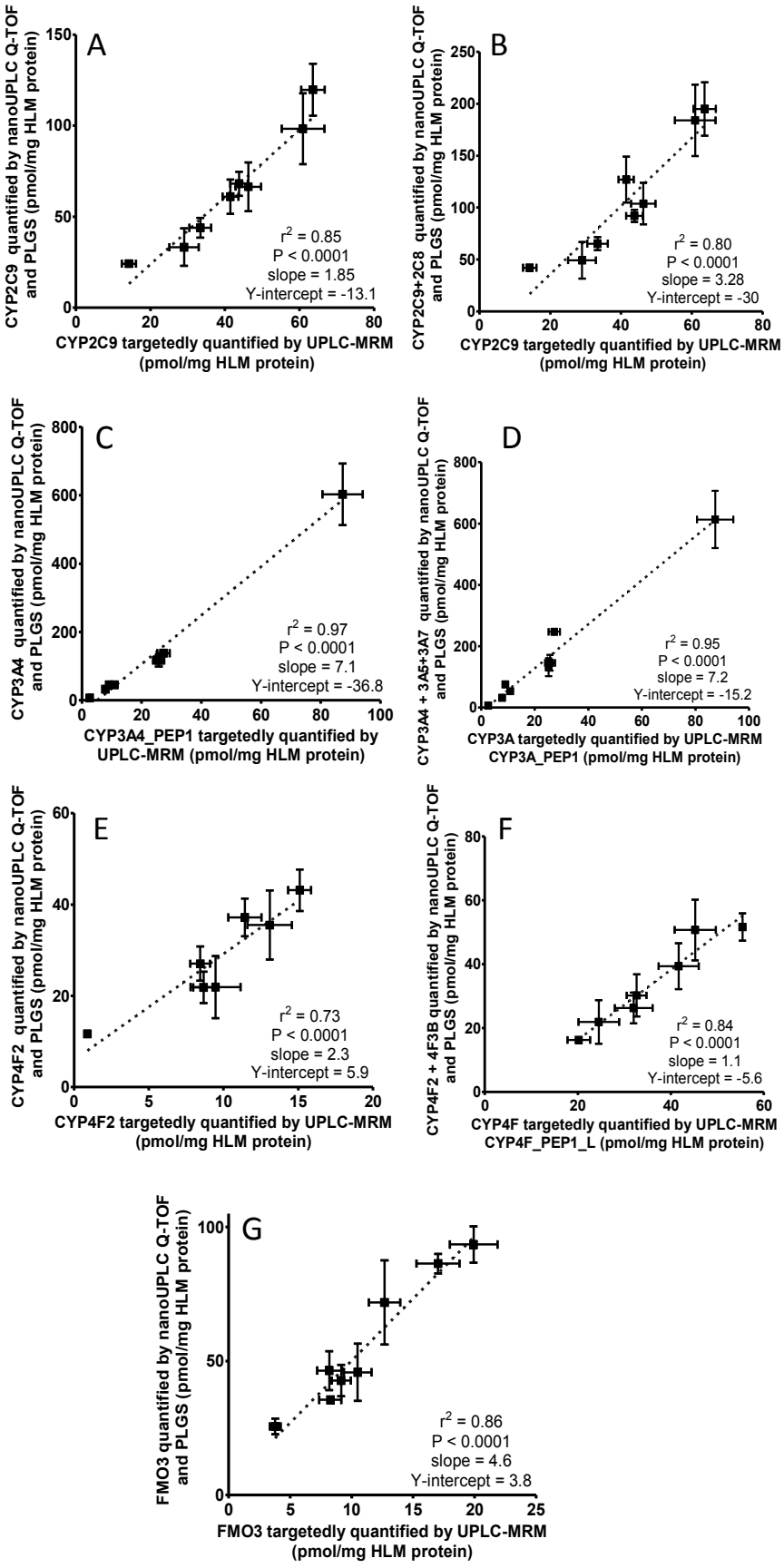
A
CYP2C9 quantified by nanoUPLC Q-TOF and PLGS (pmol/mg HLM protein)
CYP2C9 targetedly quantified by UPLC-MRM (pmol/mg HLM protein)
r2 = 0.85
P < 0.0001
slope = 1.85
Y-intercept = -13.1
B
CYP2C9+2C8 quantified by nanoUPLC Q-TOF and PLGS (pmol/mg HLM protein)
CYP2C9 targetedly quantified by UPLC-MRM (pmol/mg HLM protein)
r2 = 0.80
P < 0.0001
slope = 3.28
Y-intercept = -30
C
CYP3A4 quantified by nanoUPLC Q-TOF and PLGS (pmol/mg HLM protein)
CYP3A4_PEP1 targetedly quantified by UPLC-MRM (pmol/mg HLM protein)
r2 = 0.97
P < 0.0001
slope = 7.1
Y-intercept = -36.8
D
CYP3A4 + 3A5+3A7 quantified by nanoUPLC Q-TOF and PLGS (pmol/mg HLM protein)
CYP3A targetedly quantified by UPLC-MRM CYP3A_PEP1 (pmol/mg HLM protein)
r2 = 0.95
P < 0.0001
slope = 7.2
Y-intercept = -15.2
E
CYP4F2 quantified by nanoUPLC Q-TOF and PLGS (pmol/mg HLM protein)
CYP4F2 targetedly quantified by UPLC-MRM (pmol/mg HLM protein)
r2 = 0.73
P < 0.0001
slope = 2.3
Y-intercept = 5.9
F
CYP4F2 + 4F3B quantified by nanoUPLC Q-TOF and PLGS (pmol/mg HLM protein)
CYP4F targetedly quantified by UPLC-MRM CYP4F_PEP1_L (pmol/mg HLM protein)
r2 = 0.84
P < 0.0001
slope = 1.1
Y-intercept = -5.6
G
FMO3 quantified by nanoUPLC Q-TOF and PLGS (pmol/mg HLM protein)
FMO3 targetedly quantified by UPLC-MRM (pmol/mg HLM protein)
r2 = 0.86
P < 0.0001
slope = 4.6
Y-intercept = 3.8

Figure 11. Correlations between UPLC-MRM target quantification and nanoUPLC Q-TOF DIA quantification of CYPs and FMO3. Forty microgram of each 9 individual HLM and 1 pooled HLM were digested by qFASP. Equivalent of 2.67 ug and 1.28 ug HLM digests were loaded onto the UPLC and nanoUPLC columns respectively. CYP3A_PEP1_L (SLLSPTFTSGK) is shared by CYP3A4, CYP3A5, and CYP3A7 (D). CYP4F_PEP1_L (AEGGLWLR) is shared by CYP4F2, 4F3B, 4F12, and 4F11 (E). Enzyme quantity measured by UPLC-MRM shown on X-axis are average of two signature peptides of a protein, except CYP3A4, which only have one specific peptide monitored. Due to limited Q-TOF instrument availability, only triplicated of 8 iHLMs were analyzed, thus 8 data points were correlated in the figures.

Worth to point out, MS^E performed well in quantifying abundant species: CYP3A4, CYP2C9, and FMO3 are quantified in all injections; but lost certainty in quantifying less abundant species: CYP3A5 and FMO5 was quantified in 11 and 15 out of the 24 injections. These less abundant proteins would not be missed by targeted proteomic methods.

Another discrepancy between MS^E and targeted approach is that the MS^E quantities are almost always higher than the quantity concluded by the targeted approach, as shown by the slopes in Figure 11 were all above one. Our previous publications included experiments and discussions that dived great depth in explaining this issue (24, 66). Briefly, calibration standards used in UPLC-MRM targeted quantification are recombinant enzymes, whose nominal concentration was determined according to the prosthetic coenzyme group that only represents the amount of holoprotein in the solution. The nominal protein concentrations that defined calibrations standards are lower than the actual total protein (holoprotein + apoprotein) concentration. As a result, UPLC-MRM, which measures holoprotein, gave under-evaluated protein concentrations

compared to MS^E, which measures total protein (holo+apoprotein).

As a conclusion, this study introduced qFASP protocol that allowed full recovery of highly cleaned digested peptides and eliminated/reduced peptide adhesion during sample storage. This new protocol enabled similar or superior detection sensitivity compared to in-solution digestion, while not sacrificing digestion efficiency. We demonstrated the impact of FPD on the quantification linearity when nanoUPLC Q-TOF based MS^E was applied in quantifying highly similar protein homologs. A sample loading/direct injection method was optimized for nanoUPLC system to prevent peptide lost during online trapping process. Individual HLMs prepared by qFASP were quantified by both UPLC-MRM targeted approach and nanoUPLC-Q-TOF based MS^E methods. The two methods showed very strong correlations in many measured DMEs. We are the first to mitigate most of the problems that label free DIA technique have faced, and by applying the qFASP protocol, we observed very strong correlation between UPLC-MRM targeted protein quantification and the Q-TOF based MS^E approach. With the qFASP protocol, nanoUPLC-Q-TOF based DIA methods may release its true quantification potential.

6.4 REFERENCES

1. Wilkinson GR. Drug metabolism and variability among patients in drug response. N Engl J Med. 2005;352(21):2211-21.

2. Rushmore TH, Kong AN. Pharmacogenomics, regulation and signaling pathways of phase I and II drug metabolizing enzymes. Curr Drug Metab. 2002;3(5):481-90.

3. Guengerich FP. Cytochrome P450s and other enzymes in drug metabolism and toxicity. AAPS J. 2006;8(1):E101-11.

4. Achour B, Russell MR, Barber J, Rostami-Hodjegan A. Simultaneous quantification of the abundance of several cytochrome P450 and uridine 5'-diphospho-glucuronosyltransferase enzymes in human liver microsomes using multiplexed targeted proteomics. Drug metabolism and disposition: the biological fate of chemicals. 2014;42(4):500-10.

5. Sakamoto A, Matsumaru T, Ishiguro N, Schaefer O, Ohtsuki S, Inoue T, et al. Reliability and robustness of simultaneous absolute quantification of drug transporters, cytochrome P450 enzymes, and Udp-glucuronosyltransferases in human liver tissue by multiplexed MRM/selected reaction monitoring mode tandem mass spectrometry with nano-liquid chromatography. J Pharm Sci. 2011;100(9):4037-43.

6. Kawakami H, Ohtsuki S, Kamiie J, Suzuki T, Abe T, Terasaki T. Simultaneous absolute quantification of 11 cytochrome P450 isoforms in human liver microsomes by liquid chromatography tandem mass spectrometry with in silico target peptide selection. J Pharm Sci. 2011;100(1):341-52.

7. Chen Y, Zane NR, Thakker DR, Wang MZ. Quantification of Flavin-containing Monooxygenases 1, 3 and 5 in Human Liver Microsomes by UPLC-MRM-based Targeted Quantitative Proteomics and Its Application to the Study of Ontogeny. Drug Metab Dispos. 2016.

8. Wang MZ, Wu JQ, Dennison JB, Bridges AS, Hall SD, Kornbluth S, et al. A gel-free MS-based quantitative proteomic approach accurately measures cytochrome P450 protein concentrations in human liver microsomes. Proteomics. 2008;8(20):4186-96.

9. Michaels S, Wang MZ. The revised human liver cytochrome P450 "Pie": absolute protein quantification of CYP4F and CYP3A enzymes using targeted quantitative proteomics. Drug metabolism and disposition: the biological fate of chemicals. 2014;42(8):1241-51.

10. Peng KW, Bacon J, Zheng M, Guo Y, Wang MZ. Ethnic variability in the expression of hepatic drug transporters: absolute quantification by an optimized targeted quantitative proteomic approach. Drug Metab Dispos. 2015;43(7):1045-55.

11. Al Feteisi H, Achour B, Barber J, Rostami-Hodjegan A. Choice of LC-MS methods for the absolute quantification of drug-metabolizing enzymes and transporters in human tissue: a comparative cost analysis. AAPS J. 2015;17(2):438-46.

12. Silva JC, Gorenstein MV, Li GZ, Vissers JP, Geromanos SJ. Absolute quantification of proteins by LCMSE: a virtue of parallel MS acquisition. Mol Cell Proteomics. 2006;5(1):144-56.

13. Cheng FY, Blackburn K, Lin YM, Goshe MB, Williamson JD. Absolute protein quantification by LC/MS(E) for global analysis of salicylic acid-induced plant protein secretion responses. J Proteome Res. 2009;8(1):82-93.

14. Bostanci N, Heywood W, Mills K, Parkar M, Nibali L, Donos N. Application of label-free absolute quantitative proteomics in human gingival crevicular fluid by LC/MS E (gingival exudatome). J Proteome Res. 2010;9(5):2191-9.

15. Farrell A, Mittermayr S, Morrissey B, Mc Loughlin N, Navas Iglesias N, Marison IW, et al. Quantitative host cell protein analysis using two dimensional data independent LC-MS(E). Anal Chem. 2015;87(18):9186-93.

16. Finamore F, Pieroni L, Ronci M, Marzano V, Mortera SL, Romano M, et al. Proteomics investigation of human platelets by shotgun nUPLC-MSE and 2DE experimental strategies: a comparative study. Blood Transfus. 2010;8 Suppl 3:s140-8.

17. Mbeunkui F, Goshe MB. Investigation of solubilization and digestion methods for microsomal membrane proteome analysis using data-independent LC-MSE. Proteomics. 2011;11(5):898-911.

18. Havlis J, Shevchenko A. Absolute quantification of proteins in solutions and in polyacrylamide gels by mass spectrometry. Anal Chem. 2004;76(11):3029-36.

19. Leon IR, Schwammle V, Jensen ON, Sprenger RR. Quantitative assessment of in-solution digestion efficiency identifies optimal protocols for unbiased protein analysis. Mol Cell Proteomics. 2013;12(10):2992-3005.

20. Speicher KD, Kolbas O, Harper S, Speicher DW. Systematic analysis of peptide recoveries from in-gel digestions for protein identifications in proteome studies. J Biomol Tech. 2000;11(2):74-86.

21. Choksawangkarn W, Edwards N, Wang Y, Gutierrez P, Fenselau C. Comparative study of workflows optimized for in-gel, in-solution, and on-filter proteolysis in the analysis of plasma membrane proteins. J Proteome Res. 2012;11(5):3030-4.

22. Kristensen K, Henriksen JR, Andresen TL. Adsorption of cationic peptides to solid surfaces of glass and plastic. PLoS One. 2015;10(5):e0122419.

23. Horinek D, Serr A, Geisler M, Pirzer T, Slotta U, Lud SQ, et al. Peptide adsorption on a hydrophobic surface results from an interplay of solvation, surface, and intrapeptide forces. Proc Natl Acad Sci U S A. 2008;105(8):2842-7.

24. Mitulovic G, Stingl C, Steinmacher I, Hudecz O, Hutchins JR, Peters JM, et al. Preventing carryover of peptides and proteins in nano LC-MS separations. Anal Chem. 2009;81(14):5955-60.

25. Wegler C, editor Quantification of ADME Proteins: An Inter-laboratory Comparison. AAPS Annual Meeting and Exposition; 2015 October 29th; Orlando, FL, USA.

26. Achour B, editor A Cross-Laboratory Comparison of Enzyme and Transporter Abundance Quantification. 2015 AAPS Annual Meeting and Exposition; 2015 October 29; Orlando, FL, USA.

27. Harwood MD, editor It is a matter of trust! Performing cross-laboratory-cross-technique comparisons in quantitative ADME proteomics. America Association of Pharmaceutical Science; 2015 October 29th 2015; Orlando, Florida.

28. Wisniewski JR, Zougman A, Nagaraj N, Mann M. Universal sample preparation method for proteome analysis. Nat Methods. 2009;6(5):359-62.

29. Cunningham R, Wang J, Wellner D, Li L. Investigation and reduction of sub-microgram peptide loss using molecular weight cut-off fractionation prior to mass spectrometric analysis. J Mass Spectrom. 2012;47(10):1327-32.

30. Ismaiel OA, Halquist MS, Elmamly MY, Shalaby A, Thomas Karnes H. Monitoring phospholipids for assessment of ion enhancement and ion suppression in ESI and APCI LC/MS/MS for chlorpheniramine in human plasma and the importance of multiple source matrix effect evaluations. J Chromatogr B Analyt Technol Biomed Life Sci. 2008;875(2):333-43.

31. Bond NJ, Shliaha PV, Lilley KS, Gatto L. Improving qualitative and quantitative performance for MS(E)-based label-free proteomics. J Proteome Res. 2013;12(6):2340-53.

32. Hustoft HK, Reubsaet L, Greibrokk T, Lundanes E, Malerod H. Critical assessment of accelerating trypsination methods. J Pharm Biomed Anal. 2011;56(5):1069-78.

33. An B, Zhang M, Johnson RW, Qu J. Surfactant-aided precipitation/on-pellet-digestion (SOD) procedure provides robust and rapid sample preparation for reproducible, accurate and sensitive LC/MS quantification of therapeutic protein in plasma and tissues. Anal Chem. 2015;87(7):4023-9.

34. Felgner PL, Wilson JE. Hexokinase binding to polypropylene test tubes. Artifactual activity losses from protein binding to disposable plastics. Anal Biochem. 1976;74(2):631-5.

35. Souverain S, Rudaz S, Veuthey JL. Matrix effect in LC-ESI-MS and LC-APCI-MS with off-line and on-line extraction procedures. J Chromatogr A. 2004;1058(1-2):61-6.

36. Achour B, Barber J, Rostami-Hodjegan A. Expression of hepatic drug-metabolizing cytochrome p450 enzymes and their intercorrelations: a meta-analysis. Drug metabolism and disposition: the biological fate of chemicals. 2014;42(8):1349-56.

37. Chen Y, Zane NR, Thakker DR, Wang MZ. Quantification of Flavin-containing Monooxygenases 1, 3, and 5 in Human Liver Microsomes by UPLC-MRM-Based Targeted Quantitative Proteomics and Its Application to the Study of Ontogeny. Drug metabolism and disposition: the biological fate of chemicals. 2016;44(7):975-83.

38. Erde J, Loo RR, Loo JA. Enhanced FASP (eFASP) to increase proteome coverage and sample recovery for quantitative proteomic experiments. J Proteome Res. 2014;13(4):1885-95.

6.5 qFASP protocol

Quantitative Filter-assisted Sample Preparation (qFAS) Protocol for Label-free Data-Independent Analysis (DIA) of Human Liver Microsome (HLM) or Recombinant DME Protein Using NanoUPLC-Q-TOF

1. Reagents
    a. Millipore Microcon YM-10 10K MWCO centrifugal filters
    b. Denaturation buffer (DB): 40 mM ammonium bicarbonate (ABC), 10 Mm DTT
    c. Washing buffer A (WBA): same as DB
    d. Alkylation buffer (AB): 50 mM IAA in 40 mM ABC
    e. Washing buffer B (WBB): 40 mM ABC
    f. Trypsin Digestion buffer (TDB): keep trypsin to protein ratio between 1:30-1:50, 20 mM ABC
    g. HLM: Xenotech, Pool of 200, 20 mg/mL
    h. Certified screw top 250 uL polypropylene sample from Agilent
    i. 2 mg/mL albumin acquired from Thermo Scientific
    j. Protein LoBind Tubes from eppendorf
2. Procedure
    a. Add 200 uL water to Microcon filters, centrifuge 14000xg for 20 min for filter rinse and equilibration.
    b. Add 30-60 ug of HLM to 90 uL DB, heating up at 95 degrees for 3 min in protein Lobind vials
    c. Transfer denatured protein solution to Microcon filter. Keeping the transferring pipette tips. Wash the Lobind vials with 100 uL WBA and transfer the wash with the kept pipette tips to Microcon filters.
    d. Shake the filters at 800 RPM for 1 min, centrifuge 14000xg for 20 min, discard the flow-through
    e. Add 200 uL WBA to filters, centrifuge 14000xg for 20 min, discard the flow-through, **repeat this step** and centrifuge for 30 min
    f. Add 100 uL AB, shake the filter at 800 RPM for 1 min, and incubate in dark for 20 min. Centrifuge 14000xg for 20 min.
    g. Add 150 uL WBB to filters, centrifuge 14000xg for 20 min, discard the flow-through, **repeat this step** and centrifuge for 30-40 min until very little liquid remains on the filter
    h. Add 50 uL TDB to filter, shake 800 RPM for 1 min. Use parafilm to seal the cap and the bottom of the filter. Incubate in 37 degree for 4 hours.
    i. Discard the parafilm, add 75 uL of acetonitrile (ACN) to the filter, shake at 800 RPM for 1 min, centrifuge 14000xg for 20 min

j. Add 100 uL of 60% ACN, shake at 800 RPM for 1 min, centrifuge 14000xg for 20-30 min. **Repeat this step**
k. Add 100 uL of 60% ACN, shake at 800 RPM for 1 min, centrifuge 14000xg for 40-60 min to dry the filter membrane.
l. Collect all the eluent and transfer to protein LoBind vials, speed-vac to evaporate ACN and getting a desired volume. Note: Before speed-vac, thoroughly mix eluted peptide by vortex. Un-uniformly mixed peptide solutions may yield different remaining volume in intra-replicate samples after speed-vac. High remaining ACN jeopardies LC separation.

3. Masking sample vials
    a. Add 200 uL 2 mg/mL albumin to Agilent polypropylene sample vials. Make sure no air bubbles in albumin solution. Store in 4 degree for more than 24 h. Discard the albumin or store for another masking. Add 200 uL water, gently pipeppet up/down 3 times. Repeat the rinse again. Do not touch the wall of the vial. Discard the wash.
    b. Add digests to the masked vials for LC-MS analysis

Chapter VII: Conclusion and Future Directions

TABLE OF CONTENTS

7.1 General Conclusions

LC-MRM-based protein quantification offers unparalleled specificity, versatility, accuracy, reproducibility and ease of method development. Our efforts in the development and validation of a method for the absolute quantification of CYP2C9, CYP2C19, FMO1, FMO3 and FMO5 were successful. Good quantification linearity and reproducibility, as well as strong correlations to enzyme activity, were achieved. However, discrepancies between the use of recombinant protein and purified synthetic signature peptide for standards were identified. We concluded that recombinant protein is best for standards used in absolute protein quantification. As a result, we are calling for additional protein standards to become commercially available, thus supporting an increase in the quality of absolute protein quantifications.

Using established and existing UPLC-MRM targeted protein quantification methods, the previously reported ontogenies of CYP3A4, CYP3A5, CYP3A7, CYP2C9, FMO1 and FMO3, determined by Western blot and enzyme activity assays, were confirmed. In addition, the multiplexing capability of LC-MS allowed the simultaneous characterization of CYP4F2, CYP4F3B and FMO5 ontogeny. CYP4F2 is expressed very low during the neonatal stage, but increased with age. CYP4F3B and FMO5 expression did not change with age.

To screen CYP1B1-dependent anticancer prodrugs, a cell model, specifically KLE cells, must be characterized for the presence and expression level of CYP1B1. The characterization of this cell line using an enzyme activity assay was unsuccessful, due in part to low CYP1B1 activity; the only option remaining for characterization was CYP1B1 targeted proteomics. Utilizing microsomes isolated from different human tissues, the specificity of the targeted assay was confirmed. With this technique, KLE cells were shown to express CYP1B1 only, not CYPs 1A1 or 1A2, which is required for the first stage of screening.

UPLC-MRM targeted proteomic quantification also was used for the mechanistic elucidation of potential drug-drug interactions. We hypothesized that CYP4F2 induction by lovastatin might potentiate warfarin's therapeutic effect. To test this hypothesis, the induction of CYP4F2 by clinically significant lovastatin concentrations was examined in hepatic *in vitro* models. Although our induction studies were successful in both HepaRG and primary human hepatocytes, CYP4F2 increases could not be measured conclusively by UPLC-MRM or RT-PCR, thus the hypothesis remains unanswered.

An emerging Q-TOF-based label-free DIA approach for protein quantification is able to quantify hundreds of proteins at minimum cost, but with some problems. We developed the qFASP technique, allowing near complete recovery of cleaned, digested sample peptides. In addition, false positive discoveries in DIA were demonstrated to contribute to quantification distortion. We are the first to address a majority of the problems facing the label-free DIA technique, and by applying the qFASP protocol, we observed a very strong correlation between UPLC-MRM targeted protein quantification and the Q-TOF-based DIA approach.

7.2 Future Directions of Mass Spectrometry-Based DME Quantification

The adoption of qFASP sample preparation and analytical vial passivation, and the application of direct injection for nano-UPLC sample loading allowed the near full-recovery of clean proteomic digests. These improvements also drove the strong quantification coherence observed between the well-established UPLC-MRM targeted approach and the nano-UPLC-Q-TOF-based MS^E analysis. However, nano-UPLC-Q-TOF analysis still had intrinsic limitations, such as losing detection/quantification sensitivity for DMEs of low abundance (*e.g.*, CYP3A5 and CYP4A11), and occasional occurrences of quantity misassignment due to FPDs. These limitations are

fundamental instrument limitations and can be overcome by implementing better LC separation and mass resolution. In 2015, C. E. Doneanu *et. al.* reported the use of 2-dimensional (2D) nano-LC with an ion-mobility Q-TOF MS^E for the detection of host cell impurities (HCIs) in purified monoclonal antibodies at the 1 ppm level (1). PLGS also was used for the identification and quantification of HCI abundance. That same year, S. T. Mindaye *et. al.* also described the identification and relative quantification of over 2500 human bone marrow proteins with triplicate runs using 2D-nanoLC ion-mobility Q-TOF-based MS^E analysis(2). Improved separation of masses in space (ion-mobility) and time (2D-nano LC) enabled greater detection sensitivity and higher protein identification confidence. These same improvements are anticipated should 2D-nano LC and ion mobility Q-TOF be used for the quantification of DMEs.

Despite the excellent separation of mass achieved with 2D-LC ion mobility Q-TOF, this technique requires a great deal of training to master and effort to maintain, as well as 4-12 hours to process a single sample. It also yields enormous data files. An alternative high-throughput MS technique is QconCAT. In 2014, T. S. Batth *et. al.* performed targeted absolute quantification of over 400 *E. coli* proteins with a 5.5 min LC gradient (10 min total) using a QconCAT protein containing over 800 tryptic peptides (3). Since a majority of human DMEs have been identified, a single large QconCAT protein containing tryptic peptides for all the known DMEs could be constructed for global quantification of these enzymes.

A second application for qFASP would be MS-based quantification of human drug transporters (DTs). Previous sample preparation methods for the digestion of DTs used detergents for protein solubilization; however, many of these methods were unable to remove the detergents prior to analysis. Although SDS and urea were not used for the sake of quantification reproducibility in the qFASP method, other detergents (*e.g.* sodium deoxycholate) could be examined to enhance

the digestion of DTs and possibly preserve reproducibility simultaneously. The downstream process of qFASP would still help to remove the detergent and preserve the quantitative nature of the digested samples.

Overall, quantitative profiling of the human hepatic proteome using qFASP nanoUPLC-Q-TOF MS^E could help further characterize new DME ontogeny patterns, discover new biomarkers for liver diseases, and profile DME induction patterns under the influence of new drugs and different disease states. In addition, this method to clean up protein samples while maintaining near total recovery of the tryptic digest opens the door for new proteomic discoveries.

7.3 References

1. Doneanu CE, Anderson M, Williams BJ, Lauber MA, Chakraborty A, Chen W. Enhanced Detection of Low-Abundance Host Cell Protein Impurities in High-Purity Monoclonal Antibodies Down to 1 ppm Using Ion Mobility Mass Spectrometry Coupled with Multidimensional Liquid Chromatography. Anal Chem. 2015;87(20):10283-91.

2. Mindaye ST, Lo Surdo J, Bauer SR, Alterman MA. The proteomic dataset for bone marrow derived human mesenchymal stromal cells: Effect of in vitro passaging. Data Brief. 2015;5:864-70.

3. Batth TS, Singh P, Ramakrishnan VR, Sousa MM, Chan LJ, Tran HM, et al. A targeted proteomics toolkit for high-throughput absolute quantification of Escherichia coli proteins. Metab Eng. 2014;26:48-56.

APPENDICES

Appendix I: Quantification of Flavin-containing Monooxygenases 1, 3 and 5 in Human Liver Microsomes by UPLC-MRM-based Targeted Quantitative Proteomics and Its Application to the Study of Ontogeny

Abstract

Flavin-containing monooxygenases (FMOs) have a significant role in the metabolism of small molecule pharmaceuticals. Among the five human FMOs, FMO1, FMO3 and FMO5 are the most relevant to hepatic drug metabolism. Although age-dependent hepatic protein expression, based on immunoquantification, has been reported previously for FMO1 and FMO3, there is very little information on hepatic FMO5 protein expression. To overcome the limitations of immunoquantification, a UPLC-MRM-based targeted quantitative proteomic method was developed and optimized for the quantification of FMO1, FMO3 and FMO5 in human liver microsomes (HLM). A post-in silico product ion screening process was incorporated to verify LC-MRM detection of potential signature peptides prior to their synthesis. The developed method was validated by correlating marker substrate activity and protein expression in a panel of adult individual donor HLM (age 39-67 years). The mean (range) protein expression of FMO3 and FMO5 was 46 (26 – 65) pmol/mg HLM protein and 27 (11.5 – 49) pmol/mg HLM protein, respectively. To demonstrate quantification of FMO1, a panel of fetal individual donor HLM (gestational age 14-20 weeks) was analyzed. The mean (range) FMO1 protein expression was 7.0 (4.9 – 9.7) pmol/mg HLM protein. Furthermore, the ontogenetic protein expression of FMO5 was evaluated in fetal, pediatric and adult HLM. The quantification of FMO proteins also was compared using two different calibration standards, recombinant proteins vs. synthetic signature peptides, to assess the ratio between holoprotein vs. total protein. In conclusion, a UPLC-MRM-based targeted quantitative proteomic method has been developed for the quantification of FMO enzymes in HLM.

For complete publication see:

Chen Y, Zane NR, Thakker DR, Wang MZ. Quantification of Flavin-containing Monooxygenases 1, 3, and 5 in Human Liver Microsomes by UPLC-MRM-Based Targeted Quantitative Proteomics and Its Application to the Study of Ontogeny. Drug metabolism and disposition: the biological fate of chemicals. 2016; 44(7):975-83.

Appendix II: CYP and FMO Families Shows Age-Dependent Differences in Expression and Functional Activity

Abstract

Significant age-dependent differences in pharmacokinetic (PK) parameters exist for metabolically cleared medications. Therefore, it is essential to obtain data on gene and protein expression of drug metabolizing enzymes (DMEs), as well as their catalytic activities in fetal, pediatric, and adult hepatic tissues for the development of mechanistic models. Although the relative expression of the cytochrome P450 (CYP) 3A, CYP2C and flavin-containing monooxygenases (FMO) enzymes have been previously published, this is the first study in which quantitative gene and protein expression of these DMEs were correlated with their corresponding functional activities in the same samples from target populations. Both the CYP3A and FMO families showed a distinct switch from fetal isoforms (CYP3A7, FMO1) to adult isoforms (CYP3A4, FMO3) at birth, while the CYP2C9 enzyme showed a linear maturation from birth into adulthood. In contrast, CYP2C19 expression was higher in pediatric samples compared to fetal and adult samples. Functional activity of the CYP2C family was linearly correlated with enzyme protein expression in pediatric and adult tissues, while the catalytic efficiency of CYP2C19 was greater in pediatric hepatic tissues compared to adult tissues; this is a surprising finding and suggests that cytochrome P450 enzymes may encounter a different micro environment in children versus adults. These data are critical to understanding the mechanistic basis underlying the faster clearance of certain medications in children versus adults, and can be incorporated into mechanistic models to enhance the accuracy of pediatric PK predictions.

For complete publication see:

Zane, N. R., Chen, Y., Wang, Z. W., and Thakker, D. R. CYP and FMO Families Show Age-Dependent Differences in Expression and Functional Activity. Submitted to Journal of Pharmacology and Experimental Therapeutics, under review.

Appendix III: Development of an in vitro model to screen CYP1B1-targeted anticancer prodrugs

ABSTRACT

Cytochrome P450 1B1 (CYP1B1) is an anticancer therapeutic target due to its overexpression in a number of steroid hormone-related cancers. One anticancer drug discovery strategy is to develop prodrugs specifically activated by CYP1B1 in malignant tissues to cytotoxic metabolites. Here, we aimed to develop an in vitro screening model for CYP1B1-targeted anticancer prodrugs using the KLE human endometrial carcinoma cell line. KLE cells demonstrated superior stability of CYP1B1 expression relative to transiently transfected cells and did not express any appreciable amount of cognate CYP1A1 or CYP1A2, which would have compromised the specificity of the screening assay. The effect of two CYP1B1-targeted probe prodrugs on KLE cells was evaluated in the absence and presence of a CYP1B1 inhibitor to chemically "knockout" CYP1B1 activity (CYP1B1-inhibited). Both probe prodrugs were more toxic to KLE cells than to CYP1B1-inhibited KLE cells and significantly induced G0/G1 arrest and decreased S phase in KLE cells. They also exhibited pro-apoptotic effects in KLE cells, which were attenuated in CYP1B1-inhibited KLE cells. In summary, a KLE cell-based model has been characterized to be suitable for identifying CYP1B1-targeted anticancer prodrugs and should be further developed and employed for screening chemical libraries.

For complete publication see:

Wang, Z., Chen, Y., Wang, M. Z. Development of an in vitro model to screen CYP1B1-targeted anticancer prodrugs. Submitted to Journal of Biomolecular Screening, under 3rd review.

Appendix IV: Quantitative FASP (qFASP) Offers Nearly Full Digest Recovery and Good Quantification Correlation between Targeted UPLC-MRM and NanoUPLC-Q-TOF-Based Label-Free DIA Approach in DME Analysis

ABSTRACT

Quantification of human liver DMEs using LC-MRM targeted proteomic techniques has been well established. The high specificity and multiplexing of targeted proteomics comes at a price—cost of synthetic signature peptides increase linearly with the amount of targeted proteins, and lengthy efforts for method establishment. In comparison, label-free data independent (LFDI) MS allows quantification of hundreds of proteins simultaneously for a negligible cost. However, this quantification technique suffers from a lack of quantitative protein clean up, sample storage, and chromatography methods that offer high reproducibility and full recovery of all digested peptides. Secondly, previous parallel studies comparing LFDI quantification with targeted proteomics yielded puzzling inconsistencies, indicating deeper flaws in data independent analysis (DIA), other than non-quantitative sample preparation methods that affected quantification accuracy. This study strives to answer both challenges that jeopardize the performance of LFDI quantification. Firstly, based on a recently introduced filter-assisted sample preparation (FASP) protocol, which is known to have severe peptide lost problem, a quantitative FASP (qFASP) protocol was established. By removing detergent and denaturing-salt at digestion, eluting peptides with 60% ACN on the filter, and storing peptides in albumin masked vials, qFASP achieved almost full peptide recovery, ensured similar DME digestion efficiency, and same or better level of sample cleanness compared to the original FASP protocol. Secondly, a nanoUPLC sample loading and direct injection scheme was applied, which guaranteed no hydrophilic peptide loose, contrasting to previous online trapping method. Thirdly, false positive discoveries (FPD) occurred at LFDI quantification of homologous DMEs was evaluated on its impact on the linearity of protein quantification, which maybe another cause for the inconsistencies between LFDI and targeted proteomics. At last, 10 iHLMs were digested by

qFASP, DMEs quantified by targeted UPLC-MRM method were correlated with corresponding species quantified by nanoUPLC Q-TOF LFDI analysis. Despite FPD, good correlation coefficients (R2) between targeted UPLC-MRM proteomic method and nanoUPLC-Q-TOF-based label-free protein quantification were observed (R2=0.97 for CYP3A4; R2=0.86 for FMO3; R2=0.85 for CYP2C9, etc.).

Manuscript in preparation.

1. Doneanu CE, Anderson M, Williams BJ, Lauber MA, Chakraborty A, Chen W. Enhanced Detection of Low-Abundance Host Cell Protein Impurities in High-Purity Monoclonal Antibodies Down to 1 ppm Using Ion Mobility Mass Spectrometry Coupled with Multidimensional Liquid Chromatography. Anal Chem. 2015;87(20):10283-91.

2. Mindaye ST, Lo Surdo J, Bauer SR, Alterman MA. The proteomic dataset for bone marrow derived human mesenchymal stromal cells: Effect of in vitro passaging. Data Brief. 2015;5:864-70.

3. Batth TS, Singh P, Ramakrishnan VR, Sousa MM, Chan LJ, Tran HM, et al. A targeted proteomics toolkit for high-throughput absolute quantification of Escherichia coli proteins. Metab Eng. 2014;26:48-56.